

From the

Clinic and Policlinic for Cardiac Surgery at the University of Rostock

Director: Prof. Dr. med. habil. Gustav Steinhoff

Identification and characterization of CD4+AT2R+ T cell subpopulation in humans and rats

DISSERTATION

to obtain the academic degree

Doctor rerum humanarum (Dr. rer. hum.)

at Medical Faculty, University of Rostock



submitted by:

Anna Skórska

born on January 15, 1981 in Klimontów (Poland)

Rostock, November 2015

Aus der Klinik und Poliklinik für Herzchirurgie
Klinikdirektor: Prof. Dr. med. habil. Gustav Steinhoff

Identifizierung und Charakterisierung der CD4+AT2R+ T Zell Subpopulation bei Mensch und Ratte

DISSERTATION

zur Erlangung des akademischen Grades
doctor rerum humanarum (Dr. rer. hum.)
der medizinischen Fakultät, Universität Rostock



vorgelegt von
Anna Skórska
geb. am 15.01.1981 in Klimontow (Polen)

Rostock, November 2015

Dean: Prof. Dr. med. Emil Christian Reisinger

Assessors:

1. Assessor:

Prof. Dr. med. Gustav Steinhoff

Director of the Clinic and Polyclinic for Cardiac Surgery, Rostock University Medical Center

2. Assessor:

Prof. Dr. med. Brigitte Vollmar

Institute for Experimental Surgery, Rostock University Medical Center

3. Assessor:

Prof. Dr. med. Hans-Dieter Volk

Institute of Medical Immunology, Charité – Universitätsmedizin Berlin, Berlin-Brandenburger Center for Regenerative Therapies (BCRT)

Date of submission: 25.11.2015

Date of defence: 14.06.2016

Es ist auch schön ...

wenn man Rückschläge hinzunehmen gelernt hat, wenn man Niederlagen sich eingestehen kann, wenn man an Ungerechtigkeiten nicht mehr verzweifelt und sich selbst immer treu bleibt ohne dabei arrogant zu sein. Wer im Leben immer Glück hatte, worauf will der schon stolz sein ? Was hat der für Erfolge ? Wer nie gefallen ist, der weiß auch nicht, wie schön es ist, sich hochzurappeln, aufzustehen und den Staub abzuklopfen, über sich selbst zu lachen und dem Leben erneut die Zähne zu zeigen und alle zu verblüffen, indem er sagt:

Das Hinfallen gerade eben hat richtig gut getan ...

(Gerhard Feil)

Abbreviations

ACE	<i>Angiotensin-converting enzyme</i>
Ang I	<i>Angiotensin I</i>
AngII	<i>Angiotensin II</i>
ANP	<i>Atrial Natriuretic Peptides</i>
AT1R	<i>Angiotensin II type 1 receptor</i>
AT2R	<i>Angiotensin II type 2 receptor</i>
CK	<i>creatine kinase</i>
CVD	<i>cardiovascular diseases</i>
gp	<i>glycoprotein</i>
H ₂ O ₂	<i>Hydrogen peroxidase</i>
HF	<i>Heart Failure</i>
IL	<i>Interleukin</i>
LV	<i>left ventricle</i>
MAPK	<i>Mitogen-activated protein kinase</i>
MI	<i>myocard infarction</i>
MMP	<i>metalloproteinase</i>
RAS	<i>Renin - Angiotensin System</i>
ROS	<i>Reactive Oxygen Species</i>
TGF- β	<i>Transforming Growth Factor - β</i>
TNF- α	<i>Tumor Necrosis Factor - α</i>

Zusammenfassung

In Folge eines akuten Myokardinfarkts (MI) kommt es sowohl zu einer ischämie-induzierten, direkten myokardialen Verletzung, als auch zu einer subsequenten Herzverdickung, verursacht durch eine fehlerhafte inflammatorische Reaktion. Das Renin-Angiotensin System (RAS) spielt dabei eine besondere Rolle, da es im Zuge einer kardiovaskulären Erkrankung zur Beeinträchtigung des akuten kardialen Remodellings und der Entzündungsreaktion beiträgt. Der Angiotensin II Typ 2 Rezeptor (AT2R) ist auf immunkompetenten Zellen hochexprimiert und in die zellvermittelte Entzündungsreaktion des Herzens involviert. Angesichts dessen wird vermutet, dass der AT2R mit CD4⁺ T Zellen, die während der Entzündungsreaktion als Antwort auf die ischämische Verletzung rekrutiert werden, interagiert. Deshalb wurden aus peripherem Rattenblut nach einem experimentellen MI (MI-induziert) einerseits sowie Patienten mit Herzschwäche andererseits CD4⁺ T Zellen aufgereinigt. Zwei CD4⁺ T Zellpopulationen CD4⁺AT2R⁺ und CD4⁺AT2R⁻ wurden zunächst mittels FACS sortiert. Mittels Durchflußzytometrie, Färbung der Cytospin-Präparate und RT-PCR wurde die Reinheit der isolierten Zellen und die Expression des AT2R sowie verschiedener Zytokine bestimmt. Um den Einfluss des AT2R auf die Zytokinproduktion zu zeigen, wurden die beiden CD4⁺ T Zellpopulationen CD4⁺AT2R⁺ und CD4⁺AT2R⁻ mit AT2R Agonist (Angiotensin II) in Kombination mit AT2R Antagonist PD 123319 (PD) behandelt. Basierend auf diesen Verfahren wurde die CD4⁺AT2R⁺ T Zellpopulation im peripheren Blut der Ratte und des Menschen definiert. Die aus dem Blut gewonnenen CD4⁺AT2R⁺ T Zellen zeichneten sich zum einen durch eine hochregulierte Expression des Transkriptionsfaktors Forkhead-Box-Protein FOXP3 aus und zum anderen durch eine gesteigerte Produktion verschiedener Zytokine (anti- und proinflammatorisch). Außerdem führte die Aktivierung des AT2R zu einer erhöhten Produktion des antiinflammatorischen Zytokins IL-10 in den CD4⁺AT2R⁺ T Zellen, jedoch nicht in der CD4⁺AT2R⁻ T Zellpopulation. Darüberhinaus führte die intramyokardiale Injektion von MI-induzierten CD4⁺ATR⁺ T Zellen der Milz nach Herzinfarkt an der Ratte zu einer Reduktion der Infarktgröße und zu einer Verbesserung der kardialen Funktion. Die Ergebnisse der vorliegenden Arbeit zeigen erstmalig einen AT2R-abhängigen Mechanismus, der durch die CD4⁺AT2R⁺ T Zellpopulation vermittelt wird und die Supp-

ression der Entzündungsreaktion im Herz steuert. Damit repräsentieren CD4+AT2R+ T Zellen eine vielversprechende Zellpopulation für den Einsatz in der regenerativen Therapie, sei es durch direkte myokardiale Transplantation, durch die pharmakologische Aktivierung des AT2R oder durch eine Kombination beider Möglichkeiten.

Summary

Following acute myocardial infarction (MI) the heart suffers, beside ischemia-induced direct myocardial injury, from a subsequent indirect damage through improper inflammatory reaction. A wealth of information indicates that the renin-angiotensin system (RAS) can interfere with acute cardiac remodelling and inflammation processes during cardiovascular injury. Given the recent observations showing that AT2 receptors (AT2R) are abundantly expressed in immunocompetent cells and involved in cell-mediated inflammatory injury, it appears likely that AT2R may exert their actions through interfering with CD4⁺ T cell-involved inflammatory processes in response to ischemia-induced cardiac injury. We therefore isolated CD4⁺ T cells from peripheral blood of rats with acute myocardial infarction and donors with heart failure (HF) using Ficoll gradient centrifugation and MACS technology. The CD4⁺AT2R⁺ and CD4⁺AT2R⁻ T cell populations were further purified by FACS sorting. The purity of isolated cells and the expression of AT2R and various cytokines were confirmed using FACS analysis, cyto-spin staining and RT-PCR methods. To study the role of AT2R on cytokine production, the CD4⁺AT2R⁺ and CD4⁺AT2R⁻ T cell were treated with AT2R agonist (angiotensin II) in combination with AT2R antagonist PD 123319 (PD). Based on this, we defined the CD4⁺AT2R⁺ T cell subpopulation in the peripheral blood of rats and humans. These blood derived CD4⁺AT2R⁺ T cells were characterized by upregulated expression of the transcription factor forkhead box protein FOXP3 and various cytokines (anti- and proinflammatory). In addition, AT2R activation enhanced production of the anti-inflammatory cytokine IL-10 in the CD4⁺AT2R⁺ T cells, but not in the CD4⁺AT2R⁻ T cells. Furthermore, intramyocardial injection of MI-induced splenic CD4⁺ATR⁺ T cells into recipient rats with MI led to reduced infarct size and improved cardiac performance. This study suggests a novel AT2R-mediated cellular mechanism via the CD4⁺AT2R⁺ T cell subpopulation in suppressing inflammatory injury in the heart. The CD4⁺AT2R⁺ T cells is a promising population for regenerative therapy, *via* myocardial transplantation, pharmacological ATR activation, or a combination thereof.

Table of contents

Abbreviations	5
Zusammenfassung	3
Summary.....	5
Table of contents	6
1 Introduction	9
1.1 Heart diseases.....	9
1.1.1 Myocardial infarction.....	9
1.1.2 Heart failure – as a main consequence of coronary heart disease	11
1.2 After myocardial infarction – the healing process	14
1.2.1 From inflammatory response to the cell death	14
1.2.2 Proliferative phase.....	19
1.2.3 Maturation phase	19
1.3 The Renin-Angiotensin System (RAS).....	19
1.3.1 The classical circulating RAS. The angiotensin II.....	20
1.3.2 The local RAS in the heart.	22
1.4 Immunological aspects following MI. Cross-talk between RAS and regulatory T cells	23
2 Aim of the study	26
3 Materials and Methods.....	27
3.1 Materials.....	27
3.1.1 Devices	27
3.1.2 Plastic ware and other accessories	27
3.1.3 Chemicals	28
3.1.4 Enzymes	30
3.1.5 Kits	30
3.1.6 Antibodies	30
3.1.7 PCR primers	31
3.1.8 Media and buffers	32
3.1.9 Software	34

3.2 Methods.....	34
3.2.1 Induction of myocardial infarction (MI)	34
3.2.2 Human peripheral blood involved in <i>in vitro</i> experiments	35
3.2.3 Isolation of human/rat blood and rat spleen CD4 + T cells	35
3.2.4 Sorting of CD4+AT2R+ and CD4+AT2R- T cells.....	37
3.2.5 Cell culture of blood sorted cells	38
3.2.6 Extracellular staining for flow cytometry	38
3.2.7 Intracellular staining for flow cytometry analysis	39
3.2.8 Total RNA isolation and quantitative real-time PCR	40
3.2.9 Immunofluorescence staining	42
3.2.10 Preparation of donor CD4+AT2R+ T cells and intramyocardial transplantation	43
3.2.11 Left ventricular catheterization – pressure/volume-loop	43
3.2.12 Quantitative estimation of collagen density	44
3.2.13 Quantitative estimation of infarction size	44
3.2.14 Methods for the detection of the transplanted T cells.....	44
3.2.15 Statistical analysis	45
4 Results – Part I / human	47
4.1 The baseline characteristic of patients with heart failure.....	47
4.2 Identification of the CD4+ATR+ T-cells in human peripheral blood	48
4.3 Characterization of human blood CD4+AT2R+ T cells	53
5 Results – Part II / Rats.....	57
5.1 Identification of CD4+AT2R+ T cells in a rat MI model	57
5.2 The CD4+AT2R+ T cells as immunoregulatory players – <i>in vitro</i>	59
5.3 Cardioprotective role of CD4+AT2R+ T cells - <i>in vivo</i>	60
5.3.1 Transplanted T cells were successfully detected in the heart of recipient rats	60
5.3.2 Injection of the CD4+AT2R+ T cells effectively improves cardiac performance.....	62
5.3.3 Transplanted CD4+AT2R+ T cells ameliorate cardiac remodeling	64
6 Discussion.....	68
7 Conclusion.....	72

Financial support	73
Acknowledgements	74
References.....	77
Appendices.....	89

1 Introduction

1.1 Heart diseases

On the basis of “*the 2012 report on European Cardiovascular Disease statistics*”, diseases of the heart and circulatory system, known as cardiovascular diseases or CVD belong to the main health problem in Europe. Each year, CVD cause over 4 million deaths, reaching nearly half (47%) of all deaths (1). Thereby, the main forms of CVD are coronary heart disease (CHD) and stroke.

Among the group of CHD, there are myocardial infarction, stable angina pectoris, unstable angina pectoris, heart failure and sudden death. The following section provides an overview of coronary heart disease: *myocardial infarction* and one of its consequences: *heart failure*.

1.1.1 Myocardial infarction

Myocardial infarction (MI) is a coronary heart disease leading to myocardial necrosis due to significant and succeeding ischemia. Coronary arteries supply heart muscles with blood and oxygen. The most common etiological factor, which is responsible for MI, atherosclerotic plaque, known also as *atheroma*, consists of fatty deposits i.e. cholesterol, cells like macrophages, blood cells and some amount of connective tissue (Fig.1.1). The size/development of MI depends on plaque erosion, which happens due to the activity of metalloproteases, resulting in the thinning of the plaque. Nevertheless, by exposition of the basement membrane, it additionally initiates platelet accumulation, thrombus formation and differing degrees of vasospasm. An acute reduction of blood flow occurs, leading to an imbalance in oxygen supply and metabolic demand of myocardial cells. Such a disproportional state depends on various factors, which contribute to the irregularity of oxygen and nutrient supply, therefore causing cell death. The frequency of contractility, stress of the left ventricle (LV), and ionotropic state of myocytes are the most influencing, oxygen consumers. Myocyte death, after the ischemia onset,

takes usually a finite period to develop, in some animal models less than 20 minutes. For complete necrosis of all myocardial cells, at least 2-4 hours or longer are required, but this depends on coronary arterial occlusion, the sensitivity of the cardiomyocytes to ischemia, and/or oxygen and nutrients require. Usually several hours after myocardial necrosis, post-mortem examination of the MI size, macroscopically or microscopically is possible. MI can be classified by size: microscopic (focal necrosis), small (<10% of the LV myocardium), moderate (10-30% of the LV myocardium), and large (> 30% of the LV myocardium), and by location (2)(3)(4).

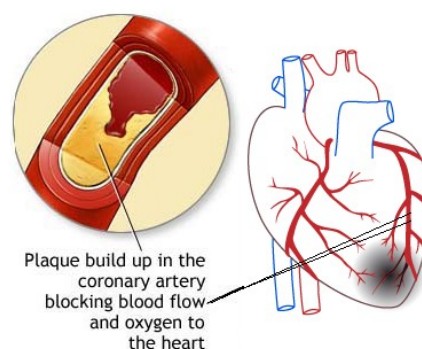


Fig.1.1: Injured heart tissue caused by formation of the plaque (modified from <http://medical-surgical-nursing.blogspot.com/>)

Myocardial infarction can be also defined pathologically (acute, healing or healed) and clinically (Tab. 1.1 types 1-5). Acute MI happens when polymorphonuclear leucocytes are present, and time needed between the onset of the infarction and death is quite fast (6h). The phase of cell infiltration can continue for up to 7 days if coronary perfusion does not increase and / or myocardial demand does not decrease. A healing infarction is characterized by the presence of mononuclear cells and fibroblasts, but polymorphonuclear cells are absent. At least 5-6 weeks are required from the healing phase until the phase of scar tissue formation, without cellular infiltration, leading to healed infarction. Clinically, the various types of myocardial infarction can be classified as shown in Tab. 1.1 (4-6)

Class	Description
<i>Type 1</i>	Spontaneous myocardial infarction related to ischemia due to a primary coronary event: plaque erosion and /or rupture, fissuring, or dissection
<i>Type 2</i>	Myocardial infarction secondary to ischemia due to either increased oxygen demand or decreased supply: coronary artery spasm, coronary embolism, anaemia, hypertension, or hypotension
<i>Type 3</i>	Sudden unexpected cardiac death, with symptoms of suggestive myocardial ischemia accompanied with a new ST elevation, or evidence of fresh thrombus in coronary artery by angiography and/or autopsy, but death occurring before blood samples could be obtained, or at a time before the appearance of cardiac biomarkers in the blood
<i>Type 4a</i>	Myocardial infarction with percutaneous coronary intervention (PCI)
<i>Type 4b</i>	Myocardial infarction documented by stent thrombosis as documented at autopsy and/or by angiography
<i>Type 5</i>	Myocardial infarction associated with coronary artery bypass graft surgery (CABG)

Tab. 1.1 Clinically classification of different types of myocardial infarction, adapted from (5)

1.1.2 Heart failure – as a main consequence of coronary heart disease

Heart failure (HF) is a complex, clinical syndrome, caused either by structural (myopathy) or functional heart disruption. The main causes for this disorder in 54-75% patients are coronary heart diseases (e.g. MI), followed by hypertension in 35-52% of patients, and further in 9-20% patients with isolated hypertension and 18-28% cases with idiopathic cardiomyopathy. Heart failure begins when an index event produces an initial decline in pumping capacity of the heart (7). Thereafter, a variety of compensatory mechanisms are activated, including the adrenergic nervous system (8), the renin-

angiotensin system (RAS) and the cytokine system. These systems are able to restore cardiac function to normal homeostatic range, in consequence, the patient remains *asymptomatic*. With time, for a period of years, the sustained activation of these systems can lead to secondary end-organ damage within the ventricle, thereby causing a worsening in cardiovascular functions, here collectively referred to as LV remodeling. These patients undergo the transition from *asymptomatic* to *symptomatic* heart failure (9). From the clinical point of view, there are some characteristic symptoms which are helpful in the diagnosis of this complex syndrome: breathless, ankle swelling and fatigue, and as the characteristic signs of congestion of systemic veins: peripheral oedema, a raised venous pressure, hepatomegaly. Further, cardiac dysfunctions e.g. decrease of the ejection fraction, increase of the ventricle dimension, abnormal diastolic flow pattern, or LV remodelling, and finally increase of the diastolic filling pressure are other signs being involved in the examination of HF. Heart failure considered as a syndrome, is not a single diagnosis, but it needs multiply-steps of examination with respect to various characteristics, or classifications to define the specific kind of heart failure, which is closest to the real picture of the heart disease, from which the patient is suffering. Therefore, beside a simple classification as acute or chronic heart failure, a more specific classification exists with respect to cardiac dysfunctions: *systolic* and *diastolic*, which describe the principal mechanisms mostly used in the clinical practice.

Systolic dysfunction means that the echocardiographically measured ejection fraction value of the left ventricle (LVEF) is less than 40%. With so-called systolic “forward” failure, blood pressure and peripheral vasoconstriction decrease. Following baroreflex activation, which stimulates alpha- and beta-receptors, the RAS is activated with sodium and water retention, and oedema formation. Due to the volume backlog, as result of the systolic dysfunction, the venous afterload increases and leads to further diastolic dysfunction (Fig. 1.2).

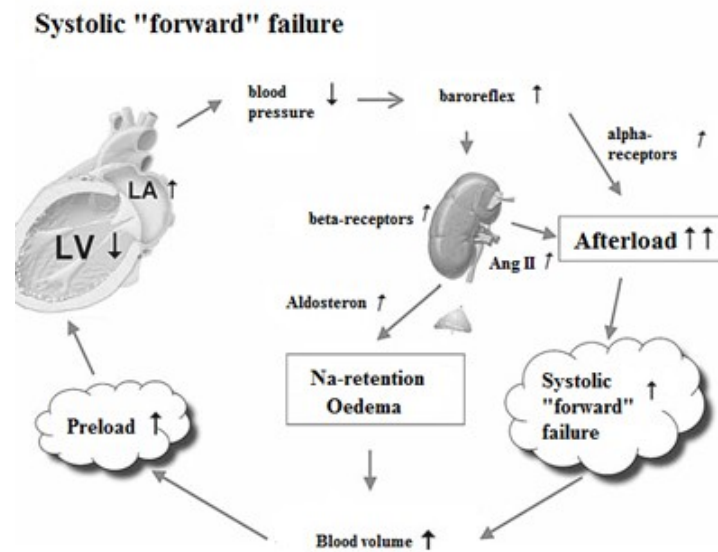


Fig. 1.2: Demonstration of systolic “forward” failure, modified from (10)

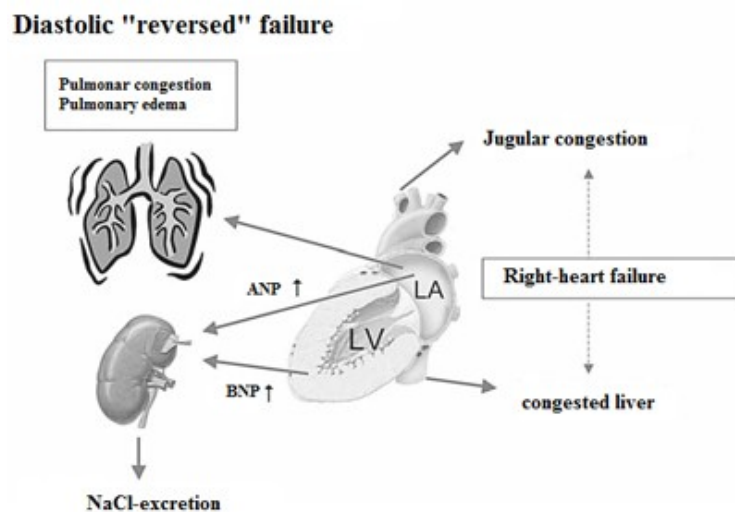


Fig. 1.3: Demonstration of diastolic “backward” failure, modified from Weber and Hermann-Lingen, 2008 (10)

Diastolic dysfunction is characterized by “backward” failure - even if values of LVEF (%) are preserved and coincide with normal range (50% or more), the diagnosis of heart failure is accepted. The structure of the myocardium is an essential factor for the diastolic features. For instance, when the connective tissue increases after myocardial infarction, this leads to a decrease in the myocardial elasticity and an increase in the filling pressure, thereby inducing the pulmonary congestion. Besides that, patients can

suffer from impaired breathing and/or pulmonary edema. In the left atrium, atrial natriuretic peptides (ANP) are released in larger amounts. Hereinafter, it collectively leads to right heart failure with peripheral edema and hepatomegaly (here: the abnormal enlargement of the liver) (Fig. 1.3)(10–15). Following that, it is classified with respect to its severity in accordance to The New York Heart Association classification (15) (NYHA classes I-IV):

- I. *Class I*. No limitation: ordinary physical exercise does not cause an inappropriate fatigue, dyspnoea or palpitations.
- II. *Class II*. Slight limitation of physical activity: comfortable at rest but ordinary activity results in fatigue, palpitations or dyspnoea.
- III. *Class III*. Marked limitation of physical activity: comfortable at rest but less than ordinary activity results in symptoms.
- IV. *Class IV*. Unable to carry out any physical activity without discomfort: symptoms of heart failure are present even at rest with increased discomfort with any physical activity.

1.2 After myocardial infarction – the healing process

1.2.1 From inflammatory response to the cell death

Myocardial infarction is associated with an *inflammatory response*, which is a prerequisite for healing and scar formation. The fact that injury causes inflammation (phlogosis) was recorded in medical literature by Galen at the beginning of the first millennium. There are several mechanisms by which injury can cause inflammation. One of the main causes is cell death. By prolonged ischemia, as a major influent of myocardial infarction, myocardial cells are not sufficiently supplied with oxygen and nutrients, and therefore are more predestined to damage and further death. There are two types of cell death: *necrosis* (oncosis) and *apoptosis*. Cells undergoing necrosis lose membrane integrity and leak their intracellular components, some of which serve as danger signals which stimulate inflammation. Necrotic cell death occurs, in response to some insults such as: trauma, infarction (as a result of prolonged ischemia) or toxins. In general, the pathological processes are responsible for necrosis. In contrast, apoptotic cell death is in majority a consequence of the physiological events (e.g., loss of trophic factors, elimi-

nation of cells during normal developmental processes, etc.) or in some cases pathological events like viral infections (16). The size of apoptotic cells seems to be smaller, but the integrity of their plasma membrane is still, at least in the very beginning, maintained. While necrotic cell death is influencing the host inflammatory response, apoptotic cells are reacting differently. The maintained integrity of the plasma membrane in apoptotic cells protects against any secretion of pro-inflammatory agents (these intracellular components). Contrastingly, these intracellular contents are released from necrotic cells. In the apoptotic process of the cell death, it does take time before such components are released. Firstly, apoptotic cells are ingested by resident phagocytes, which secrete anti-inflammatory cytokines such as interleukin-10 (IL-10) or transforming growth factor – beta (TGF- β) which are then responsible for inhibition of any inflammatory response. Apoptotic cells can transition into secondary necrosis, and start to release intracellular compartments, only when the phagocytic clearance does not appear on time (17).

The released subcellular membrane compartments are rich of mitochondria, which inclusively trigger early acting components: C1, C2, C3, C4 of the complement cascade. There is a wealth of information that mRNA and proteins for all of such components are upregulated in areas of myocardial infarcts. Moreover, activation of the complement cascade can induce infiltration of neutrophils and monocytes to the site of injured myocardium. Complement – mediated cascade may lead to leukocyte chemotactic activity as in post-ischemic cardiac lymph during the first hours of reperfusion and within the next 3 hours observed (18). Furthermore, the evidence in the whole attribution to C5a complement in cardiac lymph and blocking of the individual complement e.g. C5 by use of antibody-induced inhibition showed, that the activated complement cascade plays a role in the initiation of the *humoral* inflammatory response, particularly during the first hours of reperfusion.

In post-ischemic myocardium, many cellular mechanisms are involved. *Reactive oxygen species* (ROS) are counted among factors which in the ischemic/reperfused heart can lead to a deleterious cascade of reactions, so that further myocardial dysfunction and/or cytotoxicity are not to overcome. These molecules with unpaired electrons in their outer orbit, in normally functioning heart, are transformed as intermediate from approximately 5% of the oxygen consumed by tissue, and properly detoxified by enzy-

matic free radical scavengers (such as superoxidase dismutase, glutathione peroxidase, and catalase) or through intracellular antioxidants. At the ischemic/reperfused state or during inflammation, their exaggerated production and due to the lacking amount of oxygen, leads to the attenuating detoxification process and therefore this initiates harmful radical-mediated reactions. There are plenty of factors, which participate in the generation of the reactive oxygen species. During inflammatory response, an additional rise in the infiltration of circulating blood cells (e.g. leukocytes, platelets) and interaction of other cell types (here e.g. coronary endothelial cell and cardiac myocytes), and/or activation of cytokine cascades, induce excess in the generation of ROS. Necrotic cell death, by realising various mitochondrial, sarcoplasmic reticulum and sarcolemma compartments, targets ROS and causes myocardial dysfunction. In vitro investigations have shown that such free radicals lead to impaired functionality of the isolated mitochondria, resulting in adenosine (ATP) depletion and induction of Ca^{2+} -overload (19)(20)(21).

The elevated level of free radicals, and secretion of cytokines such as tumour necrosis factor-alpha (TNF- α) and interleukine 1-beta (IL-1 β) in myocardial infarction activates *NF- κ B* family of transcription factors. Thereafter, these induce various genes responsible for inflammatory response, cell adhesion and growth control. It has been reported that the activation of NF- κ B can mediate an injurious, but also cytoprotective response (22)(23). An inflammatory response can be demonstrated by an upregulation of various cytokines, secreted either by resident or circulating blood-derived cells. Besides of TNF- α and IL-1 cytokines which are involved in the inflammatory response, IL-6 level increase in the post-ischemic heart.

TNF- α . Release of this cytokine occurs rapidly in the central ischemic zone during infarction (at maximum in the border zone), acting on several cell types such as leukocytes, endothelial cells, fibroblasts and cardiac myocytes. It was reported that within 30 minutes after direct hemodynamic stretch, *de novo* intramyocardial production of TNF- α occurs. Furthermore, hydrogen peroxidase (H_2O_2) can activate TNF- α production via p38 mitogen-activated protein kinase (MAPK) followed by myocardial dysfunction and apoptosis. A possible role in the postinfarction inflammatory response may be clarified by a model of TNF- α deficient mice with induced myocardial infarction, where its absence was manifested by decreased expression of chemokines and adhesion

molecules. An elevated level of this cytokine may return to baseline, if the size of infarction reveals as small, but if inflammatory response and/or infarction tend to be large, an exuberant TNF- α production, predominantly in correlation with enhanced angiotensin II type 1 receptor (AT1R) expression, activates local matrix metalloproteinases (e.g. MMP) in the infarct area and increases natriuretic peptides (ANP, BNP) and collagen expression in the non-infarcted tissue(24)(25).

IL-6. All IL-6-related cytokines function through multisubunit receptors that share the transmembrane glycoprotein (gp)130. In the post-ischemic myocardium, the synthesis of these inflammatory cytokines is activated in mononuclear cells and cardiac myocytes. While one member of the IL-6 family, cardiotrophin-1 (CT-1) exhibits its functions in cardiac myocytes by an induction of hypertrophy, as by Pennica and coworkers (1995) discovered, IL-6 does not exert such a function, due to a rare presence of the IL-6 receptors on cardiomyocytes (26). Interestingly, this function was activated, when a soluble form of IL-6 (sIL-6) was present, at least *in vitro* (27). Nian et al. (2004) (28) demonstrated that beside the ischemic stress, the mechanical stretch of the myocardium can markedly stimulate cytokine production. Through a rapid induction of phosphorylation, here the activation of gp130 and STAT3 in cardiomyocyte culture, evidently showed, that IL-6-related cytokines act through the STAT3 pathway. Furthermore, the neutralizing TNF- α function, partly inhibited IL-6 upregulation suggesting an important role for TNF- α as the upstream cytokine inducer. Cross-talk between the level of TNF- α and IL-6 expression was observed in the ischemic heart after degranulation of mast cells that induced the secretion of TNF- α , and immediately influenced infiltrated mononuclear cells to release IL-6 cytokine. Moreover, in serum of patients suffering from myocardial infarction elevated levels of IL-6 were observed, as well as an increased creatine kinase (CK) activity on the first and third days of the disease, demonstrating a characteristic correlation of both parameters. Additionally, in serum of patients with transmural myocardial infarction (associated with atherosclerosis) the highest level of IL-6 was detected (29).

In the post-ischemic setting, an infiltration of neutrophils occurs and due to their large size and a stiff form, easily reach capillary endothelium where adhere. This step is locally important to amplify the initiated inflammatory response triggered by cytokines (28). The activated neutrophils can induce vasoconstriction and platelet aggregation.

The *cell-mediated inflammatory response* (innate immune response) depends on interaction of leukocytes with endothelial cells, which are usually controlled by adhesion molecules (such as selectins, β_2 -integrins and the immunoglobulin superfamily). One member of the selectin family, is L-selectin (CD62L), which with its broad expression on circulating leukocytes: neutrophils, monocytes, eosynophils, T cells and B cells (30)(28) is able to promote leukocyte attachment and rolling along post-capillary venules. Others, namely P-selectins (CD62P) were found on endothelial cells, and in normal state are stored in Weibel-Palade bodies, but after induction by oxygen radicals, thrombin, complement components, histamine or hydrogen peroxide, translocate to the surface membrane (31). It was stated that 90 minutes after ischemia onset, P-selectins were expressed on endothelial cells. The presence of the third member, E-selectin (CD62E) was observed later, during 4-6 hours of reperfusion (32).

Platelet activating factor (PAF) is one of a large group of factors responsible for β_2 -integrin activation. This integrin family, named also as CD11/CD18 complex, constitutively expressed on neutrophils, is initially stored in granules, but after activation moves to the membrane surface. The rolling process of neutrophils on the endothelium is a result of interaction of those complexes with their counterligand ICAM-1, expressed on endothelial cells. In consequence, the transendothelial migration into the myocardial parenchyma causes further physiological effects, e.g. no-reflow, necrosis (33)(31).

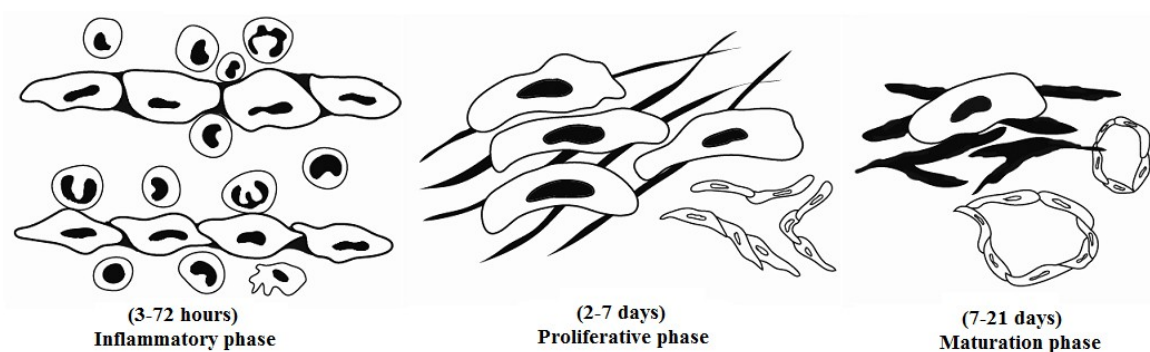


Fig. 1.4 Representative time-schedule of healing in murine myocardial infarction (modified from Nah and Rhee, 2009, (34)). Inflammatory phase is characterized by leukocyte infiltration into injured myocardium with induced cytokine and chemokine cascade, following that proliferative phase introduces, where dead cardiomyocytes are replaced with granulated tissue, including myofibroblast and fibrotic-like cells. Inflammatory reactions are suppressed. Finally, myofibroblasts undergo apoptosis leading to formation of the collagen-based scar.

Above described processes, including an activation of cytokine cascades triggering leukocytes requirement comprehends the *inflammatory phase*. This phase, as one of three known phases, belongs to healing process in myocardial infarction (Fig. 1.4).

1.2.2 Proliferative phase

Acute form of the inflammatory phase is temporarily and its resolution is associated with suppression of cytokine and chemokine cascades, followed by the entire fibrous tissue deposition (35). The myocardial tissue initiates a *proliferative phase*. After two days of reperfusion, fibroblast-like cells and myofibroblasts gather at the border of the infarct zone and contribute to the formation of granulation tissue. Myofibroblasts, due to their activation proliferate and secrete extracellular matrix proteins. For healing, wound oxygen and nutrients are provided from newly formed blood vessels. Myofibroblasts (differentiated fibroblasts) are phenotypically beneficial for injured myocardium, because they possess a contractile apparatus and can partly substitute dead cardiomyocytes, which lost the ability to divide during evolution, and therefore cannot replace themselves (3).

1.2.3 Maturation phase

When the cellular infiltration decreases, it means that the last and third phase of infarct healing, the *maturation phase* begins. During this phase, myofibroblasts undergo apoptosis and neovessels regress, resulting in collagen-based scar formation. The apoptotic processes in the cardiac scar are milder for myofibroblasts than for those of the skin. These modulated fibroblasts are able to stay in their primary form, without entering apoptosis, even up to 17 years after myocardial infarction, as observed in human model (36).

1.3 The Renin-Angiotensin System (RAS)

The renin-angiotensin system (RAS) is a hormonal regulatory system involved in various tissues, such as brain, kidney, adrenal gland, heart, vessels, with a major function in controlling of blood pressure and hypertension and further investigations on its influence on the pathogenesis of cardiovascular diseases are required.

1.3.1 The classical circulating RAS. The angiotensin II

From a historical point of view, this enzyme was discovered 100 years ago by Tigerstedt and Bergman (37). The classical RAS becomes activated with the synthesis of renin in the kidney by juxtaglomerular cells localized in the afferent arteriole. Firstly, as pro-renin it does not carry any known biological functions, but later as an active form (renin) it is released via exocytosis, controlled by renal baroreceptors, sympathetic nervous system, and angiotensin II (AngII). Renin catalytically cleaves angiotensinogen, the most important substrate derived from the liver, to form an inactive, decapeptide, angiotensin I (Ang I). Angiotensinogen controls levels of systemic circulating angiotensin (Ang) peptides. This enzyme is found also in other tissues, including heart, vasculature, kidney and adipose tissues. Furthermore, Ang I is hydrolysed by angiotensin-converting enzyme (ACE) into biological active, octapeptide Ang II. The ACE is mostly localized on plasma membranes of endothelial and neuroepithelial cells (Fig. 1.5). While angiotensinogen and renin possess long half-lives, Ang II is removed from the circulation within few seconds by peptidases, named angiotensinases (38)(39)(40)(41).

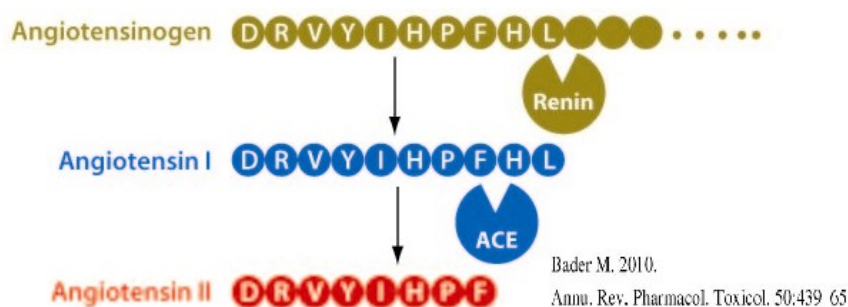


Fig. 1.5 The classical renin-angiotensin system (RAS) and its chemistry (Bader, 2010 (41))

Angiotensin II, the active octapeptide is a major factor of the RAS, and acts through its two G protein-coupled receptors: angiotensin II type 1 (AT1R) and angiotensin II type 2 (AT2R), which are seven transmembrane glycoproteins with only 32-34% homology. Ang II contributes to the regulation of blood pressure through peripheral mechanisms, inducing vasoconstriction by acting of AT1 receptors located on vascular smooth muscle cells, causing sodium retention. Angiotensin II functions via the sympathetic nervous system, and is involved in diverse effects such as proliferation, differenti-

ation, regeneration and apoptosis (42)(43). It is already well known that Ang II activity is mostly AT1R- related. Since the clinical targeting drugs are responsible for the inhibitory effects on the AT1R-mediated functions, which are regarded unfavorable, the AT2R mostly counteracts in such a scenario.

Angiotensin II type 1 receptor (AT1R). The AT1R was found to be expressed predominantly in adults. Whereas in human AT1R is as a single form, rodents possess two (with >95% amino acid sequence homology) isoforms of it: AT1Ra and AT1Rb. The AT1R is expressed, as experiments with the adult rats have shown, on VSMCs, endothelial cells, in the kidney, liver, adrenal gland, ovary, brain, testis, lung, heart and adipose tissues (37). The AT1R is known to mediate most of AngII actions in cardiovascular, renal, neuronal, hepatic manners, and it has been reported that its actions are linked to arterial blood pressure, maintenance of electrolyte and water balance, thirst, hormone secretion, renal functions and cellular growth(44) (45).

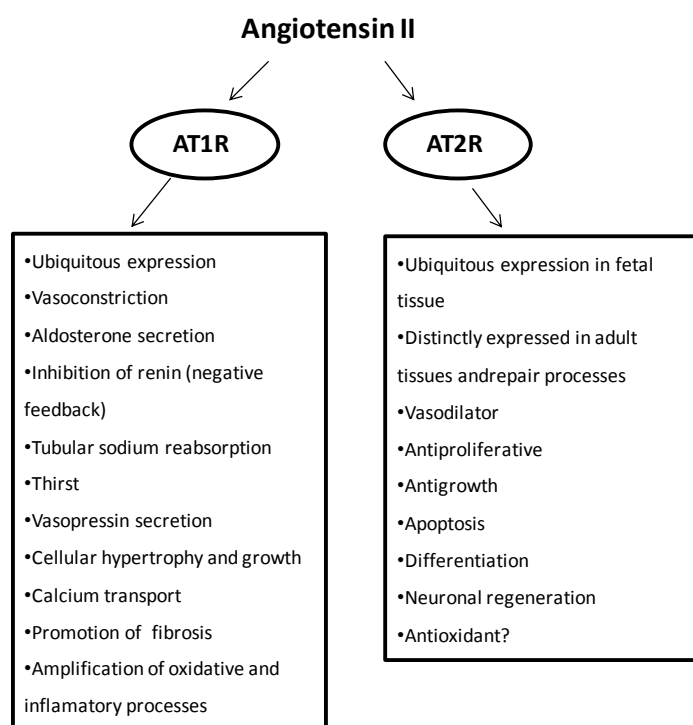


Fig. 1.6 The major hormone of the renin-angiotensin system (RAS) acts through two receptors: AT1R and AT2R, which are expressed in different tissues, and mediate various functions. Schema adapted from Volpe et al. (44)

Angiotensin II type 2 receptor (AT2R). The AT2R expression - compared to the AT1R – is in adults or in cells in cell culture very low, but is upregulated in fetal tissues

(46). The presence of the AT2R after birth is confined to a few organs such as brain, adrenal, heart, vascular endothelium, kidney and ovary. Although the AT1R is dominant in the adult organism, expression of the AT2R increases under pathological conditions as it has been observed during vascular injury (47), myocardial infarction (48)(49), congestive heart failure, renal failure, brain ischemia. Directly after the onset of injury, around 10% of the cardiomyocytes express AT2R, and this level does not change during the next 24hrs, but significantly increases in expression in 60% of the cardiomyocytes at day 7 following MI (49)(50). The AT2R signals via three transduction mechanisms:

- a. The activation of various protein phosphatases (mitogen-activated protein kinase phosphatase 1(MKP-1), SH2 domain containing phosphatase-1 (SHP-1), and protein phosphatase 2A (PP2A)) causing protein dephosphorylation
- b. Activation of the NO/cGMP system (this signal pathway is shared with AT1R, after its activation possible that bradykinin is released)
- c. Stimulation of phospholipase A2 (PLA2) with subsequent release of arachidonic acid (regulation of the intracellular pH level by $\text{Na}^+/\text{HCO}_3^-$ symporter system (NBC))

The AT2R, biologically, is involved in embryonic development, cell differentiation, apoptosis, regulation of renal function and blood pressure. The protective pathway of AT2R might be activated to avoid an overstimulation of AT1R. The AT2R-mediated functions, as well AT1R-dependent are presented in the Fig. 1.6.

1.3.2 The local RAS in the heart.

For many years, it was thought that the circulating RAS is the only one existing system. Further observations in the clinical and experimental situation showed that an application of the ACE inhibitors and Ang II antagonists protected cardiac tissue, but did not block angiotensin II in the circulation (41). After treatment with targeting drugs for RAS, measurement of Ang II levels in the plasma were normal, but blood pressure remained low. This could be due to an accumulation of this octapeptide in different tissues and organs such as the pancreas, liver, intestine, heart, kidney, vasculature, carotid body, and adipose tissue (43). It seems that the concentration of produced Ang II may depend on the amount of precursors and enzymes involved in its biosynthesis. There-

fore, besides the classical RAS, tissue-related RAS is referred to as the *local* RAS. Because the earlier sections referred to coronary heart diseases, this section describes the local renin-angiotensin system in the heart tissue, and an involvement of the RAS components in cardiac manners.

In 1987 Dzau reported about the production of AngII in the heart. One of the components of the RAS, angiotensinogen was found in the whole heart, cultured myocytes and fibroblasts (51). Mast cells, which penetrate the heart tissue, especially after myocardial injury, release renin from their granules (52), but at normal state, the amount of this enzyme reveals to be minimal. Moreover ACE is expressed in cardiac fibroblasts and coronary endothelial cells. Local AngII influences blood flow and harbour ionotropic properties. The crosstalk of Ang II and cardiac sympathetic nerve leads to a release of catecholamine. Locally produced angiotensin II plays an important role in the induction of cardiac hypertrophy and fibrosis, mediated via the AT1R, whereas the AT2R is reported to have an opposite role as already aforementioned. By an activation of ROS production, AT1R can induce cardiac hypertrophy and fibrosis, with an immoderate proliferation of cardiac fibroblasts, and further overloaded deposition of extracellular matrix in the cardiac interstitium (53). In result, it leads to ventricular stiffness and further impairment of diastolic functions. It has been stated that Ang II needs an interaction with cardiomyocytes to induce fibrosis. This evidence may be explained by paracrine effects, via release of TGF- β . Generally, the local RAS is characterized by an interaction between cardiac myocytes and fibroblasts, which then are involved in the progression of cardiac hypertrophy and fibrosis.

1.4 Immunological aspects following MI. Cross-talk between RAS and regulatory T cells

As already mentioned in the chapter „*From inflammatory response to the cell death*“, MI is associated with an immune response. Physiological inflammatory response causes self-repair and protection, while pathological autoimmune response leads to ventricular remodeling and heart failure (54).

A plethora of reports showed that inflammation is a critical factor in the pathogenesis of ventricular remodeling induced by MI (55)(56)(30)(57). At the first phase after myocardial infarction, the innate immunity is activated, leading to cytokines and chemokines

upregulation, and thereafter attracts their *immunological components* which infiltrate into infarcted area. The presence of so-called immunocompetent cells was reported in *in vitro* experiments by Jankowski M et al. (2010) showing the CD4+ and CD8+ T cells infiltration following MI (58). Other evidence of the adaptive immunity was demonstrated in an *in vivo* model, where in 1998 Maisel and associates by an adaptive implantation of the activated splenocytes derived from 6-weeks old MI rats into healthy recipients rats, observed an induced autoimmune myocardial injury (59). Moreover, the examined infarct size of recipients reflected the severity of MI-induced donors as well as exhibited cellular infiltration in the cardiac lesion.

Two years later, Varda-Bloom and coworkers (2000) reported that cultured lymphocytes (defined later as CD8 T lymphocytes using inhibition assay with anti-CD8 antibodies) obtained from MI animals with healthy neonatal cardiomyocytes led to higher cytotoxic activity against myocytes, in comparison to those derived from sham-operated group, however, this activity was to a lesser extent or hardly detectable when cultured with non-myocyte cells. This observation was related to immune-mediated injury, where the cytolytic lymphocytes revealed an autoimmune response to an autoantigen (60). The interest in understanding the role of autoimmune reaction to cardiac proteins in the failing heart was growing over the years. Following MI, a release of contractile proteins such as myosin and actin triggers autoimmune reactions. These previously “hidden” proteins changed in the infarcted milieu, and have been acting as a kind of foreign factors and led to produce antibodies (here functioning as anti-heart) and antigen - sensitized cytotoxic T lymphocytes. It has been shown that the cellular autoimmune reaction to cardiac myosin can be detected in patients with acute myocardial infarction, underlining an involvement of the immune system and its compartments as well (61)(62)(63).

Furthermore, it is well known that immune cells which are attending in the first crosstalk with the present antigens, which have been encountered tissue, can be able to keep an information (memorize it) about foreign entered proteins and during their secondary occurrence are able to react properly, thus preventing the whole organism. These cells have been termed T memory cells.

Noticing the MI as a kind of cellular autoimmune reaction to cardiac myosin, it logically demands to understand which immunocompetent cells play a role in the control of

such deleterious actions. It is well known that T regulatory cells (Treg) play an essential role in maintaining immunological insusceptibility to self-antigens and in suppressing excessive immune responses deleterious to host (64). Sakaguchi and colleagues have shown these cells as a subset of CD4⁺ T cells expressing IL-2 receptor alpha chain (CD25) and a forkhead winged helix family transcription factor (FoxP3) which are capable for immunosuppression, in *in vitro* and *in vivo* (64)(65)(66). Recent observations regarding the fluctuations in numbers or function of naturally occurring Tregs (mainly transcription factor, FoxP3) in autoimmune diseases led to the consensus, that it is consistently necessary to monitor this transcription factor also in other autoimmune-like phenomena, such as MI (67) (68). Combining the mentioned issues, researchers were intensively seeking for the interplay between adaptive immune response, T cells, T regulatory cells and the actions of major peptide of RAS, angiotensin II. Thereby, Guzik et al.(2009) (69) have shown that upon long-term infusion of AngII in mice, the number of peripheral blood T lymphocytes was increased. Kvakani et al. (70) observed a beneficial role of naturally occurring T regulatory cells after adoptive transfer into AngII-induced inflamed mice exhibiting cardiac damage. Additionally, the preventive role of post-MI activated AT2R-expressing CD8⁺ T cells secreting IL-10 has been reported by our group with the exception that only post-MI activated AT2R-expressing CD8⁺ T cells, which secreted IL-10 reduced the infarction size in MI recipient rats (71). This cell population reduced the infarction size in MI recipient rats.

2 Aim of the study

To clarify the inflammatory mechanisms following MI and the activation of RAS, following issues were questioned and should be discussed in the present study:

- Identification and characterization of the AT2 receptor within the immune cells (CD4) in two species (human, rat) and under different pathophysiological conditions (heart failure, myocardial infarction).
- Functional evaluation and therapeutic, regulatory benefits of AT2-expressing CD4 T cell subset after their intramyocardial injection in rat MI model.

3 Materials and Methods

3.1 Materials

3.1.1 Devices

Mini and QuadroMACS™ Separators	Miltenyi Biotec, Germany
MultiStand	Miltenyi Biotec
MJ Mini™ Personal Thermal Cycler	Bio-Rad, Germany
IKA – Sheaker MTS2	Fritz Gössner GmbH, Germany
FACS LSRII cytometer	Becton Dickinson, Germany
FACS Aria® sorter	Becton Dickinson
BD FACSCalibur® cytometer	Becton Dickinson
Leica DMIL, contrast microscope	Leica, Germany
Leica DMLB, fluorescence microscope	Leica
LSM 780 ELYRA PS.1, confocal microscope	Carl Zeiss , Germany
Leica Z6 APO light microscope, with DFC camera	Leica
Millar Instruments MPVS-300	FMI Foehr Medical Instruments GmbH, Germany
Syringe pump	MLW, Germany
Ventilator, SAR-830/P	IITC INC., USA
MxP Stratagene 3000™ QPCR System	Stratagene, USA
Balance CP324S	Sartorius AG, Germany
Vortex-Genie® 2	Scientific Industries, Inc., USA
Centrifuge 5417R	Eppendorf, Germany
Multifuge 1 S-R Heraeus	Thermo Scientific, Germany
Incubator BBD 6220, Heraeus	Thermo Scientific
NanoDrop™ 1000	Thermo Scientific NanoDrop Products, USA
Shandon cytospin 3 cytocentrifuge	Thermo Fisher
Safe Flow 1.2 Nunc™	Nunc, Germany
Cryostat	Leica

3.1.2 Plastic ware and other accessories

Nalgene Syringe Filter, 0.2µm	Thermo Scientific
Prolene suture: 5.0, 6.0 sizes	Ethicon, LLC, USA

Steritop™, vacuum bottle top filter, 0.22µm	Millipore, USA
Microscope slides, HistoBond®	Menzel Glaeser GmbH & Co. KG, Germany
Menzel Glaeser Superfrost® Plus	Thermo Scientific
Coverslips: 24x50mm, 22x22mm	Thermo Scientific
Neubauer Chamber, Hemacytometer	Marienfeld GmbH, Germany
Menzel Glaeser Superfrost® Plus	Thermo Scientific
Prolene 5.0 and 6.0 size	Ethicon, LLC, USA
Celstar® Tubes: 50ml, 15ml	greiner bio-one, Germany
Serum and serological pipettes, sterile	greiner bio-one
Rat Heart slicer matrix, model HSR001-1	Zivic Instruments, USA
60mm Petri dishes	greiner bio-one
96-well U-bottom	Sarstedt AG, Germany
MS, LS Columns	Miltenyi Biotec
BD 5ml falcons (with cap), sterile	Becton Dickinson
MACS pre-separation filters, 30µm	Miltenyi Biotec
Cell strainer: 100µm, 70µm, 40µm	Becton Dickinson
Syringe: 5ml, 10ml, 20ml	Becton Dickinson
Omnican® 50 syringe	B. Braun AG, Germany
Vasofix® Safety catheter with injection port, 18G x 1¾"	Becton Dickinson
Filtertips RNase/DNase free: 10µl, 20µl, 1000µl	Nerbe Plus, Germany
K-EDTA Tubes	Sarstedt AG
Millar Pressure-Volume Catheter, size 2.0 F, length 30cm, MIL-SPR-838	Foehr Medical Instruments GmbH

3.1.3 Chemicals

Novamin - Sulfon, 500mg/ml	Ratiopharm GmbH, Germany
PBS (phosphate buffered saline), without magnesium and calcium	PAA Laboratories GmbH, Germany
Ethylenediaminetetraacetic acid (EDTA)	Sigma, Germany
Bovine Serum Albumin (BSA)	Sigma
Ammonium chloride (NH ₄ Cl)	Sigma
Potassium bicarbonate (KHCO ₃)	Sigma
Sodium phosphate dibasic (Na ₂ HPO ₄)	Sigma

Sodium phosphate monobasic (NaH ₂ PO ₄)	Sigma
Potassium dihydrogen phosphate (KH ₂ PO ₄)	Merck, Germany
Sodium chloride (NaCl)	Roth, Germany
Potassium chloride (KCl)	Merck
Sucrose	Sigma
Magnesium chloride-Hexahydrate (MgCl ₂ x 6 H ₂ O)	Serva, Germany
Glycine, ACS Reagent	Sigma
Penicillin/Streptomycin	Gibco, USA
Paraformaldehyde (PFA), powder	Sigma
Formaldehyde, 37%	Roth
Fetal Bovine Serum (FBS, inactivated)	Gibco
4',6-diamidino-2-phenylindole, dihydrochloride (DAPI)	Molecular Probes , USA
Fluorosave™ Reagent	Calbiochem, USA
VECTASHIELD® Mounting medium with DAPI	Vector Laboratories, Inc., USA
FixoGum Rubber cement	Maruba GmbH & Co. KG, Germany
IGEPAL®	Sigma
Ethanol	Sigma
Isopropanol	J.K. Baker, Germany
Hydrochloric acid (HCl)	Sigma
Acetic acid, glacial	J.K. Baker
Chloroform	Sigma
DEPC-treated water	Ambion, USA
Nuclease-free water	Ambion
RNaseZAP®	Ambion
Trizol® Reagent	Invitrogen, Germany
BD Perm/Wash™ buffer (10X)	Becton Dickinson, Germany
Donkey serum	Sigma
Random primers	Promega Corporation
RNase Inhibitor	Promega Corporation
Oligo dNTPs	Promega Corporation
SYBR Green® Power universal Master Mix (2X)	Applied Biosystem, Germany
Angiotensin II	Sigma
PD123319	Tocris Bioscience, Germany

Fast Green FCF	Sigma
Sirius Red	Division Chroma, Germany
Dobutamine	Sigma
Ketamine/Xylazine	Sigma
Phorbol-12-myristate-13-acetate (PMA)	Calbiochem
Ionomycin	Calbiochem
Monensin	eBioscience, Germany
Trypsin	PAN Biotech, Germany
Tissue Tek O.C.T.	Sakura Finetek Europe B.V., the Netherlands
Pertex [®] mounting medium for histology	Medite GmbH, Germany
Protein Block serum-free	Dako, Denmark
Antibody diluent	Dako
Vybrant [™] Cell-labeling solutions	Molecular Probes
BD FACS Flow [™]	Becton Dickinson

3.1.4 Enzymes

Collagenase Type 2, CLS 2	Worthington, USA
Pepsin from porcine gastric mucosa	Sigma
SuperScript [®] II Reverse Transcriptase (10.000U/μl)	Invitrogen

3.1.5 Kits

PicoPure [™] RNA Isolation kit	Arcturus, Germany
DNase Digestion kit	Promega Corporation, USA
M-MLV Transcription kit	Promega Corporation
Rat IDetect [™] Chromosome Y FISH Paint Probe, RED	Cambio Ltd, United Kingdom
RNase Inhibitor	Promega Corporation

3.1.6 Antibodies

Primary Ab	Clone	Company	Staining
CD4-PE	SK3	eBioscience	E
AT2R rabbit polyclonal	H-143	Santa Cruz Biotechnology	E
AT2R goat polyclonal	C-18	Santa Cruz Biotechnology	E
IL-2 APC	MQ1-17H12	eBioscience	I
IL-10 eFluor 450	JES3-9D7	eBioscience	I

IL-4 Pe-Cy7	8D4-8	eBioscience	I
IFN-gamma APC	B27	Becton Dickinson	I
IL-6 PE	MQ2-13A5	Becton Dickinson	I
CD4 PerCP	SK3	Becton Dickinson	E
IFN-gamma APC	25723.11	Becton Dickinson	I
CD44 eFluor450	IM7	eBioscience	E
CD62L PeCy7	DREG-56	eBioscience	E

Fig. 3.1. Primary antibodies used for cytometry analysis of human samples (EU SICA Study); E: extracellular, I: intracellular

Secondary Ab	Company
Alexa Fluor 488 [®] donkey anti-rabbit IgG (H+L)	Molecular Probes
donkey anti-goat IgG (H+L) – APC	R&D Systems
donkey anti-rabbit IgG – PE	Santa Cruz Biotechnology

Fig. 3.2. Secondary antibodies used for cytometry analysis of human samples (EU Study)

3.1.7 PCR primers

Primers were purchased from Tib-MolBiol (Berlin, Germany)

Gene	Real –Time PCR primer sequence (5' → 3')
AT2R	Forward: AATATGAAGGGCAACTCCAC Reverse: TTAAGACACAAAGGTCTCCAT
18s	Forward: CCTGAGAAACGGCTACCACAT Reverse: TTCCAATTACAGGGCCTCGA

Fig. 3.3. Human Sybr Green[™] Real-Time PCR primers

Gene	Real –Time PCR primer sequences (5' → 3')
AT2R	Forward: AATCCCTGGCAAGCATCTTATGT Reverse: CGGAAATAAAATGTTGGCAATG
IL-6	Forward: ATATGTTCTCAGGGAGATCTTGGAA Reverse: AGTGCATCATCGCTGTTTCATACA
IL-10	Forward: AAGGCAGTGGAGCAGGTGAA Reverse: CGTAGGCTTCTATGCAGTTGATGA

β -actin	Forward: ATCGCTGACAGGATGCAGAAG Reverse: CGCTCAGGAGGAGCAATGAT
----------------	---

Fig. 3.4. Rat Sybr Green™ Real-Time PCR primers

3.1.8 Media and buffers

Aliquots of phosphate buffered saline were autoclaved before use. All prepared media and buffers were sterile filtered with available 0.2 μ m filters.

PBS/2mM EDTA buffer	0.744g EDTA ad 1L PBS (1X)
PBS/2mM EDTA/0.5% BSA (MACS Buffer)	0.744g EDTA 5g BSA ad 1L PBS (1X)
PBS/ 0.5% BSA buffer	2.5g BSA Ad 500ml PBS (1X)
Erythrocyte Lysis Buffer	1.0 g KHCO ₃ 8.3g NH ₄ Cl 0.00372g EDTA adjust pH to 7.5 ad 1L Aqua dest
Cell culture medium for lymphocytes: (RPMI 1640/10% FBS/1%P/S)	50ml FBS 5ml Pen/Strep in 500ml RPMI 1640
Cell culture medium for myocytes isolation: (DMEM/1%P/S)	5ml Pen/Strep in 500ml DMEM medium

Fig. 3.5. Overview of prepared media and buffers

Dulbecco's modified medium Eagle medium (DMEM) (with 4.5g/l glucose, L-glutamine) sterile	PAN Biotech GmbH, Germany
Roswell Park Memorial Institute 1640 (RPMI 1640) (with L-glutamine), sterile	PAA Laboratories GmbH
Lymphocyte Separation Medium (LSM, 1077 g/l)	PAA Laboratories GmbH

10% Formalin, neutral buffered (~31ml)	3.125ml Formaldehyde 37% 28.125ml DEPC –treated water 0.125g NaH ₂ PO ₄ 0.203g Na ₂ HPO ₄
1M glycine	7.5g glycine 80ml Aqua dest Adjust to pH 8.5 and fill up to 100ml, sterile filter 0.2µm
1M MgCl ₂	20.3g MgCl ₂ x 6H ₂ O ad Aqua dest to 100ml autoclave to sterilize
10X Phosphate buffered saline (PBS 10X)	2.0g NaCl 0.05g KCl 0.36g Na ₂ HPO ₄ 0.06g KH ₂ PO ₄ Fill up to 25ml with DEPC-treated water
1X PBS	5ml 10X PBS Fill up to 50ml with DEPC-treated water
2.5% Formaldehyde	2.5ml 10% Formalin, neutral buffered 7.4ml 1X PBS (in DEPC-treated water) 0.5ml 1M MgCl ₂
2X SSC buffer, pH 7.0	0.5ml 20X SSC ad 4.5ml DEPC-treated water, adjust pH to 7.0
“2X” Solution (2X SSC/0.1% IGEPAL)	5ml 20X SSC buffer 45ml DEPC-treated water 0.050ml IGEPAL [®]
“0.4X” Solution (0.4X SSC/0.3%IGEPAL)	0.4 20X SSC buffer 19.6 DEPC-treated water 0.060ml IGEPAL [®]
0.005% Pepsin Working solution	0.5ml 1N HCl 49.5ml DEPC-treated water Warm up to 37°C and ad 25µl 10% Pepsin

Fig. 3.6. Overview of prepared buffers for fluorescence *in situ* hybridization (FISH)

3.1.9 Software

IOX 1.8.3.20 software	Emka technologies, France
BD FACS Diva software	Becton Dickinson
BD CellQuest Pro [®]	Becton Dickinson
Adobe Photoshop CS	Adobe Systems Inc., USA
Software ZEN 2010 D	Carl Zeiss AG
Image J, Java image processing programme	Research Services Branch (RSB), USA
ABI Prism 7000 software	Applied Biosystems
AxioVision LE Rel. 4.5 software	Carl Zeiss AG
WinMDI (Windows Multiple Document Interface for Flow Cytometry)	The Scripps Research Institute, USA

3.2 Methods

3.2.1 Induction of myocardial infarction (MI)

For the animal experiments, we used male Wistar rats (177-200g, Charles River Laboratories, Germany). Animals were kept under standardized conditions (temperature, humidity) and housed in the 12-hour light/12-hour dark cycle with food and water *ad libitum*. All experiments were performed according to the state regulations and approved by the responsible authorities of *Landesamt für Landwirtschaft, Lebensmittelssicherheit und Fischerei Mecklenburg-Vorpommern*. Myocardial infarction in the rats was surgically induced by ligation of the left anterior descending coronary artery (LAD) as described (71–73). After anesthesia with ketamine/xylazine (80mg/10mg/kg body weight, intraperitoneally), rats were intubated and connected to a small-animal ventilator. After opening the chest, the heart was carefully cleaned with the tap with saline and the ligation using a suture (size 6.0) was performed. For the sham-operated (Sham-OP) group of animals, all steps were included besides the ligation. Only for animals which underwent the LAD ligation, 15 drops of Novamin-Sulfon were given to 300ml of water per day. Seven days after MI induction or Sham-OP, rats were sacrificed and blood from the periphery of the hearts was collected in a syringe coated with PBS/2mM EDTA, and hearts and spleens were excised. For transplantation experiments, the recipient female rats were subjected to the same standardized method for MI

induction, as described above. Randomly taken MI recipient rats were subdivided into three groups which obtained as follows either saline (as control group) or CD4+AT2R+/- T cells (as cell therapy group).

3.2.2 Human peripheral blood involved in *in vitro* experiments

Peripheral venous blood was obtained from patients with a clinical diagnosis of chronic HF according to current guidelines of the *European Society of Cardiology* and *American Heart Association* at the Department of Cardiology, Campus Virchow – Klinikum. Blood from healthy donors was obtained from the Institute for Transfusion Medicine, Charité-Universitätsmedizin Berlin. Written informed consent according to the Declaration of Helsinki was received prior to inclusion in the study. Around 25 ml of blood was obtained from an antecubital vein and transferred to K-EDTA monovettes and processed within 8 hours.

3.2.3 Isolation of human/rat blood and rat spleen CD4 + T cells

Rat and human blood. Peripheral blood, which was withdrawn from the periphery either of MI or Sham-OP rats was transferred to EDTA-K tubes and carefully mixed to avoid agglutination. Rat blood was diluted with PBS/2mM EDTA buffer in ratio: 1:3. Human blood samples were diluted with PBS/2mM EDTA buffer at least two times. Either rat or human blood samples were layered on Ficoll™ Lymphocytes Separation Medium (LSM) and centrifuged at 400xg for 35 minutes at room temperature (RT) at low acceleration and without using a brake. Mononuclear cells were collected from the white interphase, washed twice with cold PBS and red cells were lysed by adding cold Erythrocyte Lysis Buffer. Cell aggregates were removed by a filtration step with 30µM pre-separation filters, an aliquot of cell suspension was taken for counting of total cell number using Neubauer Chamber and during that, cells were washed at 300xg at 4°C for additional 10 minutes. Further immunofluorescence stainings of the isolated MI-derived rat and healthy human blood cells were performed as shown in table 3.2.1 and processed further for FACS sorting as in the next section described.

Spleen of male MI rats. After incision of peritoneal layer, spleen tissue of male MI rats was removed and transferred to a cold HBSS without Ca²⁺ and Mg²⁺. Tissue was placed in a 60mm Petri dish with 3ml cold DMEM/1% Pen/Strep, cut into 1mm pieces and

immediately filtered through 100µm filter using syringe plug. Following a centrifugation step at 300xg at 4°C for 10 minutes, erythrocytes were lysed and remaining cells were filtered through 30µm pre-separation filters to remove cell aggregates. Spleen mononuclear cells were washed once more with a cold MACS buffer, counted and stained as in the table 3.2.1 (rat spleen) presented.

Step	Rat blood (MI)	Rat spleen (MI)	Human blood (HD, HF)
Primary anti-body (<i>dilution</i>) 30min at 4°C, in the darkness	Mouse anti-rat CD4-PE (1:10), polyclonal rabbit anti-AT2R (1:50), donkey serum (1:50) Fill with a cold MACS buffer up to 200µl volume	Mouse anti-rat CD4-PE (1:10), polyclonal rabbit anti-AT2R (1:50), donkey serum (1:50) Fill with a cold MACS buffer up to 400µl volume	Mouse anti-human CD4-PE (1:10), polyclonal rabbit anti-AT2R (1:50), donkey serum (1:50) Fill with a cold MACS buffer up to 400µl volume
Washing step I	Add 5ml of a cold MACS buffer and washed at 300xg at 4°C for 10 minutes		
Secondary anti-body (<i>dilution</i>) 30min at 4°C, in the darkness	anti-PE MicroBeads (1:10), donkey anti-rabbit Alexa Fluor 488 (1:50) in volume up to 200µl in MACS buffer	anti-PE MicroBeads (1:10), donkey anti-rabbit Alexa Fluor 488 (1:50) in volume up to 400µl in MACS buffer	anti-PE MicroBeads (1:10), donkey anti-rabbit Alexa Fluor 488 (1:50) in volume up to 400µl in MACS buffer
Washing step II	Add 5ml of a cold MACS buffer and washed at 300xg at 4°C for 10 minutes		

Fig. 3.7 Tabular protocol of an indirect immunofluorescence staining (I) combined with anti-PE MicroBeads labeling. **HD:** healthy donors, **HF:** heart failure

Cardiac cells of MI rats. Rats were anesthetized, the abdomen sterilized, beating heart was surgically removed and transferred in HBSS (w/o Mg, Ca). The remaining blood was flushed out with PBS and the heart was cut into small pieces. Following trypsin (O.N. at 4°C, 0.25%, PAN) and Collagenase Type II (0,25mg/ml, 37°C up to 25 min) treatment, heart cells were released by passing the tissue aggregates several times using a 25ml serological pipette. Subsequently, cells were filtered through 70µm and then

40µm cell strainers. Cells were re-pelleted, counted for their viability and used for immunofluorescence staining as described in **Tab. 3.8**.

Step	Rat heart (MI)
Primary antibody (<i>dilution</i>) 30min at 4°C, in the darkness	Mouse anti-rat CD4-FITC (1:10), polyclonal goat anti-AT2R (1:50), donkey serum (1:50) Fill with a cold MACS buffer up to 200µl volume
Washing step I	Add 5ml of a cold MACS buffer and washed at 300xg at 4°C for 10 minutes
Secondary antibody (<i>dilution</i>) 30min at 4°C, in the darkness	Anti-mouse IgG MicroBeads (1:5), donkey anti-goat APC (1:20) in volume up to 200µl in MACS buffer
Washing step II	Add 5ml of a cold MACS buffer and washed at 300xg at 4°C for 10 minutes

Fig. 3.8 Tabular protocol of an indirect immunofluorescence staining (II) combined with MicroBeads labeling

Stained mononuclear blood, spleen or cardiac cells were further applied onto preconditioned MS columns and processed using MACS technology. Columns were placed onto a MiniMACS Separator attached to a MultiStand. While magnetically labelled CD4+T cells were retained in the column due to the existing magnetic field, unlabeled cells were passed through it into a falcon tube as a *negative fraction*. The CD4+ T cells were then eluted by removing the column from the separator and placing onto fresh falcon tube (*positive fraction*). MACS isolated CD4+ T cells of rat or human origin were further processed for sorting of CD4+AT2R+ and CD4+AT2R- T cell subpopulations by BD FACS Aria[®] device.

3.2.4 Sorting of CD4+AT2R+ and CD4+AT2R- T cells

Flow sorting is a process that allows the physical separation of a cell or particle of interest from a heterogeneous population. After MACS isolation, cells were resuspended in a cold MACS buffer at a concentration less than 2000 cells per second (events/s). Cell suspension greater than 2000 events/s declines the efficiency of the sorting process. Before sorting, nuclei dye DAPI was added at a final concentration of 300nM to distinguish between dead and living cells. The established pressure in the whole FACS sys-

tem allowed an ejection of cells into air in a stream of sheath fluid (i.e. buffer on the basis of phosphate buffered saline). Cells were passed through one or more laser beams and information about the fluorescence characteristics of the acquired cell (event) was gathered. The different cell fractions were collected, when the cell broke off from the solid stream in a droplet. At this moment, cells were charged and then passed through two high-voltage deflection plates and were deflected into collection tubes or aspirated to waste. Sorted CD4+AT2R+ and CD4+AT2R- T cells were re-pelleted at 400xg at room temperature for 15 minutes, to ensure that the sorted cells were settled in the bottom of tube. While rat and human blood T cell fractions were used for cell culture experiments and cardiac T cells for RNA isolation, rat spleen cells were prepared for further intra-myocardial transplantation.

3.2.5 Cell culture of blood sorted cells

Freshly sorted CD4+AT2R+ and CD4+AT2R- from MI rat or human control blood were plated in a U-bottom 96-well plate at a density 10^6 cells per ml and cultured in RPMI 1640 medium supplemented with 10% FBS and 1% Pen/Strep and 2mM Glutamine under standard cell culture conditions at 37°C, 5% CO₂ with 20% humidity. T cells were cultured without treatment (control) or treated with AT2 receptor agonist angiotensin II (AngII, 0.5nM), pre-treated with AT2R blocker PD123319 (PD, 5nM) for one hour and immediately stimulated with angiotensin II (0.5nM). Only human sorted T cells were subjected to the treatment. Rat blood cells were cultured without any treatment as a control. After one day of culture, cells were harvested and processed for intracellular staining as described in the next section.

3.2.6 Extracellular staining for flow cytometry

Blood mononuclear cells of human origin were stained for surface markers (CD4, AT2R, CD25), and subjected to an *extracellular* staining protocol. Firstly, cells were blocked with donkey serum to reduce unspecific binding (1:50), indirectly labelled with polyclonal rabbit anti-AT2R antibody (1:50), additionally stained with PE-conjugated mouse anti-human CD4 and APC-conjugated mouse anti-human CD25 (1:10) antibodies. Secondly, staining for AT2 antigen was complemented by labelling with donkey anti-rabbit Alexa Fluor 488 (1:50). Incubation time and washing steps were performed as already shown in Tab. 3.7 or 3.8

3.2.7 Intracellular staining for flow cytometry analysis

Following 24-hours culture, cells were stimulated for another 6 hours with phorbol myristic acid (PMA, 10ng/ml) and ionomycin (500ng/ml). To keep secreted cytokines within cells, monensin (2 μ M) was added to medium for the remaining 3 hours. The extracellular staining with anti-CD4 and anti- AT2R antibodies, performed before sorting and one day of cultivation did not markedly attenuate fluorescence intensity. Therefore, harvested cells were immediately washed once with cold MACS buffer and fixed with 4% paraformaldehyde for 10 minutes on ice, in darkness. By addition of 0.5 ml of a cold PBS and centrifugation at 300xg, 4°C for 10 minutes, fixatives were removed. Fixation was followed by a permeabilisation step with the commercial detergent Perm/Wash[™] (diluted 10-times with Aqua dest) for another 15 minutes on ice. Above mentioned steps were performed in the same way for rat and human cells. Thus fixed and permeabilized cells were processed for various direct intracellular stainings.

Cytokine patterns. The antibodies used for human T cell fractions were: allophycocyanin (APC)-conjugated rat anti-human interleukine-10 (IL-10-APC, 1:50), APC-conjugated mouse anti human interferon gamma (IFN- γ -APC, 1:10) and phycoerythrin-Cy7 (PE-Cy7)-conjugated mouse anti-human tumour necrosis factor-alpha (TNF- α -PE-Cy7, 1:20), and rat T cells were stained with phycoerythrin (PE)-conjugated mouse monoclonal anti-rat IL-10 (IL-10-PE, 1:50) for 30 minutes at 4°C, in darkness. Perm/Wash[™] buffer served here as the antibody diluent. Stained cells were washed with cold PBS, resuspended in 0.3 ml PBS and acquired using a BD FACS Calibur[®] and /or a BD FACS LSRII. At least 10³ cells were recorded and analyzed via WinMDI Software and/or FACS DIVA Software 6.2.1.

Forkhead protein box (FoxP3). The extracellular immunofluorescence stainings, i.e. 3.2.6 were performed. In rat and human mononuclear blood cells, the transcription factor forkhead protein box (FoxP3) was detected intracellularly. Rat blood mononuclear cells were previously stained with PE-conjugated mouse anti-rat CD4 (1:10) and indirectly labelled with APC-anti-AT2R (1:50) antibodies. Fixation and permeabilisation steps followed as stated in the beginning of this section, and cells were then incubated with FITC-conjugated anti-mouse/rat FoxP3 (FoxP3-FITC, 1:10) for 30 minutes in Perm/Wash buffer at 4°C, in darkness. By contrast, human blood mononuclear cells,

with regard to the extracellular staining section (3.2.6), were stained with APC-conjugated rat anti-human FoxP3 (FoxP3-APC, 1:10) during the same incubation time and way as that of rat origin. Data were acquired on a BD FACSCalibur[®] and at least 5×10^4 events of the CD4⁺ gate were recorded. The frequency of the FoxP3-positive cells was analyzed among two sub-populations: CD4⁺AT2R⁺ and CD4⁺AT2R⁻.

3.2.8 Total RNA isolation and quantitative real-time PCR

Some samples of sorted or/and stimulated T cells were taken for RNA isolation. Total RNA of small cell pellets (3.2.4) was purified by a PicoPure Kit according to manufacturer's recommendations. Collected cells were washed in MACS buffer at 3000xg for 10 minutes, then after removing the supernatant for additional 5 minutes. Next, 100 μ l of supplied Extraction Buffer was added and cells were extracted at 42°C for 30 minutes. After a five-minute washing step at 3000xg, supernatant with the extracted RNA was removed and mixed with an equal volume of 70% ethanol. Complete mixture was applied onto preconditioned purification column and following centrifugation and washing steps, pure RNA was eluted with Elution Buffer into microcentrifuge tubes provided in the kit. An alternative method used for RNA extraction was the application of Trizol[™] Reagent accordingly to the conventional method (74). Cells were extracted in Trizol reagent for 15 minutes at room temperature. By applying chloroform and 15 minutes centrifugation step at 12000xg, 4°C, aqueous phase contained RNA was carefully transferred into a new tube, and precipitated with isopropanol. RNA was centrifuged into a gel-like pellet and washed with 75% ethanol (diluted in nuclease-free water). RNA pellet was dried and dissolved in nuclease-free water. The amount of RNA was estimated using a NanoDrop device at 260 nm. Reverse transcription to cDNA was performed using either Promega reagents (5x M-MLV buffer, M-MLV enzyme, dNTPs, Rnasin Inhibitor) or SuperScript II kit, especially when the amount was less than 250ng of total RNA. Table 3.9 shows reverse transcription of the purified RNA into cDNA when Promega reagents were used.

Reagents	Volume, Time, Temperature
0.5-1 μ g of total RNA	8 μ l
DNase	1 μ l

DNase Buffer	1 μ l
	10 μ l of the mixture incubated at 37°C for 30minutes
DNase Stop solution	1 μ l -> 10 minutes at 65°C
Random primers	1 μ l -> 5 minutes at 70°C
5xM-MLV Buffer	5 μ l
M-MLV reverse transcriptase	0.5 μ l
dNTPs (25 mM)	2 μ l
RNase inhibitor	0.5 μ l
Nuclease-free water	5 μ l
	total volume: 25 μ l -> 1 hour at 37°C then 4°C and stored at -20°C

Fig. 3.9 DNase digestion and reverse transcription of isolated RNA

Quantitative real-time PCR was performed using an ABI Prism 7000 and Stratagene 3000 MXP PCR cyler with the SybrGreen PCR Master Mix (table 3.10) according to the following steps demonstrated in the table 3.11.

Reagents	Volume
SybrGreen [®] PCR Master mix (2x)	12.5 μ l
Forward primer (20 μ M)	0.4 μ l
Forward primer (20 μ M)	0.4 μ l
Nuclease-free water	6.7 μ l
cDNA	5 μ l

Fig. 3.10 PCR reaction mixture

1. Hot start	95°C	10min
2. Denaturation	95°C	15s
3. Primer annealing	60°C	30s
4. Elongation	60°C	30s, 40 cycles
5. End	72°C	1min, 1 cycle
6. Pause	4°C	∞

Fig. 3.11 PCR-temperature profiles and number of cycles

3.2.9 Immunofluorescence staining

Cytospin of cell suspension. Suspensions of the human MACS isolated CD4⁺ T cells were washed once with PBS/BSA 0.5% buffer, counted and resuspended in the RPMI1640/2%FBS medium using $1-2 \times 10^5$ total cells and kept cold. Cytospin slides were prepared as follows: cytocentrifuged at 1000rpm for 5min, fixed in 1% PFA for 5min and subsequently blocked with PBS/5% donkey serum/2% BSA for one hour. Finally, cytopins were stained by indirect double-step immunocytochemistry with primary antibody polyclonal rabbit anti – AT2R (1:50) for 3 hr at RT and secondary donkey anti-rabbit Alexa Fluor 488 (1:100) for 1hr at RT. Nuclei were counterstained with DAPI dye for 10 min at RT (300nM). Cytospin slides were visualized by a Zeiss LSM 780 Microscope with 63x objective magnification and processed using free software ImageJ.

Preparation of cryosections. Following the left ventricular catheterization (or 7 days after MI induction), rats were sacrificed (5% KCl), heart tissue was excised and remaining blood removed by flushing with cold PBS. Using a rat heart matrix slicer (model with 1.0 mm coronal section slice intervals) the aorta of the base was truncated and then heart was embedded in Tissue Tek O.C.T., snap-frozen and stored at -80°C. Samples were sectioned into 5 μ m from 4 levels (10mm thick) on a Leica Cryostat and placed onto HistoBond[®] adhesion microscope slides.

Staining of heart cryosections from MI rats (7 days). Five-micron cryosections were fixed in 4% PFA, blocked with DAKO Protein Block for 10min at RT, and stained indirectly with primary goat polyclonal CD4, rabbit polyclonal AT2 (1:50, both) at 4°C overnight and the following secondary antibodies: donkey anti-goat Alexa Fluor 647, donkey anti-rabbit Alexa Fluor 568 (Invitrogen, 1:300, both) for 2 hours at RT, respectively. The nuclei were counterstained with DAPI. Control slides were defined as those without primary antibodies.

3.2.10 Preparation of donor CD4+AT2R+ T cells and intramyocardial transplantation

Donor CD4+AT2R+ and CD4+AT2R- T cells were prepared from spleens of male rats seven days after induction of MI. Immediately after LAD ligation, 2.5×10^5 CD4+AT2R+ or CD4+AT2R- T cells resuspended in 50 μ l saline were injected into the border zone of the ischemic myocardium of each recipient female rat. MI rats injected with saline served as control group.

3.2.11 Left ventricular catheterization – pressure/volume-loop

Four weeks after transplantation, female rats underwent pressure-volume (P/V) loop measurements using the Millar Pressure-Volume System (Catheter model SPR-838 (size 2F, length 12.5cm), Millar Pressure Conductance Unit (model MPCU-200) and PowerLab data acquisition hardware (emka Technologies). Following a small incision in the external jugular vein, a plastic catheter was inserted and 200UI/kg of heparin was administered. After a short period, up to 0.4 ml blood was collected, immediately applied into two cylindrical holes with defined volumes (95, 300 μ l) and calibration of volume was performed. Thereafter, calibration of pressure at 0 and 100 mmHg was performed. The right carotid artery was subsequently exposed by a small incision on the neck and the lateral retraction of the osmohyoid muscles. After a small incision between the two ligatures, the Millar catheter was carefully inserted. To secure the catheter, the loose ligature around it was tied. Values of parallel conductance volume (V_p) were acquired via triple injection of saline (5%), averaged and used for correction of conductance volume. IOX Version 1.8.3.20 software was used to analyze all P/V loop data recorded at steady state (baseline) and under stress conditions (dobutamine, 10 μ g/kg/min

intravenously). Collected data on cardiac performance were divided into three groups: hemodynamic parameters and systolic and diastolic indices.

3.2.12 Quantitative estimation of collagen density

From the four-week-old rats which underwent myocardial infarction plus cell implantation, excised hearts were snap-frozen as described above and divided into two groups: induction of MI plus transplantation of the CD4+AT2R+ T cells (MI+CD4+AT2R+) and induction of MI + transplantation of CD4+AT2R- T cells (MI+CD4+AT2R-). Sliced five-micron sections were fixed in 10% formalin. Following Sirius Red (collagen) and Fast Green FCF (myocytes) staining, incubation with increasing alcohol changes, slides were mounted with Pertex[®] and recorded on Leica DMLB microscope, analyzed with Adobe Photoshop.

3.2.13 Quantitative estimation of infarction size

The same slides, which were stained for the quantification of collagen density (3.2.12), were used for the infarction size estimation. Each section was recorded with the same settings using a Leica Z6 APO apochromatic, light microscope (connected to LAD camera and computer). Images were further processed with Axio Vision LE Rel. 4.5 software, and the infarcted area (%) was calculated with respect to the whole heart section.

3.2.14 Methods for the detection of the transplanted T cells

Labeling of donor cells with Vybrant[®] DiD dye. There are three different tracking dyes available: DiO, DiL, DiD. We chose DiD (V-22887), which usually is detected at 665nm. Sorted T cells were washed once with PBS and kept overnight at 4°C in DMEM medium. Following one more washing step, cells were resuspended at 1×10^6 /ml density and usually 5 μ l of DiD dye was added to one ml of cell suspension. After 10 minutes incubation at 37°C (conditions optimal for splenocytes), cells were washed twice at 400xg for 5 minutes. Donor cells were resuspended in a defined volume and implanted into the heart after myocardial infarction induction in female Wistar rats. Aliquots of stained cells were taken and positive DiD- labeled cells were acquired on FACS LSRII cytometer to optimize settings and gating strategy. Two days post MI and transplantation, hearts were excised, cardiac mononuclear cell isolation was performed and data were directly acquired on a cytometer to detect presence of donor cells in recipient

hearts. The percentage of positive DiD – labeled donor cells was calculated among all acquired cardiac cells.

Detection of the chromosome Y in recipients rats (4 weeks). Slides were subsequently processed for fluorescence via *in situ* hybridization (FISH) to detect Y chromosomes of donor rat cells. For detection, Rat IDetect™ Chromosome Y FISH Paint Probe Red was used and staining was performed according to manufacturer's recommendations. All buffers and reagents were prepared freshly using DEPC-treated water before staining, if necessary. Heart slides were transferred from -20°C to room temperature to allow them to completely dry. Following denaturation steps by placing slides in 2XSSC buffer at 73°C for 2 minutes, slides were then transferred into pre-warmed 0.005% pepsin working solution and incubated at 37°C for 10 minutes. Following washing step with PBS for 5 minutes at RT, each tissue was fixed by covering it completely in 2.5% formaldehyde solution. After 5 minutes, slides were rinsed in PBS (with few drops of 1M glycine) for another 5 minutes, and dehydrated with 1 minute in each 70%, 85% and 100% ethanol solutions at RT. A mixture of the probe and Hybridization Buffer, which were supplied in the kit, were prepared and applied onto tissue, covered with coverslips and sealed with rubber cement. Next, probe and chromosomal DNA were co-denatured on a hot plate at 69°C for 2 minutes and hybridized at 37°C for 16 hours in humidified chamber. Before washing, rubber cement was carefully removed with fine forceps and slides were periodically shaken to remove coverslips, and immediately transferred to hot "0.4X" solution (set at 73°C) for 2 minutes, and briefly in "2X" solution for 1 minute. Rinsed slides with DEPC-treated water were air dried and mounted with Vectashield® medium, containing DAPI at 1.5µg/ml concentration. Images were recorded using a Zeiss LSM EYLRA P S.1 microscope with 63x objective. Co-localization of Y⁺ cells was analysed by use of the Ortho function available in ZEN 2010 software. Recorded images were processed using Adobe Photoshop® software.

3.2.15 Statistical analysis

All results are presented as mean ± SEM. For two group comparisons, two-tailed Student *t* test was used. For multiple groups statistical analysis, one-way-ANOVA method

with Bonferroni post-hoc multiple comparisons was used. Differences at a value $P \leq 0.05$ were considered as a significant.

4 Results – Part I / human

4.1 The baseline characteristic of patients with heart failure.

Nine patients who donated whole blood within the SICA Study (no. 241558), were enclosed to the present dissertation and the relevant parameters were included and are presented as baseline characteristics, see **Tab. 4.1**.

Parameters	Heart Failure n=9
Age (years)	65.7 ± 4.4
Sex (male/female)	(4/5)
NYHA functional class (II/III)	(4/5)
Etiology:	
ischemic and others	9
LVEF (%)	32.78 ± 5.8
PM	1
ICD	4
CRT	1
CRT-D	1
No PM	2
Medication (%):	
ACE inhibitors	5 (55.6)
β-blockers	9 (100)
AT1R-antagonists	4 (44.4)
Diuretics	7 (77.8)
Aldosterone-antagonists	6 (66.7)
Statins	3 (33.3)
Digoxin	4 (44.4)
Aspirin	7 (77.8)

Tab. 4.1 Baseline characteristics of patients with heart failure. Taken from Skorska A et al., *JCMM* (2015)

Values are shown as mean ± SEM. **DCM**: dilated cardiomyopathy, **ICD**: Implantable Cardioverter Defibrillator, **CRT**: Cardiac Resynchronization Therapy, **PM**: Pacemaker, **AT1R**: angiotensin II type 1 receptor, **ACE**: angiotensin-converting enzyme

The above baseline characteristics show that ischemia was a major cause which led to the progression of heart failure. Among the functional NYHA classes, patients were classified as II and III. This could explain minimal physical activity caused by an attenuated heart function with heart damage and wall thinning during the healing process. Moreover, to avoid the second heart attack, patients had undergone drug therapy by administration of β -blockers (all patients), AngII-, AT1R- and Aldosterone antagonists, ACE and thrombocyte inhibitors (aspirin), and to the less extent (three of nine patients), statins, to decrease the cholesterol level. Twenty eight healthy donors were included in the present work and served as a control.

4.2 Identification of the CD4+ATR+ T-cells in human peripheral blood

The mononuclear cells obtained either from whole blood of healthy donors or patients with HF, were subjected to flow cytometric analysis. The frequency of CD4+ T cells in peripheral blood of patients with heart failure (**Fig. 4.1**) showed a significant increase,

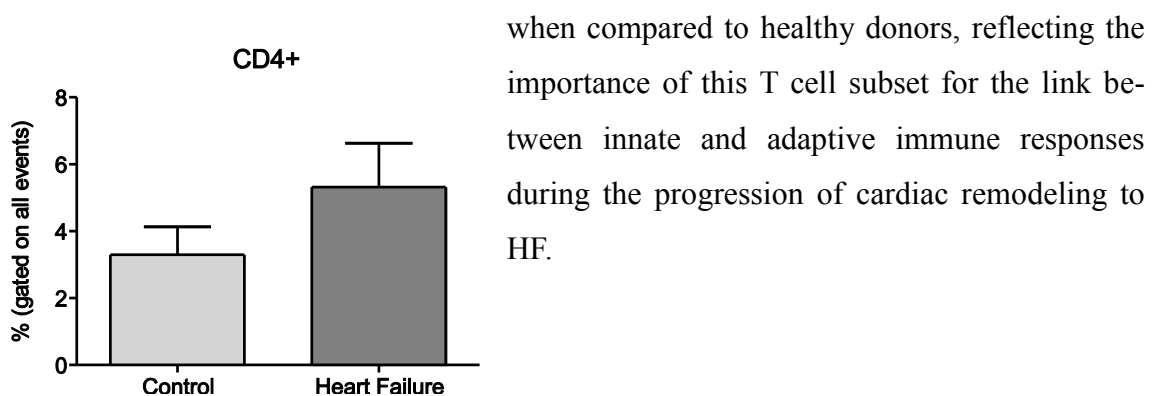


Fig. 4.1 CD4 expression in human blood mononuclear cells. Mononuclear cells (MNCs) were isolated using Ficoll centrifugation method and analyzed by FACS. The frequency of CD4+ T cells is decreased in MNCs of patients with ischemic heart failure compared to healthy donors. n= 7 (HF), n=5 (control); no significance observed between both groups. Taken from Skorska A et al., *JCMM* (2015)

As immunofluorescence analysis of mononuclear cells showed expression of AT2R within the CD4+ T cell population (**Fig. 4.2**), both identified T-cell subpopulations expressing or lacking the AT2R were sorted accordingly to the CD4+AT2R+ or the CD4+AT2R- T-cell subpopulations.

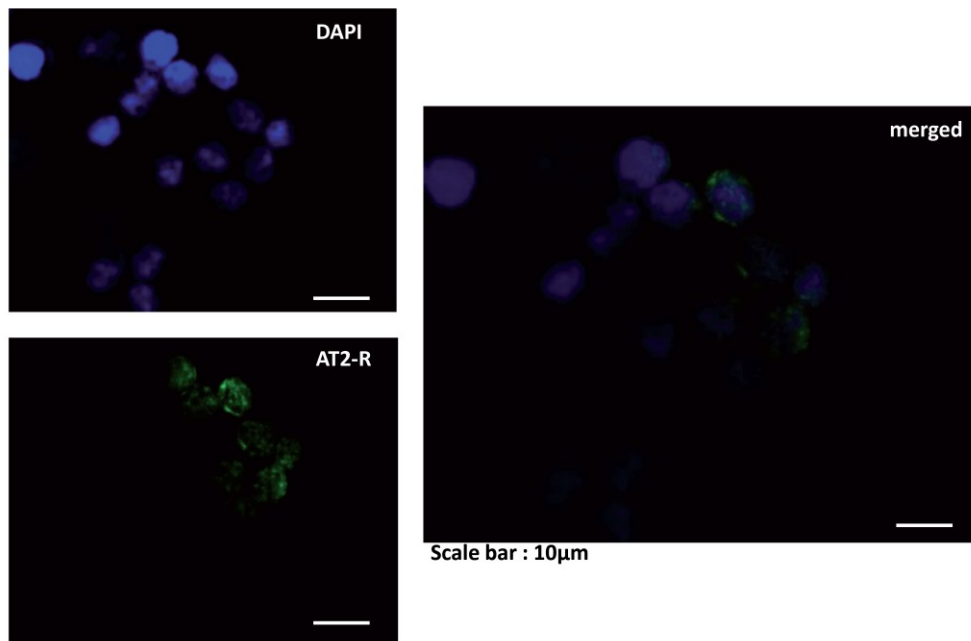


Fig. 4.2 Identification of the AT2R +- expressing T cells in human peripheral blood. MACS isolated CD4+ T cells were cyto-centrifuged, blocked and double-indirect stained with polyclonal rabbit anti- AT2 antibody followed with donkey anti- rabbit Alexa Fluor 488 secondary antibody. AT2R+ cells (green), nuclei (blue), CD4+AT2R+ (merged), scale bar= 10µm

Representative re-analysis of such sorted T-cell subpopulations in peripheral blood of healthy controls and patients with HF and confirmation of the expression of AT2R on mRNA level are shown in **Figure 4.3 A and B**, respectively.

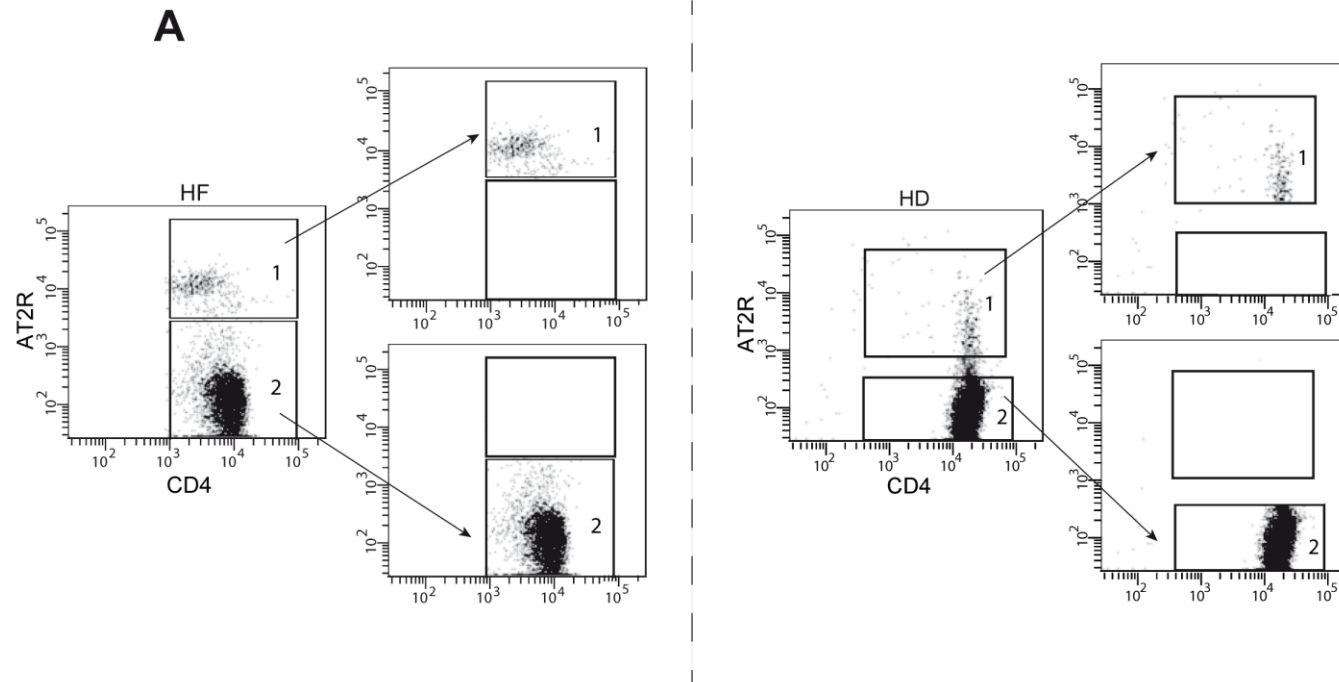
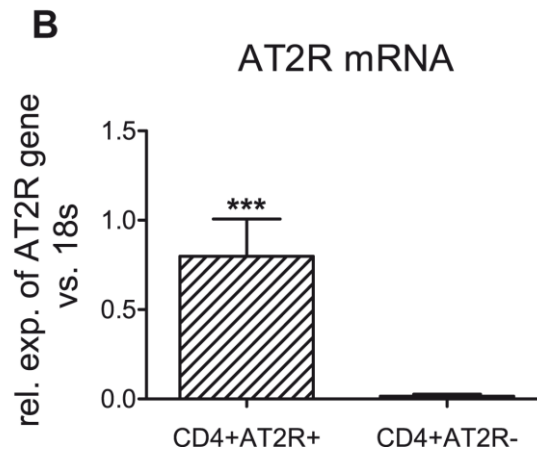


Fig. 4.3 Identification of human blood CD4+AT2R+ T cell population. A. Representative FACS plots of sorted CD4+AT2R+ (1) and CD4+AT2R- (2) T cells from peripheral blood of patients with heart failure (HF) and healthy donors (HD). Taken from Skorska A et al., *JCMM* (2015)

All FACS dot plots showing the analysis of CD4+AT2R+ vs. CD4+AT2R- within the CD4+ fraction of mononuclear blood cells, either of healthy donors or patients with HF are presented at the end of this thesis as **Appendix 1** and **2**, respectively.



4.3(continued): B. Predominant AT2R mRNA level in sorted human blood CD4+AT2R+ (vs. CD4+AT2R-) T cells, n=3, *** p <0.001. Taken from Skorska A et al., *JCMM* (2015)

Further, to study the adaptive distribution of CD4+AT2R+ T cells during cardiac injury, the frequency of these cells in peripheral blood of patients with HF was compared with that of healthy controls. The frequency of CD4+AT2R+ T cells in blood CD4+ T cells was reduced from $2.6 \pm 0.2\%$ in healthy controls to $1.7 \pm 0.4\%$ in patients with HF (**Fig.4.4**), revealing a potential accumulation of CD4+AT2R+ T cells infiltrating the failing heart.

Due to the essential role of regulatory T cells (Treg) in controlling the immune response under physiological and pathological conditions, the expression of the immunoregulatory transcription factor FoxP3 and the Treg surface marker CD25 within the CD4+AT2R+ T cell subset was investigated. In human CD4+AT2R+ T cells, the frequency of FoxP3-positive cells was increased by 2.1-fold (**Fig. 4.5 A**, p <0.0001). The potential to produce anti-inflammatory IL-10 cytokine by both T-cell populations was also evaluated, whereby the predominantly IL-10-secreting subset resided within the CD4+AT2R+ T-cells and increased by 12.6-fold (healthy donors) and 41.2-fold (heart failure) when compared to CD4+AT2R- T cells (p <0.01, p <0.05 respectively) (**Fig. 4.5 B, C**). However, no difference in CD25 expression was detected (**Fig. 4.5 A**, right plot).

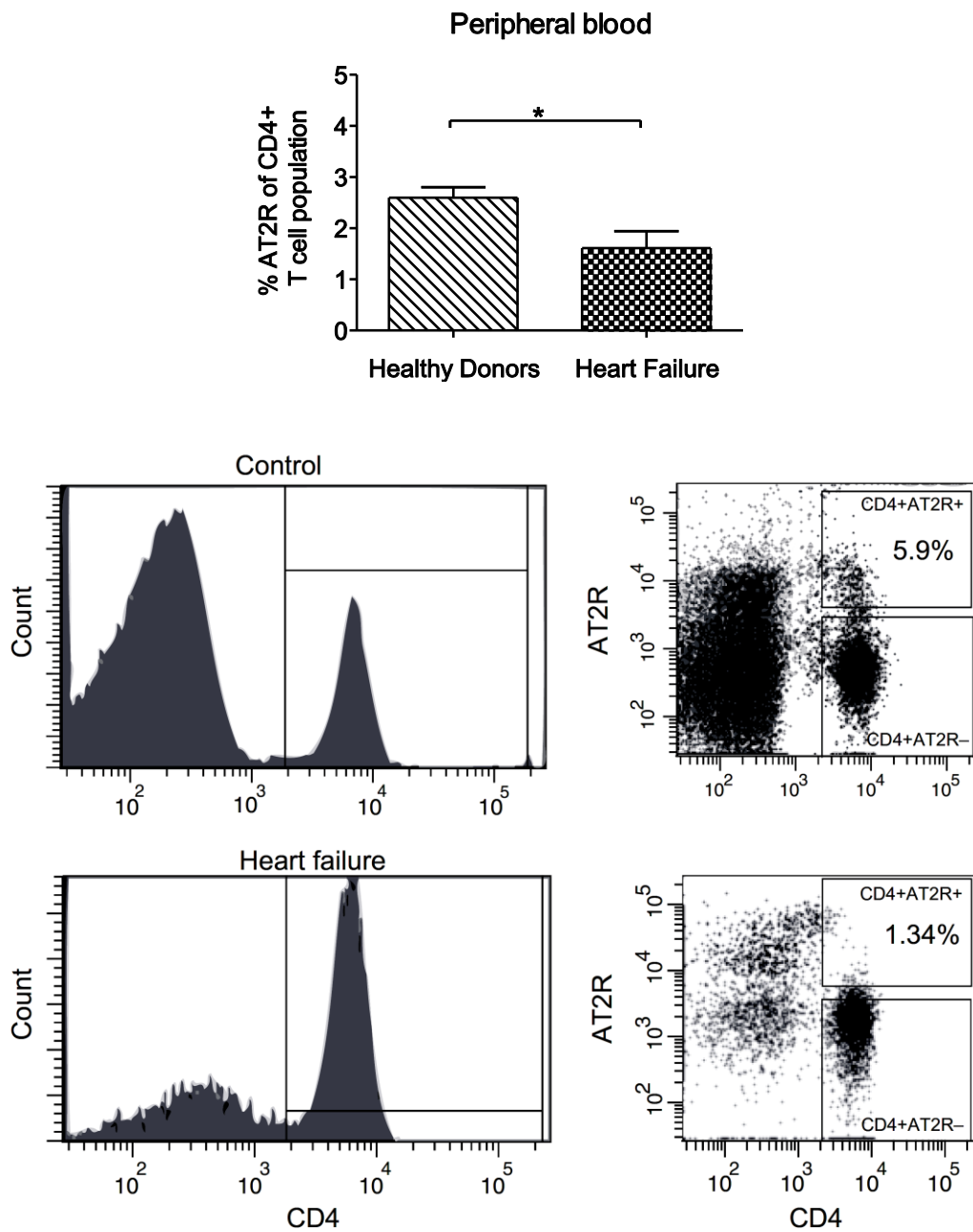


Fig.4.4 CD4+AT2R+ T cells were reduced in HF patients. * $p < 0.05$, (heart failure, $n=9$, healthy donors, $n=27$). Representative FACS plots from healthy controls (upper panel) and HF patients (lower panel). Taken from Skorska A et al., *JCMM* (2015)

4.3 Characterization of human blood CD4+AT2R+ T cells

To address a potential cardioprotective role of AT2R, we determined whether AT2R influences the regulation of the inflammatory-related cytokines IL-10 and TNF- α in the CD4+AT2R+ T cell population.

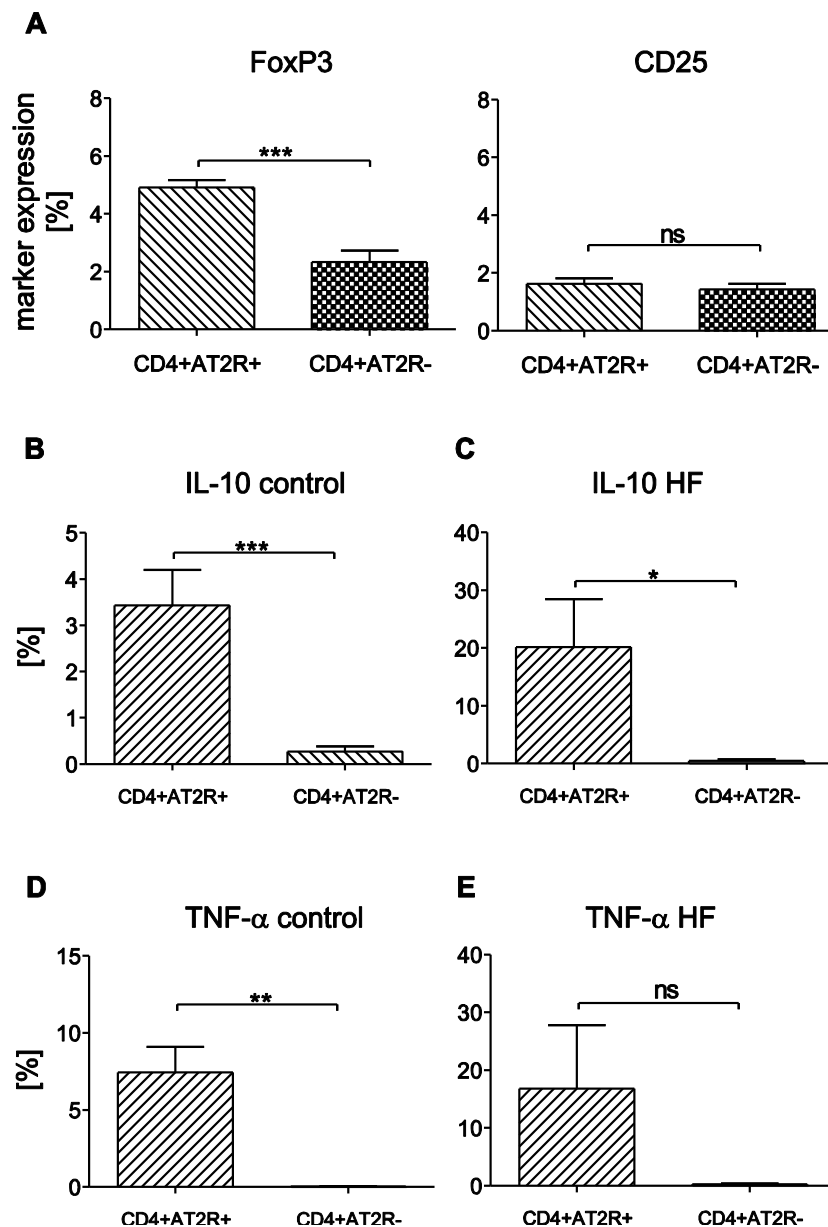
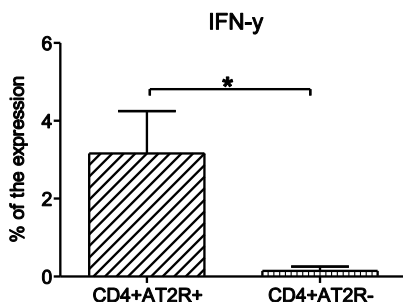


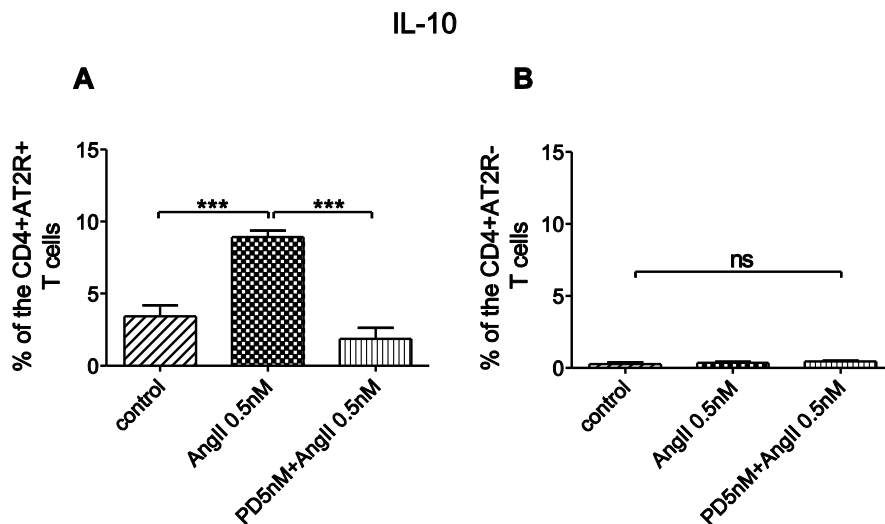
Fig. 4.5 Characterization of human blood CD4+AT2R+ T cells. Flow cytometric analysis was performed on gated CD4+AT2R+ and CD4+AT2R- subpopulations of mononuclear cells (MNCs) from healthy donors (A, Foxp3, n=8; CD25, n=11); Predominant IL-10 expression was observed in the CD4+AT2R+ (vs. CD4+AT2R-) T cells of healthy controls (B, n=6) and HF patients (C, n=7). Increased TNF- α expression was observed in the CD4+AT2R+ (vs. CD4+AT2R-) T cells of healthy controls (D, n=6) but not HF patients (E, n=7). ns, not significant; ** $p < 0.01$, *** $p < 0.001$. Taken from Skorska A et al., *JCMM* (2015)

Upon AngII stimulation, IL-10 expression in the CD4+AT2R+, but not in CD4+AT2R- T cells was significantly increased (2.6-fold in comparison to the control group, **Fig. 4.7 A, B**), while TNF- α expression in the CD4+AT2R+ T cells was reduced 2.0-fold (**Fig.**



4.7 C, D). Both effects were completely abolished by the AT2R blocker PD123319. In particular, a highly increased level of TNF- α expression was observed exclusively in the CD4+AT2R+ T cells (**Fig. 4.5 D, E**). In addition to that this T cell subpopulation secreted IFN- γ significantly more than those T cells without AT2Rs (**Fig 4.6**).

Fig. 4.6 Characterization of human blood CD4+AT2R+ T cells. The frequency of IFN- γ - positive cells within the CD4+AT2R+ subset is increased in patients with ischemic heart failure compared to CD4+AT2R- T cells. n = 3, * $p < 0.05$. Taken from Skorska A et al., *JCMM* (2015)



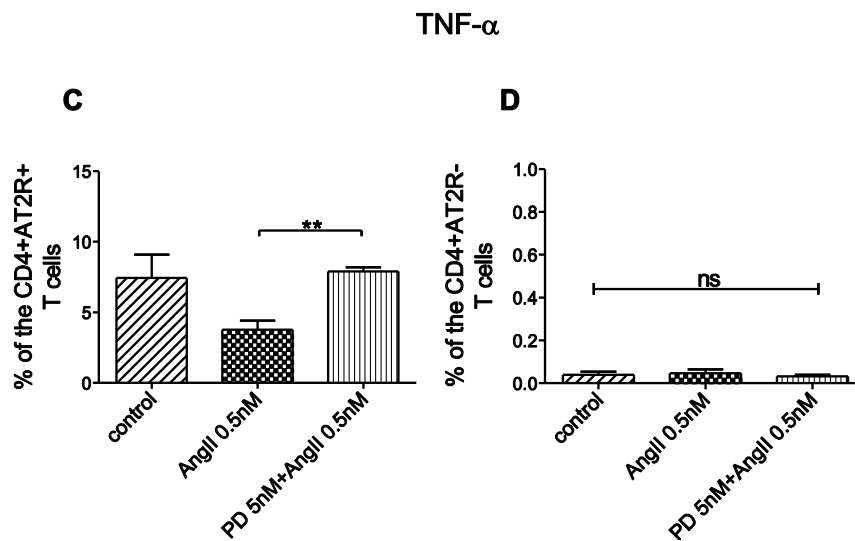


Fig. 4.7 IL-10 and TNF- α expression in human blood CD4+AT2R+ T cells. Sorted cells were analyzed after one day of cultivation. AT2R mediated IL-10 production in the CD4+AT2R+ (A) but not in the CD4+AT2R- (B) T cells of healthy controls as observed after AT2R stimulation with angiotensin II (AngII) in presence or absence of AT2R blocker PD123319 (PD).

AT2R shows a tendency to downregulate TNF- α production in the CD4+AT2R+ (C) but not in CD4+AT2R- (D) T cells of healthy donors, as shown after AT2R stimulation with angiotensin II (AngII) in the presence or absence of the AT2R blocker PD123319 (PD). ns, not significant; ** $p < 0.01$. Taken from Skorska A et al., *JCMM* (2015)

A further detailed analysis of the distribution of CD4+AT2R+ T cells within CD4+CD44+CD62L- or CD4+CD44+CD62L+ T cell subsets (**Fig. 4.8 A, B**) showed that a significant decrease of blood CD4+AT2R+ T cells in patients with HF was exclusively assigned to the CD4+CD44+CD62L- T cell subset, a known activated T cell fraction located mainly at inflammatory sites(75).

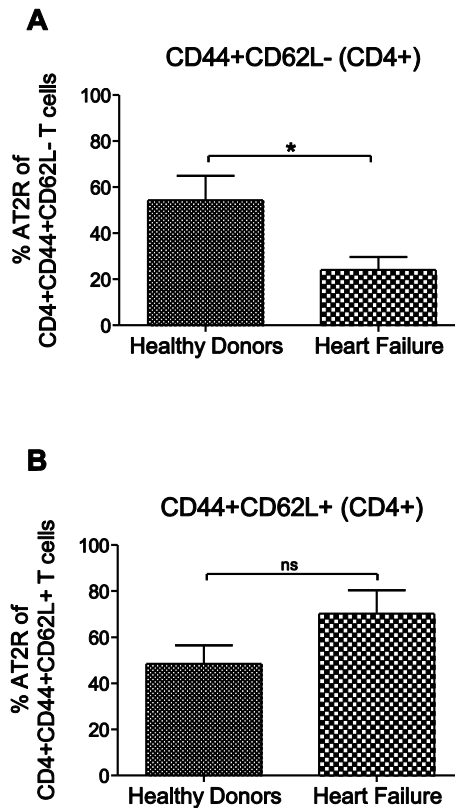


Fig. 4.8 Distribution of the CD4+AT2R+ T cells within CD4+CD44+CD62L- or CD4+CD44+CD62L+ T cell subsets A. A decreased frequency of CD4+AT2R+ T cells within the CD4+CD44+CD62L- cell subset was observed in patients with HF. No significant difference was detected within the CD4+CD44+CD62L+ T cell subset (B). ns, not significant; * $p < 0.05$, $n = 5$. Taken from Skorska A et al., *JCMM* (2015)

5 Results – Part II / Rats

5.1 Identification of CD4+AT2R+ T cells in a rat MI model

In rats, myocardial infarction was induced by permanent ligation of the left descending artery (LAD). These seven day old MI rats enabled to study the relevance of AT2R in response to ischemic injury. Further, the method of cardiac cell isolation with slightly altered MACS technology, which had been established during a previous AT2R-related project of our group (71) allowed to clarify a potential functional relevance of AT2R for cardiac infiltration within CD4+ T cell subsets. Here, **Fig. 5.1** shows the CD4+AT2R+ - T cells infiltrating the myocardium, which were mainly detected in the peri-infarct zone.

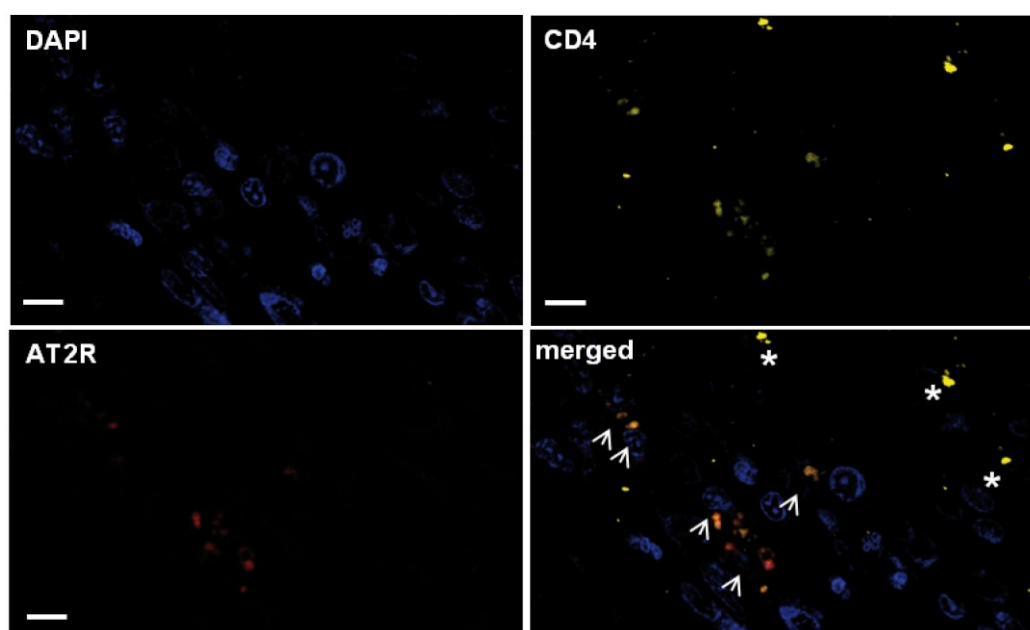


Fig. 5.1 Identification of CD4+AT2R+ T cells in a rat MI model. Co-localization of AT2R in a fraction of infiltrating CD4 T cells in peri-infarct myocardium. Arrows indicate CD4+ (yellow) AT2R+(red) cells. Sections were counterstained with DAPI (nuclei, blue). Scale bar = 10 μ m. (The present staining was performed by Ms Stephanie Zirkel within the bachelor thesis, 2011 and included in Skorska A et al., *JCMM* (2015).

Besides the infarcted myocardium (representative FACS dot plot analysis, **Fig. 5.2** and middle of the **Fig. 5.4**), the CD4+AT2R+ T cells were found in circulating blood and spleen (**Fig. 5.4**). In addition, the verification of AT2R expression on the mRNA level in sorted CD4+AT2R+ T cells was performed as shown in **Fig. 5.3**.

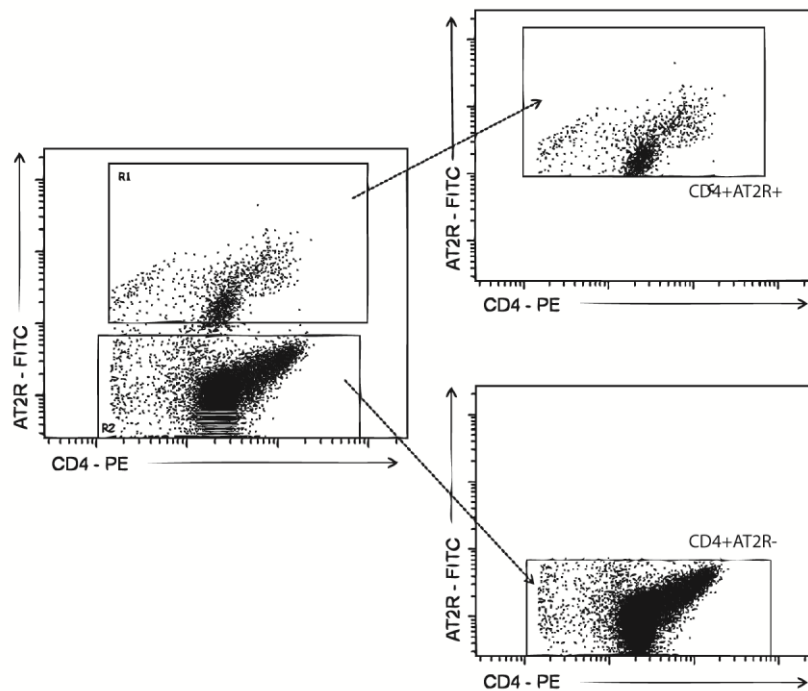


Fig. 5.2 Identification of CD4+AT2R+ T cells in a rat MI model. Representative FACS plots of post-infarction cardiac CD4+AT2R+ and CD4+AT2R- T cells. Taken from Skorska A et al., *JCMM* (2015)

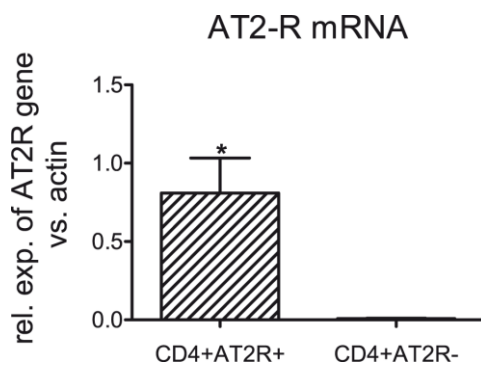


Fig. 5.3 Verification of the AT2R mRNA level. Accumulated AT2R mRNA levels (normalized to beta-actin) in sorted post-infarct cardiac CD4+AT2R+ (vs. CD4+AT2R-) T cells, n=3, *p<0.05. Taken from Skorska A et al., *JCMM* (2015)

In blood, infarcted heart and spleen, $3.8 \pm 0.4\%$, $23.2 \pm 2.7\%$ and $22.6 \pm 2.6\%$ of CD4+ cells expressed AT2R, respectively, (**Fig. 5.4**). Quantitative analysis reveals a significant increase of CD4+AT2R+ T cells in post-infarct heart and spleen, whereas it decreased in circulating blood.

Collectively, the CD4+AT2R+ T cell population seems to be recruited selectively and adaptively into the myocardium in response to ischemia.

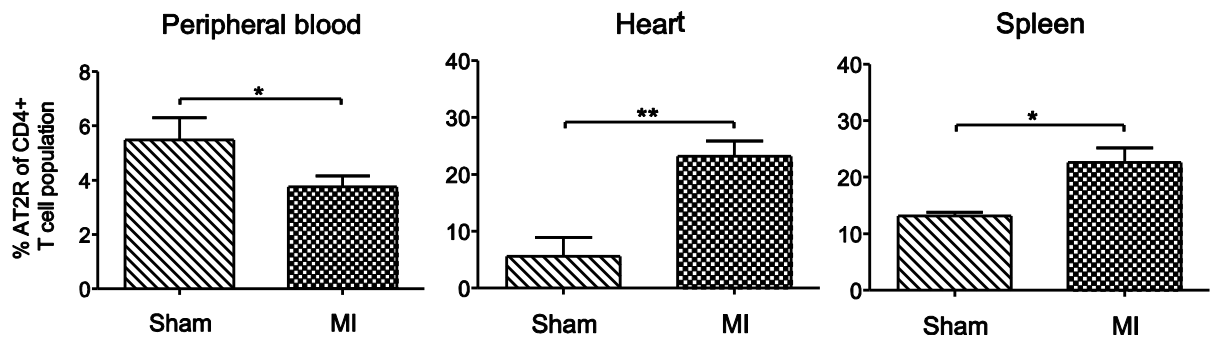


Fig. 5.4 Adaptive redistribution of the CD4+AT2R+ T cell population in response to myocardial infarction in rats. Frequency of the CD4+AT2R+ T cells in CD4+ T cells of blood (sham, n= 7; MI, n=14), heart (sham, n=5; MI, n=12), and spleen (sham, n=3; MI, n=7) was evaluated by flow cytometric analysis. * $p < 0.05$, ** $p < 0.01$. Taken from Skorska A et al., *JCMM* (2015).

5.2 The CD4+AT2R+ T cells as immunoregulatory players – *in vitro*

A better understanding of the functionality of the detected CD4+AT2R+ in response to ischemic insult will enable a selection of ideal and well defined cells for cardiac therapy approaches. Therefore, this T cell subpopulation was analysed for expression of the immunoregulatory transcription factor FoxP3 (**Fig. 5.5**, left) and secretion of the cytokine IL-10 in the CD4+AT2R+ T cells derived from the peripheral blood of rats with MI was evaluated (**Fig. 5.5**, right plot). As shown, the intracellular production of FoxP3 and IL-10 was significantly upregulated 4- and 74-fold, respectively, in CD4+AT2R+ T cells, when compared with CD4+AT2R- T cells ($p < 0.05$). These increased IL-10 expression levels in the CD4+AT2R+ T cells were confirmed by real-time PCR analysis of IL-10 mRNA (**Fig. 5.6**).

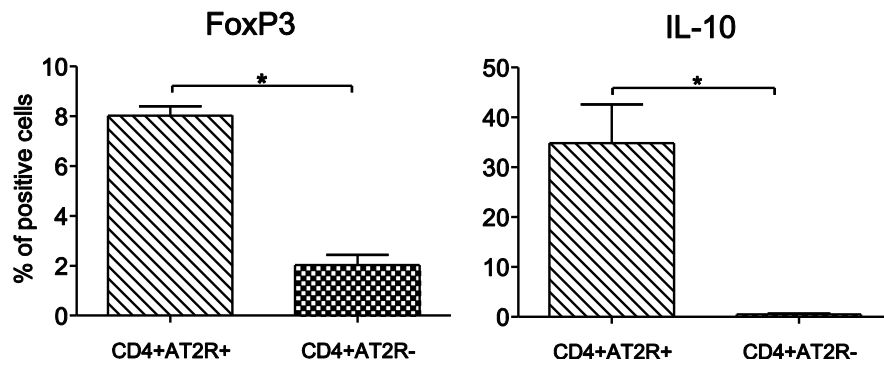


Fig. 5.5 Characterization of CD4+AT2R+ T cells in rats after myocardial infarction. FoxP3 and IL-10 were significantly upregulated in blood CD4+AT2R+ T cells. * $p < 0.05$, $n = 5$. Taken from Skorska A et al., *JCMM* (2015)

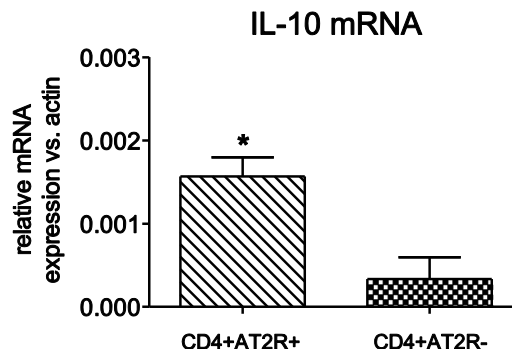


Fig. 5.6 Confirmation of IL-10 mRNA level in CD4+AT2R+ T cells . * $p < 0.05$, $n = 5$. Taken from Skorska A et al., *JCMM* (2015)

Hence, these data indicate an immunoregulatory potential of CD4+AT2R+ T cells.

5.3 Cardioprotective role of CD4+AT2R+ T cells - *in vivo*

To determine whether the immunoregulatory potential of CD4+AT2R+ T cells has functional relevance *in vivo*, we evaluated the effects of intramyocardial transplantation of splenic CD4+AT2R+ T cells on cardiac remodeling and performance in rats with MI.

5.3.1 Transplanted T cells were successfully detected in the heart of recipient rats

Initially, splenic CD4+AT2R+ T cells - sorted and stained with Vybrant DiD dye - were transplanted into MI-induced rat hearts. Using flow cytometric analysis after two days, we could detect an average 2.8% of Vybrant DiD-positive cells as shown on FACS histogram, **Fig. 5.7**. In addition, four weeks after transplantation, the engraftment of the

transplanted cells from male donor rats in peri-infarct myocardium of female recipient rats was proven via single-color FISH using a Y-chromosome-specific probe (Fig. 5.8).

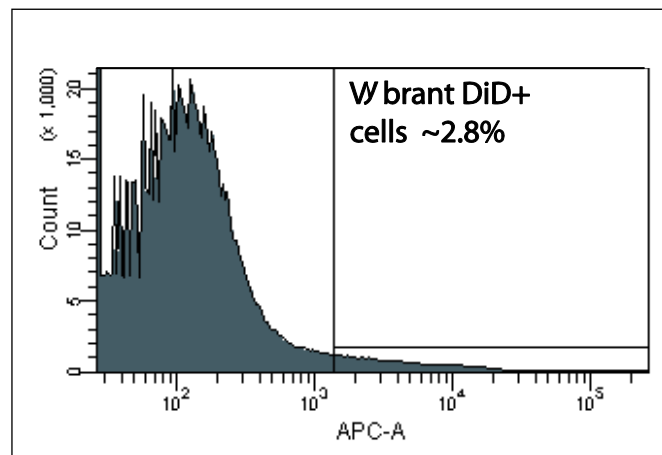


Fig. 5.7 Detection of transplanted CD4+AT2R+ T cells in heart tissue of recipient rats 2 days post MI. Hearts were excised, digested and direct flow cytometric acquisition was performed. A representative FACS histogram shows Vybrant DiD+ cells which were gated on all acquired cardiac mononuclear cells.

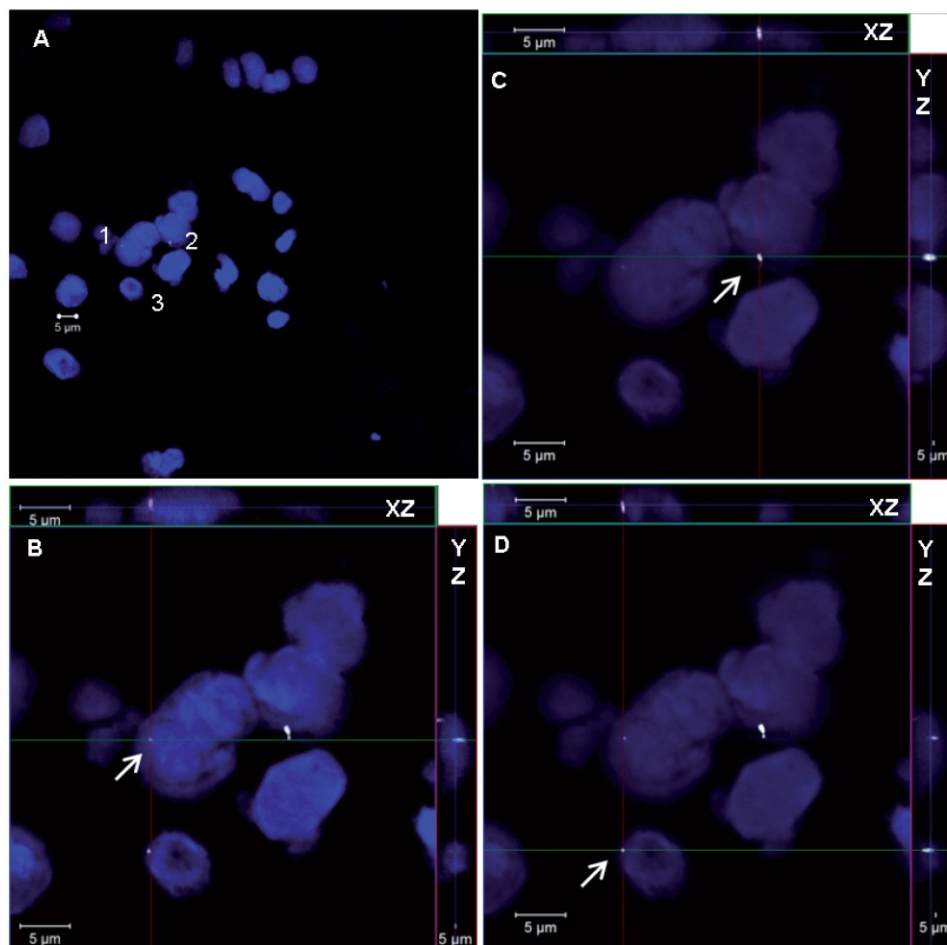


Fig. 5.8 Detection of male donor cells in the myocardium of female recipient rats by fluorescence *in situ* hybridization. **A.** Four weeks after cell transplantation, donor cells were detected via fluorescence *in situ* hybridization (FISH), based on probes specific for the Y chromosome.

Donor nuclei within the recipient heart are numerically labeled (nuclei 1-3). The probes were labeled with IDYETM 556 (white) for Y chromosomes. Slides were mounted with VECTASHIELD[®] medium containing DAPI for counter-staining of nuclei. Z-stack images were obtained via laser scanning confocal microscopy (LSM 780, Zeiss). Y-chromosomes present within nucleus 1, 2 and 3 are also shown in *xz* and *yz* positions, respectively (Arrows in **B**, **C** and **D**). Scale bar, 5 μ m. Taken from Skorska A et al., *JCMM* (2015)

5.3.2 Injection of the CD4+AT2R+ T cells effectively improves cardiac performance

For further *in vivo* characterization of a cardioprotective role of the CD4+AT2R+ T cell subpopulation, PV-loop measurements at baseline and during stress (dobutamine) were performed. The complete results (hemodynamic parameters, systolic and end-diastolic indices) of this evaluation are shown in the end of this chapter (**Tab. 5.1**). The data of cardiac catheterization of the recipient group in which the CD4+AT2R+ T cells were intramyocardially injected showed a significant improvement in cardiac performance when compared with CD4+AT2R- T cells and control (saline) groups. In detail, the ejection fraction at steady-state of MI plus CD4+AT2R+ animals was increased by 1.5-fold and 1.2-fold, compared with control and MI plus CD4+AT2R- animals, respectively (**Fig. 5.9A** and **Tab. 5.1**). An additional parameter relevant for cardiac systolic function, namely the maximal peak rate of LVP (dP/dtmax, mmHg/s) under both baseline and stress conditions was increased in the CD4+AT2R+. At baseline, respective values were enhanced 1.7-fold and 1.4-fold as compared to the control and the CD4+AT2R- groups (**Fig. 5.9A**). Under stress, the values were elevated 1.2-fold and 1.3-fold in comparison to the control and the CD4+AT2R- groups (**Fig. 5.9B** and **Tab. 5.1**).

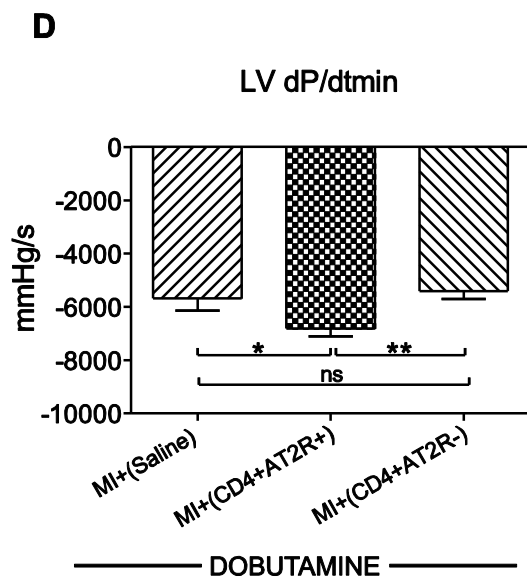
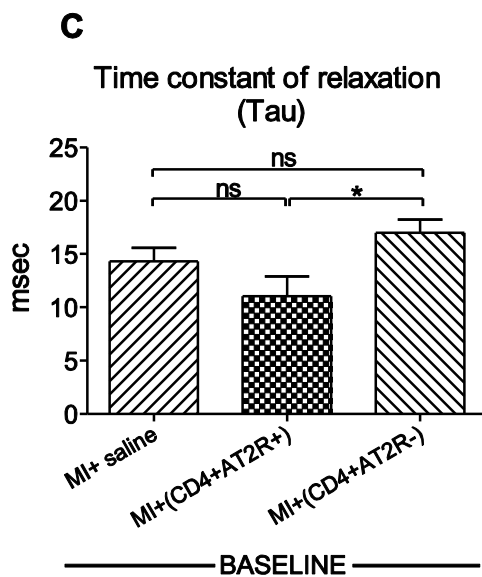
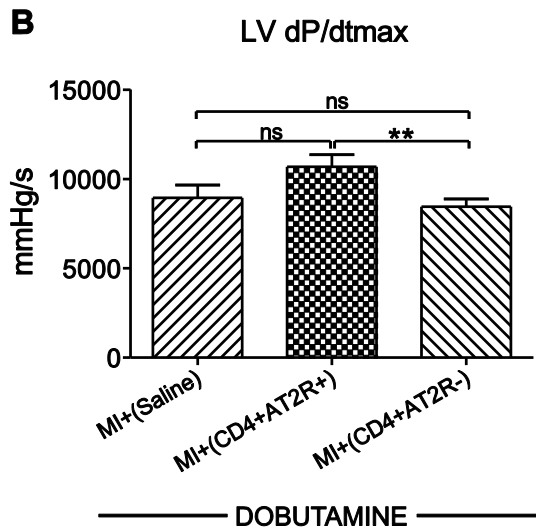
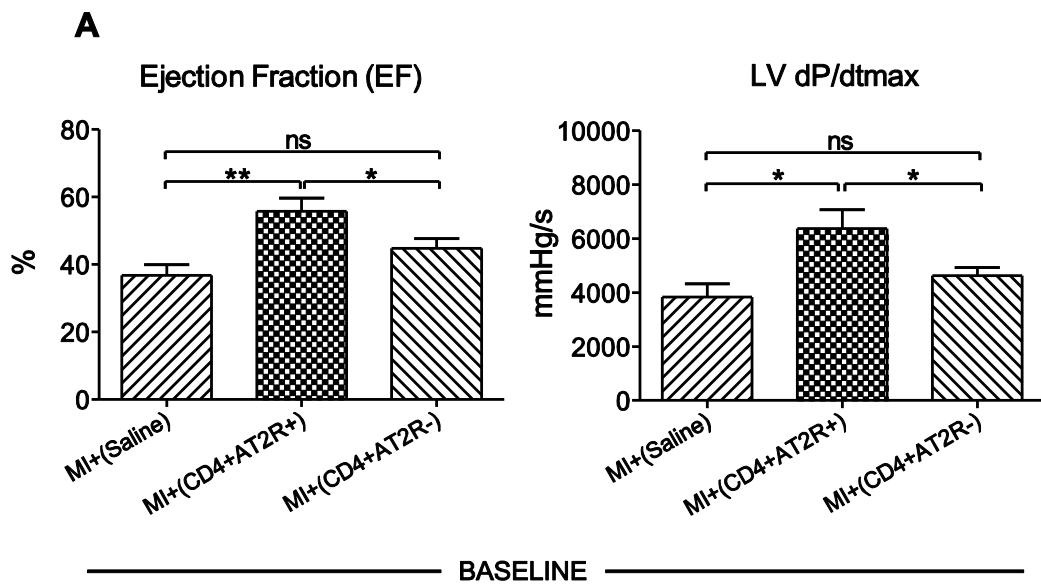


Fig. 5.9 Assessment of left ventricular functions in recipient MI rats via pressure-volume loops. Intramyocardial transplantation of splenic CD4+AT2R+ T cells led to an increase in ejection fraction (EF) at steady state and a maximal peak rate of LVP (dP/dtmax, mmHg/s) under both baseline and stress condition (Dobutamine, 10µg/min/kg) (**A, B**), and improved diastolic indices including reduced time during relaxation (Tau) at steady state and improved minimal (-dP/dtmin, mmHg/s) peak rate under stress condition (**C, D**) as evaluated with conductance-catheter method. Around 2.5×10^5 splenic cells one of the T cell subpopulation were injected in 50µl saline into the border zone. MI+(Saline), n=10, MI+(CD4+AT2R+), n=10; MI+(CD4+AT2R-), n=15; ns: not significant, *p<0.05, **p<0.01. Taken from Skorska A et al., *JCMM* (2015)

Adoptive transfer of CD4+AT2R+ T cells also markedly improved diastolic indices as shown by a reduced relaxation time at steady state (Tau, from 17.0 ± 1.3 to 11.0 ± 1.9 ; **Fig. 5.9C**). It likewise improved the minimal peak rate (-dP/dtmin, mmHg/s) under stress conditions from -6808 ± 292.2 to -5408 ± 296.0 when compared with the CD4+AT2R- animal group (**Fig. 5.9D** and **Tab. 5.1**).

5.3.3 Transplanted CD4+AT2R+ T cells ameliorate cardiac remodeling

The CD4+AT2R+ T cells seemed to be therapeutically effective due to their significant influence on cardiac remodeling in recipient rats when compared to controls. In addition, CD4+AT2R+ T cells from the same donor rats, led to a significant reduction of infarction size (1.8- and 1.2- fold, respectively, **Fig. 5.10**). No significant differences were observed between the control and the CD4+ATR- groups (p=0.3171). Representative images of heart slices stained with Sirius Red/ Fast Green are presented in the lower panel of this figure.

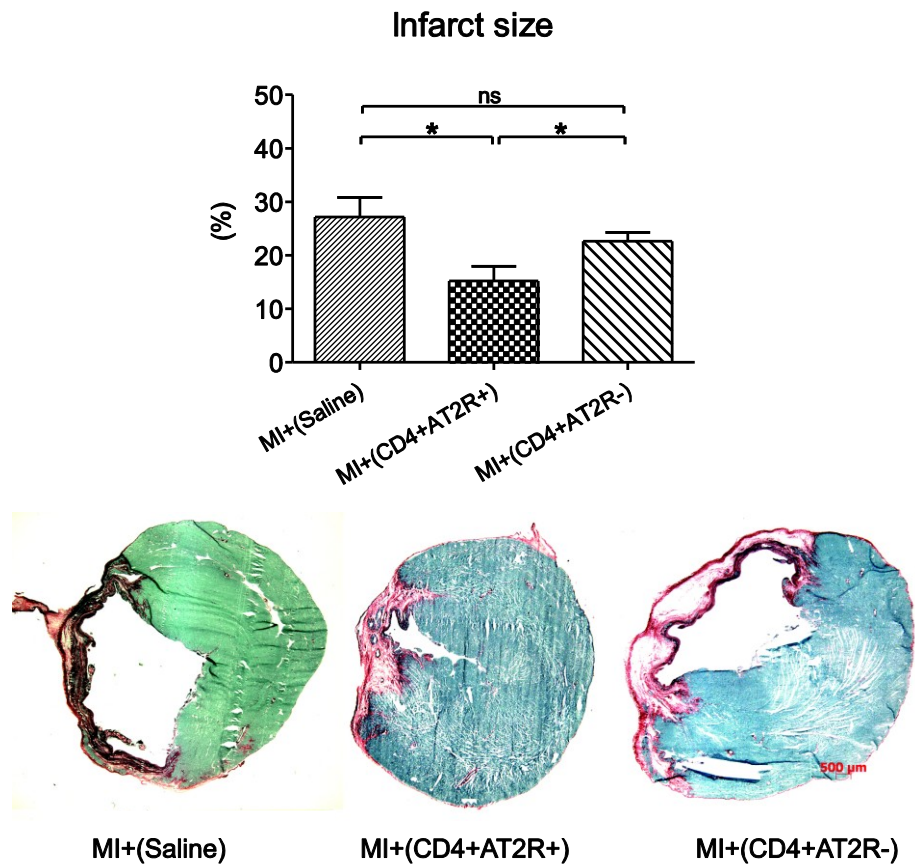


Fig. 5.10 Effects of CD4+AT2R+ T cells on cardiac injury in recipient MI rats. Intramyocardial transplantation of splenic CD4+AT2R+ T cells (vs. MI+(Saline) and CD4+AT2R-) significantly reduced infarction size in recipient MI rats four weeks after transplantation. Therapy groups obtained around 2.5×10^5 splenic cells, either of CD4+AT2R+ or CD4+AT2R-, resuspended in 50 μ l saline and injected into a border zone. Control group received only 50 μ l saline. Representative ventricular cross sections of infarct areas are shown in lower panels. * $p < 0.05$, ** $p < 0.01$; n=8; scale bar=500 μ m. Taken from Skorska A et al., *JCMM* (2015)

Overall, these data support a cardioprotective role for the CD4+AT2R+ T cell population by ameliorating post-infarction inflammatory injury *in vivo*.

	MI+(Saline), n=10		MI+(CD4+AT2R+), n=10		MI+(CD4+AT2R-), n=15		P Value					
	Baseline	Dobutamine	Baseline	Dobutamine	Baseline	Dobutamine	P1	P2	P3	P4	P5	P6
Hemodynamic parameters												
Body weight [g]	252± 46.9		274.1 ± 5.902		279.8 ± 5.257		ns					
HR [bmp]	384.1 ± 16.09	424.8 ± 14.60	370.1 ± 15.38	434.9 ± 7.232	387.2 ± 9.814	436.1 ± 7.292	ns	ns	ns	ns	ns	ns
Pmax [mmHg]	93.17 ± 6.47	109.3 ± 3.912	105.6 ± 5.159	117.3 ± 3.802	92.08 ± 3.027	108.4 ± 2.341	ns	ns	<0.05 *	ns	ns	<0.05 *
PES [mmHg]	88.49 ± 7.133	103.3 ± 4.444	93.14 ± 6.692	104.0 ± 4.068	77.79 ± 2.804	91.23 ± 2.915	ns	ns	<0.05 *	ns	<0.05 *	<0.05 *
PED [mmHg]	9.686 ± 0.927	9.578 ± 0.774	11.66 ± 0.9256	10.80 ± 0.7961	14.25 ± 1.154	12.83 ± 0.9883	ns	<0.01 **	ns	ns	<0.05 *	ns
ESV [μl]	148.7 ± 13.26	121.7 ± 13.49	143.6 ± 12.48	59.54 ± 6.920	133.1 ± 8.838	114.7 ± 20.09	ns	ns	ns	<0.01 **	ns	ns
EDV [μl]	206.4 ± 13.13	201.8 ± 11.27	224.5 ± 13.88	244.4 ± 18.18	289.7 ± 28.82	241.5 ± 20.02	ns	<0.05 *	ns	ns	ns	ns
SV [μl]	73.90 ± 5.491	106.4 ± 13.37	124.5 ± 8.259	185.0 ± 15.86	152.5 ± 16.75	157.8 ± 15.81	<0.01 **	<0.01 **	ns	<0.01 **	<0.05 *	ns
CO (μl/min)	30430 ± 3993	48340 ± 6979	54190 ± 5533	79890 ± 6541	56940 ± 5903	69290 ± 7054	<0.01 **	<0.01 **	ns	<0.01 **	<0.05 *	ns
Systolic indices												
EF (%)	36.80 ± 3.171	49.90 ± 5.448	55.75 ± 3.851	69.54 ± 4.880	44.74 ± 2.960	57.02 ± 4.081	<0.01 **	ns	<0.05 *	<0.05 *	ns	ns
dP/dtmax (mmHg/s)	3828 ± 496.6	8946 ± 714.5	6370 ± 700.1	10690 ± 669.7	4620 ± 304.3	8444 ± 439.2	<0.05 *	ns	<0.05 *	ns	ns	<0.01 **
SW (μl x mmHg)	4597 ± 661.5	8075 ± 1241	8740 ± 653.4	12910 ± 1676	7897 ± 813.0	13430 ± 1333	<0.01 **	<0.01 **	ns	<0.05 *	<0.05 *	ns

	MI+(Saline)		MI+(CD4+AT2R+)		MI+(CD4+AT2R-)		P Value					
	Baseline	Dobutamine	Baseline	Dobutamine	Baseline	Dobutamine	P1	P2	P3	P4	P5	P6
Diastolic indices												
-dP/dtmin (mmHg/s)	-4736 ± 747.8	-5689 ± 447.1	-5333 ± 570.8	-6808 ± 292.2	-4298 ± 293.9	-5408 ± 296.0	ns	ns	ns	<0.05*	ns	<0.01**
Tau (msec)	14.32 ± 1.250	11.96 ± 0.920	11.03 ± 1.866	10.40 ± 1.482	16.99 ± 1.257	12.98 ± 0.9085	ns	ns	<0.05*	ns	ns	ns

Fig.5.11: Hemodynamic characteristics. Hemodynamic characteristics measured in the left ventricular artery using pressure-volume loop (P/V-loop) method in 4-week-old rats, which undergone LAD ligation plus saline, intra-myocardial transplantation with splenic CD4+AT2R+ or CD4+AT2R- T cells. Mean ± SEM, *P1*: MI+CD4+AT2R+ vs. MI+Saline (Baseline), *P2*: MI+CD4+AT2R- vs. MI+Saline (Baseline), *P3*: MI+CD4+AT2R+ vs. MI+CD4+AT2R- (Baseline), *P4*: MI+CD4+AT2R+ vs. MI+Saline (Dobutamine), *P5*: MI+CD4+AT2R- vs. MI+Saline (Dobutamine), *P6*: MI+CD4+AT2R+ vs. MI+CD4+AT2R- (Dobutamine), ns: not significant, Student T-test. Taken from Skorska A et al., *JCMM* (2015)

HR: heart rate, **Pmax**: maximal pressure, **PES**: end systolic pressure, **PED**: end diastolic pressure, **ESV**: end systolic volume, **EDV**: end diastolic volume, **SV**: stroke volume, **CO**: cardiac output (=SV x HR), **EF**: ejection fraction, **dP/dtmax**: maximum rate of pressure change in left ventricle (LV), **-dP/dtmin (mmHg/s)**: minimum rate of pressure change in LV, **SW**: stroke work, **Tau**: isovolumic relaxation of time

6 Discussion

MI is a frequent cause of heart failure and death. A vast body of evidence showed AngII as a major inflammatory agent, acting through modulation of responses of immune and inflammatory cells. Actions of AngII are mediated by two receptors, AT1R and AT2R. Research on the renin-angiotensin system with respect to cardiac diseases, in particular on actions of angiotensin II via the AT2 receptor, is constantly increasing. Therefore, the understanding of the crosstalk between the RAS system and the immune system, especially the participating (immunocompetent) cells was the major topic in the present study.

In this thesis, for the first time AT2R expression on CD4⁺ T cells of humans as well as rats was assessed and its regulation in cardiac disease was described. AT2R expression on human peripheral blood CD4⁺ T cells was higher in healthy donors than in HF patients. In a rat MI model displaying cardiac remodeling with fibrosis/elevated collagen density and loss of heart function, as is typical for HF, CD4⁺AT2R⁺ T cell number was increased in the heart and spleen but diminished in blood compared to sham-treated animals. Our findings are in accordance with previous reports of elevated AT2R levels in the adult heart after MI induction (72) and specific AT2R activation after MI induction (73). Whereas previous work has mostly addressed AT2 receptor levels in whole tissues: Altarache-Xifro et al. (2009) showed ATR up-regulation in c-kit⁺ stem cells of rats subjected to MI, and Curato et al. (2010) detected splenic AT2R⁺ - expressing CD8 T cells. Based on this and on our novel findings in animal models, it is likely that the mobilization of CD4⁺AT2R⁺ T cells to the heart after RAS activation may cause their reduction in peripheral blood. Given previous observations of AT2R stimulating cell differentiation and migration (72,76), it seems likely that AT2R is actively involved in the selective extravasation of effector CD4⁺AT2R⁺ T cells into injured myocardium. The elevated levels of AT2R detected on CD4⁺ T cells in the infarcted heart might be the consequence of that. Moreover, flow cytometric analysis of the frequency of CD4⁺ T cells in peripheral blood of patients with heart failure showed a significant increase compared to healthy donors, indicating the importance of this T cell subset during the progression of cardiac remodeling to HF. It has long been appreciated that T cell subsets in inflammatory sites, like cardiac allografts and ischemic injury (77,78) down-regulate

CD62L (also known as L-selectin), the lymphoid homing receptor, but up-regulate CD44, a marker of activated effector T cells (79). A reduction of CD4+AT2R+ T cells was also found in blood CD44+CD62L- effector T cells of patients with HF, but not in CD44+CD62L+ cells, confirming our hypothesis that AT2R is influenced specifically on T cell subsets involved in cardiac inflammation and regeneration.

Pathologic processes such as congestive heart failure lead to remodeling of the heart and reduce the ability to function as a syncytium (80). Moreover, contractility is also influenced by expansion of the extracellular matrix with fluid, as observed in inflammatory states. These so-called intracellular edema results in functional ischemia and irreversible damage of the myocardium leading to scar formation. This damage is due to the abnormal failure of self-tolerance, where infiltrated lymphocytes are reacting against self-antigens. To elucidate the role that infiltrating CD4+AT2R+ T cells may play in this process, we analyzed inflammatory properties of these cells. CD4+AT2R+ T cells from MI rats as well as healthy and HF human donors overexpressed FoxP3 compared to CD4+AT2R- T cells, whereas CD25 remained unchanged. Treg cells were reported to contribute to prevention of autoimmune disease through expression of FoxP3 (81), and Tang et al.(82)(83) observed reduced CD4+CD25+ FoxP3+CD127low Treg cells in heart failure, suggesting that defective Treg might be involved in disturbed immune homeostasis and also responsible for uncontrolled T cell activation in HF. While AT2R does not seem to be selective for Treg, the detected overexpression of FoxP3 suggests an anti-inflammatory potential of CD4+AT2R+ cells. Thus, it underlines the importance of FoxP3 in the actions mediated via AT2R. Very recently, publications reported factors involved in FoxP3 expression, such as Sp1, NFATc2, AP1 and STAT5 binding to the *Foxp3* promotor (83) (75). Also our RT-PCR data showed an elevated trend towards NFATc2 mRNA in CD4+AT2R+ T cells compared to CD4+AT2R- T cells although not at a statistically significant level (data not shown).

One of the immunosuppressive properties characteristic for Treg cells is the potential to secrete IL-10 (84). Noteworthy, CD4+AT2R+ T cells produced significantly more IL-10 than CD4+AT2R- T cells *in vitro*, and AngII stimulation further induced IL-10 up- as well as TNF α and IFN- γ downregulation in these cells. AT2R was required for this regulation, as evident from selective inhibition with the AT2R antagonist, PD123319. The anti-inflammatory cytokine IL-10 activates JAK and/or STAT proteins leading to an

induction of JAK1/Tyk2 proteins, which further activate STAT3 and SOCS3 responsible for central anti-inflammatory responses of IL-10 in macrophages. IL-10 indirectly inhibits NF- κ B activation induced via TNF- α (**Fig. 6.1**) (85). The elevated IL-10 secretion by CD4+AT2R+ T cells might inhibit the activation of TNF- α and/or IFN- γ .

Here we postulated that when the actions of IFN- γ signaling are blocked, due to the elevated level of IL-10 cytokines, it plays an important role in inhibitory Smad7 downstream pathways, interfering with Smad2 and Smad3 binding and elicits a reduced inflammatory response (**Fig.6.1**). CD4+AT2R+ T cells markedly exerted cytokine secretion when compared to CD4+AT2R- T cells, which is likely mediated by AT2R. This indicates CD4+AT2R+ T cells as being regulatory cells.

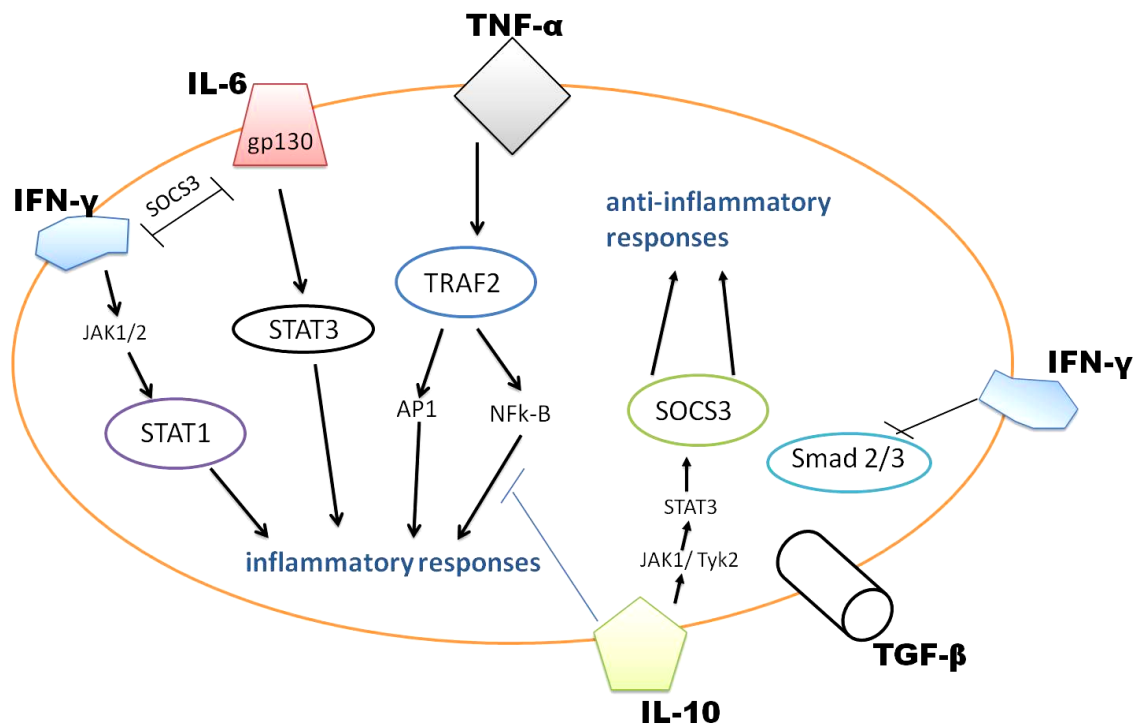


Fig. 6.1 Potential interactions of the pro- and anti-inflammatory cytokines towards immune response under ischemia conditions. The CD4+AT2R+ T cells reveal immunoregulatory properties, due to their elevated secretion of IL-10 and downregulation in production of pro-inflammatory cytokines (TNF- α , IFN- γ). Additionally, the predominant levels of IL-10 might inhibit IFN- γ actions promoting the anti-inflammatory actions. **SOCS3** – suppressor of cytokine 3; **JAK** – Janus kinase; **STAT** - signal transducers and activators of transcription; **TRAF** – TNF receptor-associated factor; **AP1** – activator protein 1; **NF- κ B** – nuclear factor “kappa-light-chain-enhancer” of activated B cells; **Tyk** - tyrosine kinase; **Smad** - intracellular protein of TGF β family; **TGF- β** – transforming growth factor- β ; **IL** – interleukin; **IFN- γ** – interferon- γ ; **TNF- α** - tumor necrosis factor- alpha.

Taking into account the above described evidence of CD4+AT2R+ T cell anti-inflammatory potential, especially in HF individuals or under RAS stimulation, we hypothesized that CD4+AT2R+ T cells of MI rats transplanted to recipient MI hearts might improve cardiac function. Indeed, pressure and volume assessment in the left ventricles of rats with MI plus injected splenic CD4+AT2R+ T cells showed improved myocardial performance in comparison to those rats with CD4+AT2R- injected cells. Hearts derived from rats with MI+(CD4+AT2R+) presented a significant reduction in infarct size compared to hearts from the MI+(CD4+AT2R-) group. Our findings align well with studies of AT2R stimulation with Compound 21 (C21), which led to an improvement in hemodynamics and reduction of infarct size due to C21-suppressed inflammatory actions as shown by significant decrease of cytokines (IL-1 β , MCP-1, IL-2, IL-6) in plasma and peri-infarct zone(73).

In an animal model of autoimmune diabetes, injected regulatory T cells were markedly present in lymph nodes rather than at the site of inflammation (86). In contrast, in a model of multiple sclerosis, transplanted cells accumulated directly at the site of inflammation in the nervous system (87). Therefore, it remains to be clarified whether the beneficial actions of transferred CD4+AT2R+ cells observed by us occur directly in the inflamed heart or whether draining lymph nodes are involved.

Irrespective of the final site of action, we provide evidence that AT2R+CD4+ cells possess high regenerative potential. Their selective stimulation may open up promising treatment opportunities for cardiac therapy. Here, the AT2R agonist Compound 21 may be a suitable candidate for future applications (88).

In sum, we identified CD4+AT2R+ as a novel regulatory T cell subset with beneficial impact on cardiac function after MI. CD4+AT2R+ T cells were upregulated in HF patients as well as MI rats and displayed anti-inflammatory properties (induction of FoxP3 and IL-10, downregulation of TNF- α and IFN- γ) compared to CD4+AT2R- cells. Myocardial transplantation of CD4+AT2R+ T cells led to improved cardiac function and reduced infarct size in a rat MI model. Our results introduce the AT2 receptor as a beneficial AngII-mediating receptor, implying that CD4+AT2R+ cells are a highly promising population for regenerative therapy, as they are suitable for myocardial transplantation, pharmacological AT2R activation or a combination thereof.

7 Conclusion

Taken together, our study contributes to the understanding of CD4+AT2R+ cell function after MI. We identified this potential novel regulatory T cell subset, which expresses FoxP3 and various cytokines (i.e. IL-10, TNF- α , IFN- γ), improves cardiac function and reduces infarct size. The underlying results indicate the AT2 receptor as a beneficial AngII-mediating receptor of the RAS system, implying that CD4+AT2R+ cells can be included in therapeutic approaches for the treatment of cardiac diseases, due to its upregulation in the infarcted state. The application of this T cell subset may improve the healing process of compromised heart tissue and contribute to a better quality of life in affected patients.

Financial support

This work was supported by:

BMBF (FKZ 0312138A, FKZ 0316159); DFG (DA1296-2/1); European Social Fonds (FKZ V230-630-08-TFMV-F/S-035; ESF/IV-WM-B34-0011/08), (FKZ V630-F-075-2010/183; V630-S-075-2010/185; ESF/IV-WM-B34-0030/10), European Commission (FP7) SICA-HF (no. 241558), National Natural Science Fundation of China (no. 81370321) and Shanghai Pujiang Program (no. 13PJ1405800).

Acknowledgements

This work was carried out in the Research Laboratories for Cardiac Tissue and Organ Replacement (Forschungslaboratorien für kardialen Gewebe- und Organersatz; FKGO), Reference- and Translation Center for Cardiac Stem Cell Therapy (RTC), Department of Cardiac Surgery, Universitätsmedizin Rostock, Germany.

I greatly appreciate my mentor Prof. Dr. Gustav Steinhoff, Director of the Department of Cardiac Surgery for his scientific supervision, instructive advice and useful suggestions. Working in his laboratory I got the opportunity to conduct my experiments in very well-equipped place, close to the clinical environment gave me the chance to understand how to transfer the basic knowledge into the development of therapies and clinical application for cardiac regeneration.

Prof. Dr. Robert David, Group Leader of the FKGO I am deeply thankful for his supervision especially at the compilation of the data, for new ideas during the writing process of the publication and this dissertation. Moreover, I express my grateful acknowledgements to Prof. Dr. Jun Li (currently leading the Clinical Stem Cell Research Center and Department of Cardiovascular Surgery, Renji Hospital, Shanghai Jiao Tong University, School of Medicine) for his supervision in the entire part of my dissertation, for interesting discussions about the AT2 receptor.

I also want to thank Prof. Dr. Thomas Unger (former Director of the Center for Cardiovascular Research (CCR) and Institute of Pharmacology, Charité - Universitätsmedizin Berlin) for support and scientific advice over the first months when I collected first experience in the field of RAS and angiotensin II type 2.

I am deeply indebted to my former mentor Dr. Milan C. Pesič, who regrettably left us last year. Thanks to his deep trust, patient guidance and helpful instruction during the first years I spent in Germany working at his praxis (Bad Harzburg) I got the opportunity to develop myself working on a new project and from then on I've begun my journey with research and stem cells. Thanks to him I wished to learn more about it and decided to start the PhD which he supported during the entire time.

Yet, I would like to hand on my gratitude to his companion Mrs. Ruth Barg, daughters (Dr. Katrin Pesič, Annette Baudrexl) and family, who I could meet over the years.

I also want to say thank you to all former staff members of the company Biofactor GmbH, LyContract GmbH: Heidi Reinecke, Samira Musolik, Elvira Mund and medical

praxis: Mrs. Marquardt, Anja Kricke. First months I spent in Bad Harzburg were not easy, not only because of a new language, but also a different place, culture without my family. I am deeply thankful to Anja for her help, trust and power she gave me during our excursions, hikes and mountain walks. Our friendship remained exactly the same way over the years even I moved to other cities.

I would like to thank my former colleagues from Berlin: Dr. Caterina Curato, Dr. Svetlana Slavič, Dr. Wassim Altarche-Xifro. I had a wonderful time with you, we were a great team and so extremely determined during our numerous MACS/FACS isolations of cells. You gave me power over the first months of my scientific journey, which then helped me immediately after moving to another city. I also thank Dr. Veronica Valero, Pawel Namsolleck, Miranda Schröder, Dr. Marie Brinckmann and Melanie Timm for their constant assistance.

To my Rostock friends I say a big thank! I will be honest and admit that I have been warmly received by ALL of you immediately after moving from Berlin to your city. I would especially like to extend my sincere gratitude to Dr. Ralf Gäbel, Dr. Marion Ludwig, Dr. Cornelia A. Lux, Anita Tölk, Gabriela Kleiner, Dr. Christian Klopsch, Christian Maschmeier, Paula Müller, Frauke Hausburg, Praveen Vasudevan. I wish to thank my previous and current colleagues: Margit Fritsche, Madeleine Bartsch, Dr. Heiko Lemcke, Peter Mark, Karina Müller-Brown, Evgenya Delyagina, Anna Schade, Natalia Voronina, Sandra Bubritzki, Dr. Cajetan Lang, Dr. Julia Nesteruk, Julia Jung, Haval Sadraddin, Saifullah Abubaker, Dr. Christian Rimmbach, Thomas Michael, Dr. Frauke Stähler, Dr. Sandra Kurzawski, Dr. Dario Furlani, Erik Pittermann, Dr. Koji Hirano, Anke Wagner, Stephanie Zirkel and Dr. Yue Zhang. Thanks to all of them for creating such a comfortable learning and working atmosphere in which everybody profits from the scientific discussion and efficient cooperation.

High tribute shall be paid to RTC/GxP team: Dr. Gudrun Tiedemann, Dr. Jana Große, Dr. Ulrike Ruch; physicians: PD Dr. Alexander Kaminski, PD Dr. Peter Donndorf, Dr. Catharina Nesselmann; secretary's office: Jana Gabriel and Katrin Höfer. They provided essential help to my work and study. Moreover, I love to thank all students who I supervised independently during all kinds of projects (master, bachelor, medical students) or the duration of the internship. Such experience was very valuable not only for any scientific development, but also my person.

The progress of this work is indispensably based on the collaboration with the following scientists and research institutes: Prof. Dr. Brigitte Vollmar, Institute for Experimental Surgery, Universitätsmedizin Rostock, PD. Dr. Dr. Stephan von Haehling, Center for Cardiovascular Research and Department of Cardiology, Campus Virchow-Klinikum, Charité – Universitätsmedizin Berlin, Prof. Dr. Brigitte Müller-Hilke and Dr. Robby Engelmann from FACS Core Facility, Rostock University, Medical Center, Dr. Jun Dong, Deutsches Rheuma-Forschungszentrum (DRFZ), Berlin, Toralf Kaiser and Jenny Kirsch from Flow Cytometry Core Facility at DRFZ. I greatly acknowledge their collaboration and support.

Marco Maasch, Ralf Gäbel; Anita Tölk, Cornelia Lux, Svetlana Gerter, Christian Maschmeier, Paula Müller, Praveen Vasudevan thank you for every time I spent with you after lab work, whether during the coffee break fulfilled with informative discussions, in nature active (at seaside, hiking, barbecue, cycling, dancing, and sailing) or by listening to the music.... This place is with YOU very special.

I also thank my dear good friend from study Anna Paszkiewicz for her long-term friendship. Despite the distance and rare possibilities to talk to each other, you were always present in my life without any doubt. I am also grateful to meet you, dear family Maasch: Marco, Gertrud, Claus, Andre, Jörg, Cornelia and Rainer Speer. Last but not least, I truly thank my parents Christina and Christoph Skórski, my sister Małgorzata Skórska-Kućma and her husband Grzegorz, my brother Dominik and his wife Magdalena, and my brother Robert for their sisterly/brotherly help, advice and belief in me, especially during the last years.

References

1. 2012 European Cardiovascular Disease Statistics [Internet]. Available from: <http://www.escardio.org/The-ESC/Initiatives/EuroHeart/2012-European-Cardiovascular-Disease-Statistics>
2. Jennings RB. Historical perspective on the pathology of myocardial ischemia/reperfusion injury. *Circ Res*. 2013;**113**:428–438.
3. Frangogiannis NG. The mechanistic basis of infarct healing. *Antioxid Redox Signal*. 2006;**8**:1907–1939.
4. Thygesen K, Alpert JS, Jaffe AS, Simoons ML, Chaitman BR, White HD, Joint ESC/ACCF/AHA/WHF Task Force for Universal Definition of Myocardial Infarction, Authors/Task Force Members Chairpersons, Thygesen K, Alpert JS, White HD, Biomarker Subcommittee, Jaffe AS, Katus HA, Apple FS, Lindahl B, Morrow DA, ECG Subcommittee, Chaitman BR, Clemmensen PM, Johanson P, Hod H, Imaging Subcommittee, Underwood R, Bax JJ, Bonow JJ, Pinto F, Gibbons RJ, Classification Subcommittee, Fox KA, et al. Third universal definition of myocardial infarction. *J Am Coll Cardiol*. 2012;**60**:1581–1598.
5. Thygesen K, Alpert JS, White HD, Joint ESC/ACCF/AHA/WHF Task Force for the Redefinition of Myocardial Infarction. Universal definition of myocardial infarction. *J Am Coll Cardiol*. 2007;**50**:2173–2195.
6. Paiva L, Providência R, Barra S, Dinis P, Faustino AC, Gonçalves L. Universal definition of myocardial infarction: clinical insights. *Cardiology*. 2015;**131**:13–21.
7. Braunwald E. Heart failure. *JACC Heart Fail*. 2013;**1**:1–20.
8. Esler M, Alvarenga M, Pier C, Richards J, Osta A El-, Barton D, Haikerwal D, Kaye D, Schlaich M, Guo L, Jennings G, Socratous F, Lambert G. The neuronal noradrenaline transporter, anxiety and cardiovascular disease. *J Psychopharmacol Oxf Engl*. 2006;**20**:60–66.
9. Mann DL, Bristow MR. Mechanisms and models in heart failure: the biomechanical model and beyond. *Circulation*. 2005;**111**:2837–2849.
10. Heinz Weber, Christoph Herrmann-Lingen, Rainer Spinka, Ferdinand Rudolf Waldenberger H. Herzinsuffizienz: vom Symptom zum Therapie-Erfolg.
11. Remme WJ, Swedberg K, Task Force for the Diagnosis and Treatment of Chronic Heart Failure, European Society of Cardiology. Guidelines for the diagnosis and treatment of chronic heart failure. *Eur Heart J*. 2001;**22**:1527–1560.

-
12. Hobbs RE. Guidelines for the diagnosis and management of heart failure. *Am J Ther.* 2004;**11**:467–472.
 13. Hess OM. Risk stratification in hypertrophic cardiomyopathy: fact or fiction? *J Am Coll Cardiol.* 2003;**42**:880–881.
 14. Chatterjee K, Rame JE. Systolic heart failure: chronic and acute syndromes. *Crit Care Med.* 2008;**36**:S44–S51.
 15. Classes of Heart Failure. Available from:
http://www.heart.org/HEARTORG/Conditions/HeartFailure/AboutHeartFailure/Classes-of-Heart-Failure_UCM_306328_Article.jsp
 16. Rock KL, Kono H. The inflammatory response to cell death. *Annu Rev Pathol.* 2008;**3**:99–126.
 17. Mozaffari MS, Liu JY, Abebe W, Baban B. Mechanisms of load dependency of myocardial ischemia reperfusion injury. *Am J Cardiovasc Dis.* 2013;**3**:180–196.
 18. Dreyer WJ, Michael LH, Nguyen T, Smith CW, Anderson DC, Entman ML, Rossen RD. Kinetics of C5a release in cardiac lymph of dogs experiencing coronary artery ischemia-reperfusion injury. *Circ Res.* 1992;**71**:1518–1524.
 19. Lefer DJ, Jones SP, Girod WG, Baines A, Grisham MB, Cockrell AS, Huang PL, Scalia R. Leukocyte-endothelial cell interactions in nitric oxide synthase-deficient mice. *Am J Physiol.* 1999;**276**:H1943–H1950.
 20. Ventura-Clapier R, Garnier A, Veksler V. Energy metabolism in heart failure. *J Physiol.* 2004;**555**:1–13.
 21. Katz AM. The ‘modern’ view of heart failure: how did we get here? *Circ Heart Fail.* 2008;**1**:63–71.
 22. Gordon JW, Shaw JA, Kirshenbaum LA. Multiple facets of NF- κ B in the heart: to be or not to NF- κ B. *Circ Res.* 2011;**108**:1122–1132.
 23. Valen G. Signal transduction through nuclear factor kappa B in ischemia-reperfusion and heart failure. *Basic Res Cardiol.* 2004;**99**:1–7.
 24. Saini HK, Xu Y-J, Zhang M, Liu PP, Kirshenbaum LA, Dhalla NS. Role of tumour necrosis factor-alpha and other cytokines in ischemia-reperfusion-induced injury in the heart. *Exp Clin Cardiol.* 2005;**10**:213–222.
 25. Schulz R, Aker S, Belosjorow S, Heusch G. TNFalpha in ischemia/reperfusion injury and heart failure. *Basic Res Cardiol.* 2004;**99**:8–11.

-
26. Pennica D, King KL, Shaw KJ, Luis E, Rullamas J, Luoh SM, Darbonne WC, Knutzon DS, Yen R, Chien KR. Expression cloning of cardiotrophin 1, a cytokine that induces cardiac myocyte hypertrophy. *Proc Natl Acad Sci U S A*. 1995;**92**:1142–1146.
 27. Saito M, Yoshida K, Hibi M, Taga T, Kishimoto T. Molecular cloning of a murine IL-6 receptor-associated signal transducer, gp130, and its regulated expression in vivo. *J Immunol Baltim Md 1950*. 1992;**148**:4066–4071.
 28. Nian M, Lee P, Khaper N, Liu P. Inflammatory cytokines and postmyocardial infarction remodeling. *Circ Res*. 2004;**94**:1543–1553.
 29. Kucharz null, Wilk null. Dynamics of serum interleukin-6 level in patients with acute myocardial infarction. *Eur J Intern Med*. 2000;**11**:253–256.
 30. Frangogiannis NG, Smith CW, Entman ML. The inflammatory response in myocardial infarction. *Cardiovasc Res*. 2002;**53**:31–47.
 31. Jordan JE, Zhao ZQ, Vinten-Johansen J. The role of neutrophils in myocardial ischemia-reperfusion injury. *Cardiovasc Res*. 1999;**43**:860–878.
 32. Weyrich AS, Buerke M, Albertine KH, Lefer AM. Time course of coronary vascular endothelial adhesion molecule expression during reperfusion of the ischemic feline myocardium. *J Leukoc Biol*. 1995;**57**:45–55.
 33. Gumina RJ, Newman PJ, Kenny D, Warltier DC, Gross GJ. The leukocyte cell adhesion cascade and its role in myocardial ischemia-reperfusion injury. *Basic Res Cardiol*. 1997;**92**:201–213.
 34. Nah D-Y, Rhee M-Y. The inflammatory response and cardiac repair after myocardial infarction. *Korean Circ J*. 2009;**39**:393–398.
 35. Dewald O, Frangogiannis NG, Zoerlein MP, Duerr GD, Taffet G, Michael LH, Welz A, Entman ML. A murine model of ischemic cardiomyopathy induced by repetitive ischemia and reperfusion. *Thorac Cardiovasc Surg*. 2004;**52**:305–311.
 36. Christia P, Bujak M, Gonzalez-Quesada C, Chen W, Dobaczewski M, Reddy A, Frangogiannis NG. Systematic characterization of myocardial inflammation, repair, and remodeling in a mouse model of reperfused myocardial infarction. *J Histochem Cytochem Off J Histochem Soc*. 2013;**61**:555–570.
 37. Gasparo M de, Catt KJ, Inagami T, Wright JW, Unger T. International union of pharmacology. XXIII. The angiotensin II receptors. *Pharmacol Rev*. 2000;**52**:415–472.

-
38. Reid IA. THE RENIN-ANGIOTENSIN SYSTEM: PHYSIOLOGY, PATHOPHYSIOLOGY, AND PHARMACOLOGY. *Adv Physiol Educ.* 1998;**275**:S236–S245.
 39. Paul M, Poyan Mehr A, Kreutz R. Physiology of local renin-angiotensin systems. *Physiol Rev.* 2006;**86**:747–803.
 40. Carey RM, Padia SH. Angiotensin AT2 receptors: control of renal sodium excretion and blood pressure. *Trends Endocrinol Metab TEM.* 2008;**19**:84–87.
 41. Bader M. Tissue renin-angiotensin-aldosterone systems: Targets for pharmacological therapy. *Annu Rev Pharmacol Toxicol.* 2010;**50**:439–465.
 42. Kaschina E, Unger T. Angiotensin AT1/AT2 receptors: regulation, signalling and function. *Blood Press.* 2003;**12**:70–88.
 43. Leung PS. Frontiers in research of the renin-angiotensin system on human disease. Dordrecht, Netherlands: Springer; 2007.
 44. Volpe M, Musumeci B, Paolis P De, Savoia C, Morganti A. Angiotensin II AT2 receptor subtype: an uprising frontier in cardiovascular disease? *J Hypertens.* 2003;**21**:1429–1443.
 45. Volpe M, Savoia C, Paolis P De, Ostrowska B, Tarasi D, Rubattu S. The renin-angiotensin system as a risk factor and therapeutic target for cardiovascular and renal disease. *J Am Soc Nephrol JASN.* 2002;**13 Suppl 3**:S173–S178.
 46. Grady EF, Sechi LA, Griffin CA, Schambelan M, Kalinyak JE. Expression of AT2 receptors in the developing rat fetus. *J Clin Invest.* 1991;**88**:921–933.
 47. Nakajima M, Hutchinson HG, Fujinaga M, Hayashida W, Morishita R, Zhang L, Horiuchi M, Pratt RE, Dzau VJ. The angiotensin II type 2 (AT2) receptor antagonizes the growth effects of the AT1 receptor: gain-of-function study using gene transfer. *Proc Natl Acad Sci U S A.* 1995;**92**:10663–10667.
 48. Nio Y, Matsubara H, Murasawa S, Kanasaki M, Inada M. Regulation of gene transcription of angiotensin II receptor subtypes in myocardial infarction. *J Clin Invest.* 1995;**95**:46–54.
 49. Busche S, Gallinat S, Bohle RM, Reinecke A, Seebeck J, Franke F, Fink L, Zhu M, Summers C, Unger T. Expression of angiotensin AT(1) and AT(2) receptors in adult rat cardiomyocytes after myocardial infarction. A single-cell reverse transcriptase-polymerase chain reaction study. *Am J Pathol.* 2000;**157**:605–611.

-
50. Steckelings UM, Kaschina E, Unger T. The AT2 receptor--a matter of love and hate. *Peptides*. 2005;**26**:1401–1409.
 51. Dzau VJ. Implications of local angiotensin production in cardiovascular physiology and pharmacology. *Am J Cardiol*. 1987;**59**:59A – 65A.
 52. Mackins CJ, Kano S, Seyedi N, Schäfer U, Reid AC, Machida T, Silver RB, Levi R. Cardiac mast cell-derived renin promotes local angiotensin formation, norepinephrine release, and arrhythmias in ischemia/reperfusion. *J Clin Invest*. 2006;**116**:1063–1070.
 53. Booz GW, Baker KM. Molecular signalling mechanisms controlling growth and function of cardiac fibroblasts. *Cardiovasc Res*. 1995;**30**:537–543.
 54. Tang T-T, Yuan J, Zhu Z-F, Zhang W-C, Xiao H, Xia N, Yan X-X, Nie S-F, Liu J, Zhou S-F, Li J-J, Yao R, Liao M-Y, Tu X, Liao Y-H, Cheng X. Regulatory T cells ameliorate cardiac remodeling after myocardial infarction. *Basic Res Cardiol*. 2012;**107**:232.
 55. Walcher D, Vasic D, Heinz P, Bach H, Durst R, Hausauer A, Hombach V, Marx N. LXR activation inhibits chemokine-induced CD4-positive lymphocyte migration. *Basic Res Cardiol*. 2010;**105**:487–494.
 56. Abbate A, Biondi-Zoccai GGL, Baldi A. Pathophysiologic role of myocardial apoptosis in post-infarction left ventricular remodeling. *J Cell Physiol*. 2002;**193**:145–153.
 57. Beyersdorf N, Gaupp S, Balbach K, Schmidt J, Toyka KV, Lin C-H, Hanke T, Hünig T, Kerkau T, Gold R. Selective targeting of regulatory T cells with CD28 superagonists allows effective therapy of experimental autoimmune encephalomyelitis. *J Exp Med*. 2005;**202**:445–455.
 58. Jankowski M, Bissonauth V, Gao L, Gangal M, Wang D, Danalache B, Wang Y, Stoyanova E, Cloutier G, Blaise G, Gutkowska J. Anti-inflammatory effect of oxytocin in rat myocardial infarction. *Basic Res Cardiol*. 2010;**105**:205–218.
 59. Maisel A, Cesario D, Baird S, Rehman J, Haghighi P, Carter S. Experimental autoimmune myocarditis produced by adoptive transfer of splenocytes after myocardial infarction. *Circ Res*. 1998;**82**:458–463.
 60. Varda-Bloom N, Leor J, Ohad DG, Hasin Y, Amar M, Fixler R, Battler A, Eldar M, Hasin D. Cytotoxic T lymphocytes are activated following myocardial infarction and can recognize and kill healthy myocytes in vitro. *J Mol Cell Cardiol*. 2000;**32**:2141–2149.

-
61. Hofmann U, Frantz S. Role of lymphocytes in myocardial injury, healing, and remodeling after myocardial infarction. *Circ Res*. 2015;**116**:354–367.
 62. Scheerder I De, Vandekerckhove J, Robbrecht J, Algoed L, Buyzere M De, Langhe J De, Schrijver G De, Clement D. Post-cardiac injury syndrome and an increased humoral immune response against the major contractile proteins (actin and myosin). *Am J Cardiol*. 1985;**56**:631–633.
 63. Moraru M, Roth A, Keren G, George J. Cellular autoimmunity to cardiac myosin in patients with a recent myocardial infarction. *Int J Cardiol*. 2006;**107**:61–66.
 64. Sakaguchi S, Yamaguchi T, Nomura T, Ono M. Regulatory T cells and immune tolerance. *Cell*. 2008;**133**:775–787.
 65. Sakaguchi S, Sakaguchi N, Asano M, Itoh M, Toda M. Immunologic self-tolerance maintained by activated T cells expressing IL-2 receptor alpha-chains (CD25). Breakdown of a single mechanism of self-tolerance causes various autoimmune diseases. *J Immunol Baltim Md 1950*. 1995;**155**:1151–1164.
 66. Asano M, Toda M, Sakaguchi N, Sakaguchi S. Autoimmune disease as a consequence of developmental abnormality of a T cell subpopulation. *J Exp Med*. 1996;**184**:387–396.
 67. Levings MK, Allan S, Hennezel E d', Piccirillo CA. Functional dynamics of naturally occurring regulatory T cells in health and autoimmunity. *Adv Immunol*. 2006;**92**:119–155.
 68. Piccirillo CA, d'Hennezel E, Sgouroudis E, Yurchenko E. CD4+Foxp3+ regulatory T cells in the control of autoimmunity: in vivo veritas. *Curr Opin Immunol*. 2008;**20**:655–662.
 69. Guzik TJ, Hoch NE, Brown KA, McCann LA, Rahman A, Dikalov S, Goronzy J, Weyand C, Harrison DG. Role of the T cell in the genesis of angiotensin II induced hypertension and vascular dysfunction. *J Exp Med*. 2007;**204**:2449–2460.
 70. Kvakan H, Kleinewietfeld M, Qadri F, Park J-K, Fischer R, Schwarz I, Rahn H-P, Plehm R, Wellner M, Elitok S, Gratze P, Dechend R, Luft FC, Muller DN. Regulatory T cells ameliorate angiotensin II-induced cardiac damage. *Circulation*. 2009;**119**:2904–2912.
 71. Curato C, Slavic S, Dong J, Skorska A, Altarche-Xifró W, Miteva K, Kaschina E, Thiel A, Imboden H, Wang J, Steckelings U, Steinhoff G, Unger T, Li J. Identification of noncytotoxic and IL-10-producing CD8+AT2R+ T cell population in response to ischemic heart injury. *J Immunol Baltim Md 1950*. 2010;**185**:6286–6293.

-
72. Altarache-Xifró W, Curato C, Kaschina E, Grzesiak A, Slavic S, Dong J, Kappert K, Steckelings M, Imboden H, Unger T, Li J. Cardiac c-kit+AT2+ cell population is increased in response to ischemic injury and supports cardiomyocyte performance. *Stem Cells Dayt Ohio*. 2009;**27**:2488–2497.
 73. Kaschina E, Grzesiak A, Li J, Foryst-Ludwig A, Timm M, Rompe F, Sommerfeld M, Kemnitz UR, Curato C, Namsolleck P, Tschöpe C, Hallberg A, Alterman M, Hucko T, Paetsch I, Dietrich T, Schnackenburg B, Graf K, Dahlöf B, Kintscher U, Unger T, Steckelings UM. Angiotensin II type 2 receptor stimulation: a novel option of therapeutic interference with the renin-angiotensin system in myocardial infarction? *Circulation*. 2008;**118**:2523–2532.
 74. Chomczynski P, Sacchi N. Single-step method of RNA isolation by acid guanidinium thiocyanate-phenol-chloroform extraction. *Anal Biochem*. 1987;**162**:156–159.
 75. DeGrendele HC, Estess P, Siegelman MH. Requirement for CD44 in activated T cell extravasation into an inflammatory site. *Science*. 1997;**278**:672–675.
 76. Côté F, Do TH, Laflamme L, Gallo JM, Gallo-Payet N. Activation of the AT(2) receptor of angiotensin II induces neurite outgrowth and cell migration in micro-explant cultures of the cerebellum. *J Biol Chem*. 1999;**274**:31686–31692.
 77. Ochando JC, Yopp AC, Yang Y, Garin A, Li Y, Boros P, Llodra J, Ding Y, Lira SA, Krieger NR, Bromberg JS. Lymph node occupancy is required for the peripheral development of alloantigen-specific Foxp3+ regulatory T cells. *J Immunol Baltim Md 1950*. 2005;**174**:6993–7005.
 78. Huebener P, Abou-Khamis T, Zymek P, Bujak M, Ying X, Chatila K, Haudek S, Thakker G, Frangogiannis NG. CD44 is critically involved in infarct healing by regulating the inflammatory and fibrotic response. *J Immunol Baltim Md 1950*. 2008;**180**:2625–2633.
 79. DeGrendele HC, Estess P, Siegelman MH. Requirement for CD44 in activated T cell extravasation into an inflammatory site. *Science*. 1997;**278**:672–675.
 80. Taqueti VR, Mitchell RN, Lichtman AH. Protecting the pump: controlling myocardial inflammatory responses. *Annu Rev Physiol*. 2006;**68**:67–95.
 81. Tone Y, Furuuchi K, Kojima Y, Tykocinski ML, Greene MI, Tone M. Smad3 and NFAT cooperate to induce Foxp3 expression through its enhancer. *Nat Immunol*. 2008;**9**:194–202.
 82. Tang T-T, Ding Y-J, Liao Y-H, Yu X, Xiao H, Xie J-J, Yuan J, Zhou Z-H, Liao M-Y, Yao R, Cheng Y, Cheng X. Defective circulating CD4CD25+Foxp3+CD127(low) regulatory T-cells in patients with chronic heart

-
- failure. *Cell Physiol Biochem Int J Exp Cell Physiol Biochem Pharmacol*. 2010;**25**:451–458.
83. Tang T-T, Yuan J, Zhu Z-F, Zhang W-C, Xiao H, Xia N, Yan X-X, Nie S-F, Liu J, Zhou S-F, Li J-J, Yao R, Liao M-Y, Tu X, Liao Y-H, Cheng X. Regulatory T cells ameliorate cardiac remodeling after myocardial infarction. *Basic Res Cardiol*. 2012;**107**:232.
84. Hara M, Kingsley CI, Niimi M, Read S, Turvey SE, Bushell AR, Morris PJ, Powrie F, Wood KJ. IL-10 is required for regulatory T cells to mediate tolerance to alloantigens in vivo. *J Immunol Baltim Md 1950*. 2001;**166**:3789–3796.
85. Schottelius AJ, Mayo MW, Sartor RB, Baldwin ASJ. Interleukin-10 signaling blocks inhibitor of kappaB kinase activity and nuclear factor kappaB DNA binding. *J Biol Chem*. 1999;**274**:31868–31874.
86. Szanya V, Ermann J, Taylor C, Holness C, Fathman CG. The subpopulation of CD4+CD25+ splenocytes that delays adoptive transfer of diabetes expresses L-selectin and high levels of CCR7. *J Immunol Baltim Md 1950*. 2002;**169**:2461–2465.
87. McGeachy MJ, Stephens LA, Anderson SM. Natural recovery and protection from autoimmune encephalomyelitis: contribution of CD4+CD25+ regulatory cells within the central nervous system. *J Immunol Baltim Md 1950*. 2005;**175**:3025–3032.
88. Namsolleck P, Recarti C, Foulquier S, Steckelings UM, Unger T. AT(2) receptor and tissue injury: therapeutic implications. *Curr Hypertens Rep*. 2014;**16**:416.

The most of the work was published at JCMM. Figures/Tables, which were included in the thesis, were appropriately labeled:

Skorska A, Haehling S von, Ludwig M, Lux CA, Gaebel R, Kleiner G, Klopsch C, Dong J, Curato C, Altarache-Xifró W, Slavic S, Unger T, Steinhoff G, Li J, David R. The CD4(+) AT2R(+) T cell subpopulation improves post-infarction remodelling and restores cardiac function. *J Cell Mol Med*. 2015;19:1975–1985

Selbständigkeitserklärung

Ich versichere, die vorliegende Arbeit zum Thema „ Identification and characterization of CD4+AT2R+ T cell subpopulation in humans and rats“ selbständig verfasst und keine anderen Hilfsmittel, als die angegebenen benutzt zu haben. Stellen, die anderen Werken dem Wortlaut oder dem Sinn nach entnommen sind, habe ich in jedem einzelnen Fall durch Angabe der Quelle kenntlich gemacht.

Rostock, November 2015

Anna Skorska

Veröffentlichungen:

1. Curato C, Slavic S, Dong J, **Skorska A**, Altarche-Xifró W, Miteva K, Kaschina E, Thiel A, Imboden H, Wang J, Steckelings U, Steinhoff G, Unger T, Li J. Identification of noncytotoxic and IL-10-producing CD8+AT2R+ T cell population in response to ischemic heart injury. *J Immunol*. 2010;185:6286–6293.
2. Mark P, Tölk A, Lux CA, **Skorska A**, Pittermann E, Scharfenberg D, Li W, Ma N, Steinhoff G. Difference in proliferation potential and gene expression pattern of c-kit+ HSC subpopulations. *J Stem Cells Regen Med*. 2010;6:99–100.
3. **Skorska A**, Curato C, Altarche-Xifró W, Slavic S, Unger T, Steinhoff G, Li J. Identification and characterization of the CD4+AT2R+ T cell subpopulation in rats and humans. *J Stem Cells Regen Med*. 2010;6:131–132.
4. Ludwig M, **Skorska A**, Tölk A, Hopp H-H, Patejdl R, Li J, Steinhoff G, Noack T. Characterization of ion currents of murine CD117(pos) stem cells in vitro and their modulation under AT2 R stimulation. *Acta Physiol (Oxf)*. 2013;208:274–287.
5. Schade A, Delyagina E, Scharfenberg D, **Skorska A**, Lux C, David R, Steinhoff G. Innovative strategy for microRNA delivery in human mesenchymal stem cells via magnetic nanoparticles. *Int J Mol Sci*. 2013;14:10710–10726.
6. Delyagina E, Schade A, Scharfenberg D, **Skorska A**, Lux C, Li W, Steinhoff G. Improved transfection in human mesenchymal stem cells: effective intracellular release of pDNA by magnetic polyplexes. *Nanomedicine (Lond)*. 2014;9:999–1017.
7. Klopsch C, Kleiner G, **Skorska A**, Ludwig M, Gaebel R, Mueller K, Mela P, Jockenhoevel S, David R, Steinhoff G. Epicardial Erythropoietin patch most efficiently improves myocardial regeneration and performance after infarction. *Thorac Cardiovasc Surg*. 2014;62:SC6.
8. Laupheimer M, **Skorska A**, Große J, Tiedemann G, Steinhoff G, David R, Lux CA. Selective Migration of Subpopulations of Bone Marrow Cells along an SDF-1 α and ATP Gradient. *Bone Marrow Res*. 2014;2014:182645.
9. Schade A, Müller P, Delyagina E, Voronina N, **Skorska A**, Lux C, Steinhoff G, David R. Magnetic Nanoparticle Based Nonviral MicroRNA Delivery into Freshly Isolated CD105(+) hMSCs. *Stem Cells Int*. 2014;2014:197154.
10. Donndorf P, Lube L, Lux C, **Skorska A**, Steinhoff G, Kraft K. Mobilization of Bone Marrow-Derived Endothelial Progenitor Cells following Finnish Sauna: A Pilot Study. *Forsch Komplementmed*. 2015;22:246–250.
11. Hausburg F, Na S, Voronina N, **Skorska A**, Müller P, Steinhoff G, David R. Defini-

ing optimized properties of modified mRNA to enhance virus- and DNA- independent protein expression in adult stem cells and fibroblasts. *Cell Physiol Biochem*. 2015;35:1360–1371.

12. Ludwig M, Tölk A, **Skorska A**, Maschmeier C, Gaebel R, Lux CA, Steinhoff G, David R. Exploiting AT2R to Improve CD117 Stem Cell Function In Vitro and In Vivo--Perspectives for Cardiac Stem Cell Therapy. *Cell Physiol Biochem*. 2015;37:77–93.
13. **Skorska A**, Haehling S von, Ludwig M, Lux CA, Gaebel R, Kleiner G, Klopsch C, Dong J, Curato C, Altarache-Xifró W, Slavic S, Unger T, Steinhoff G, Li J, David R. The CD4(+) AT2R(+) T cell subpopulation improves post-infarction remodelling and restores cardiac function. *J Cell Mol Med*. 2015;19:1975–1985.

Ausgewählte Vorträge:

2010:

Workshop Kardiale Stammzelltherapie und Tissue engineering 2010, 28.– 30. April 2010 ; Internationale Naturschutzakademie Insel Vilm

und

44. DGBMT Jahrestagung 3 Länder Tagung D-A-CH, 05.-08. Oktober 2010, Rostock-Warnemünde

„Identification and characterization of the CD4+AT2R+T cell subpopulation in rats and humans“

Anna Skorska (Reference- and Translation Centre for Cardiac Stem Cell Therapy, DE); Curato C. (Center for Cardiovascular Research (CCR) and Institute of Pharmacology); Altarache-Xifró W. (Reference- and Translation Centre for Cardiac Stem Cell Therapy, DE); Slavic S., Unger T. (Center for Cardiovascular Research (CCR) and Institute of Pharmacology); Gustav Steinhoff, Li J. (University of Rostock, DE)

2012:

European Society for Artificial Organs (ESAO) Congress 2012 “from replacement to regeneration – from science to clinic. September 26th – 29th, 2012, Rostock

„Identification od cardioprotective CD4+AT2R+ T cell subpopulation in response to ischemic heart injury“

Poster Präsentation:

2010:

40th Annual Meeting of the German Society for Immunology (DGfI), 22 – 25 September 2010, in Leipzig

und

5th Annual Meeting of the German Society for Stem Cell Research (GSZ), 30 September – 2 October 2010, in Lübeck.

"Identification and characterization of the CD4+AT2R+ T cell subpopulation in rats and humans"

2012:

„Cardiac Regeneration and Vascular Biology“ Conference 2012, San Servolo – Venedig, Venice (Italy), May 24th – 26th 2012

und

3rd EACTS Meeting on Cardiac and Pulmonary Regeneration Berlin-Brandenburgische Akademie, Berlin, Germany, 14-15 December 2012.

THE CD4 + AT2R+ T CELL SUBPOPULATION IN RESPONSE TO ISCHAEMIC HEART INJURY

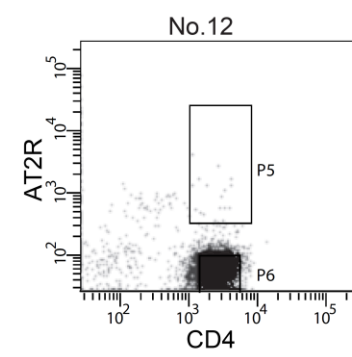
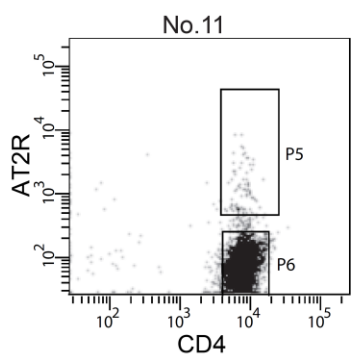
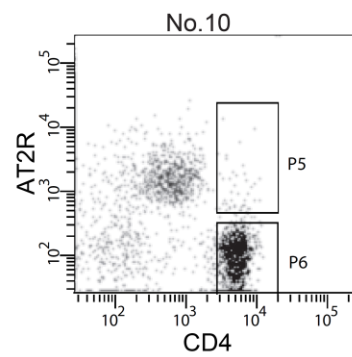
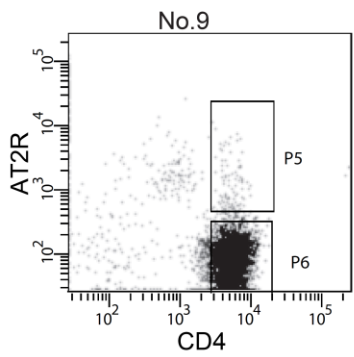
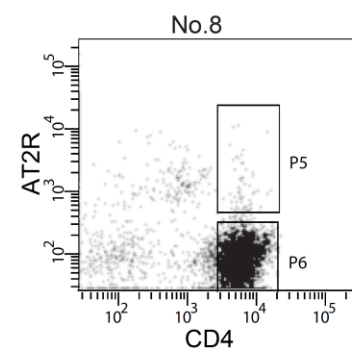
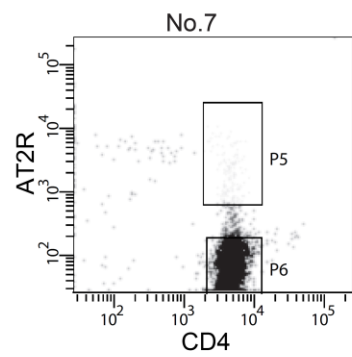
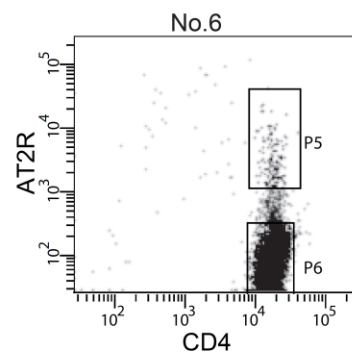
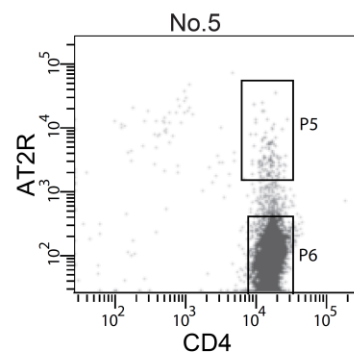
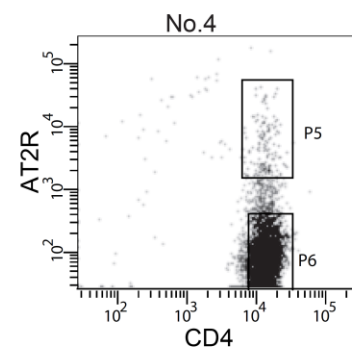
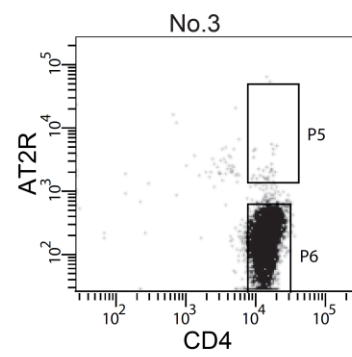
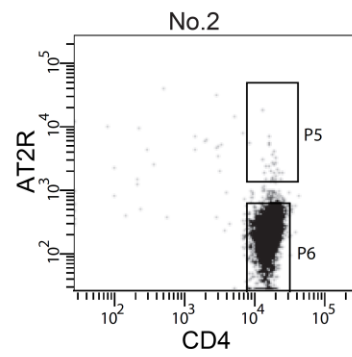
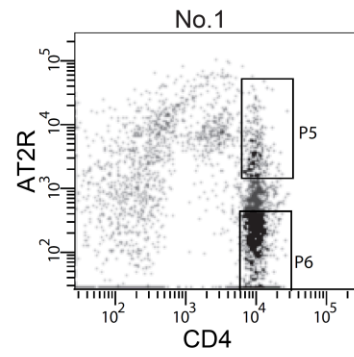
A. Skorska¹, S. von Haehling^{2,3}, M. Ludwig¹, S. Slavic³, C. Curato³, W. Altarache-Xifro³, T. Unger³, G. Steinhoff¹, J. Li^{1,3}

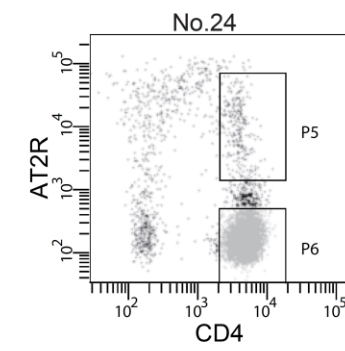
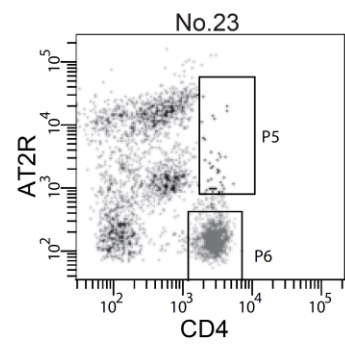
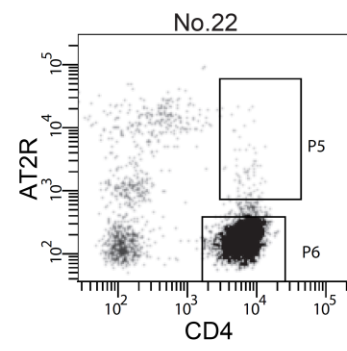
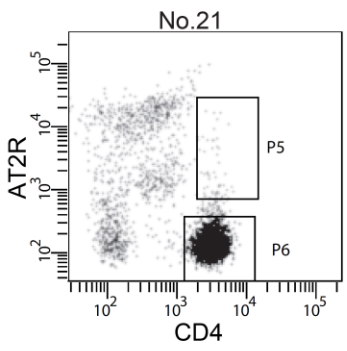
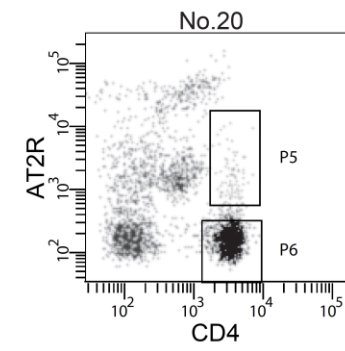
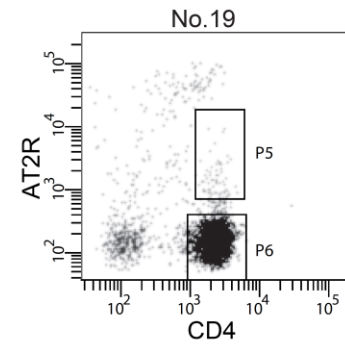
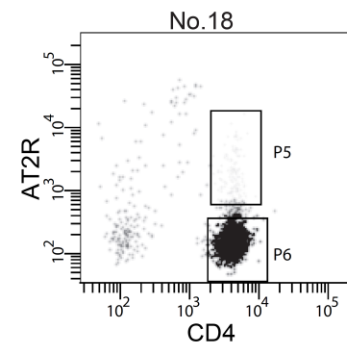
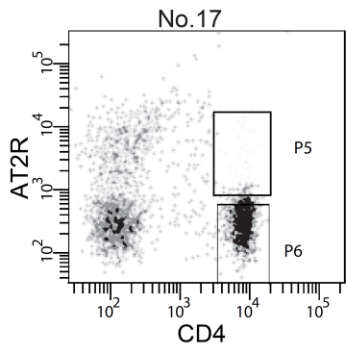
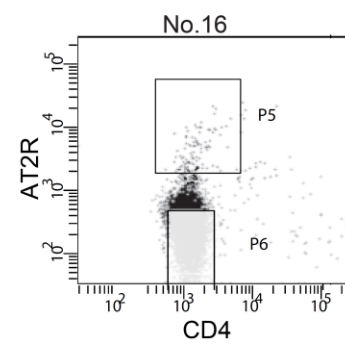
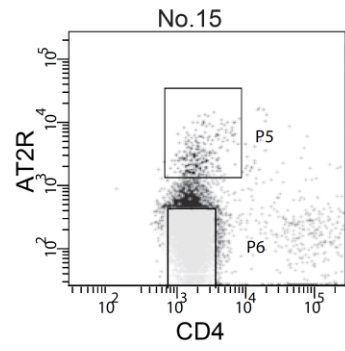
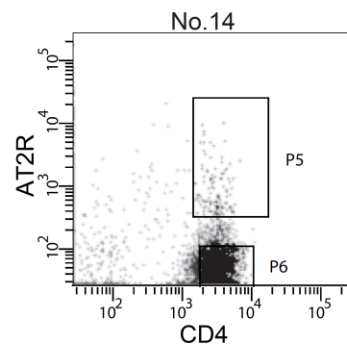
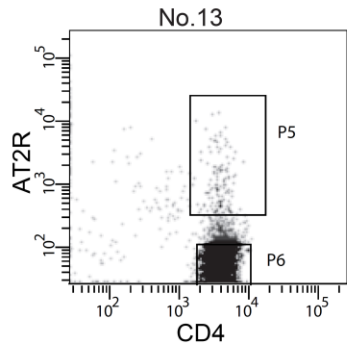
¹Reference and Translation Center for Cardiac Stem Cell Therapy, University of Rostock, Germany; ²Department of Cardiology, Charité, Berlin, Germany; ³Center for Cardiovascular Research, Charité, Berlin, Germany

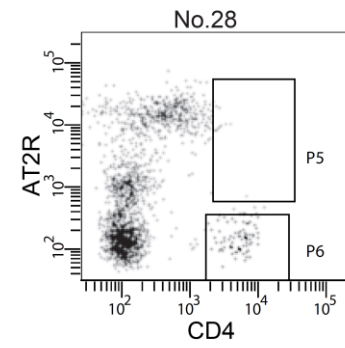
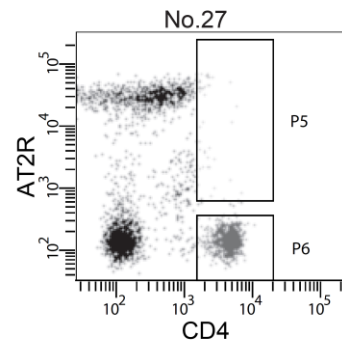
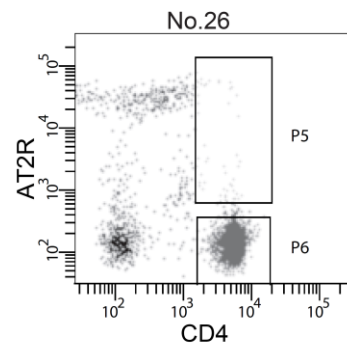
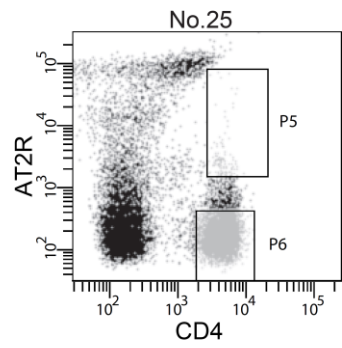
Appendices

Appendix 1. FACS dot plots of healthy donors (n=28)

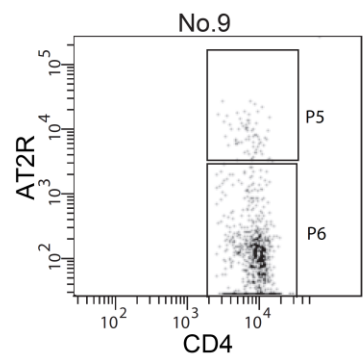
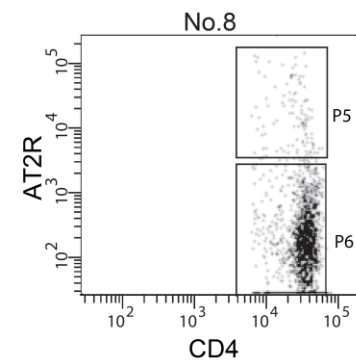
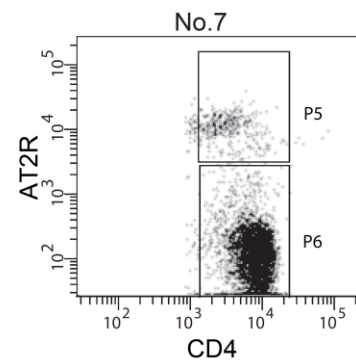
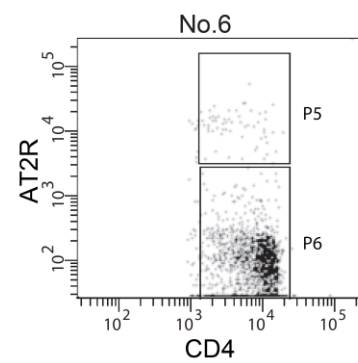
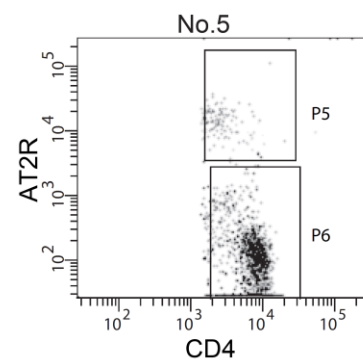
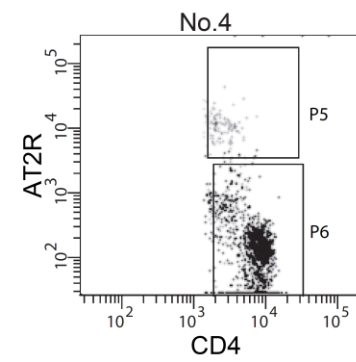
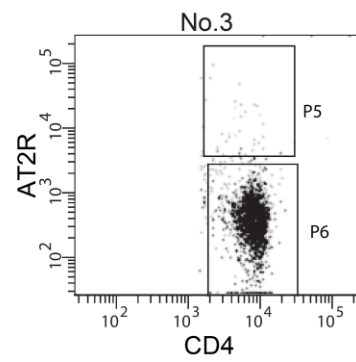
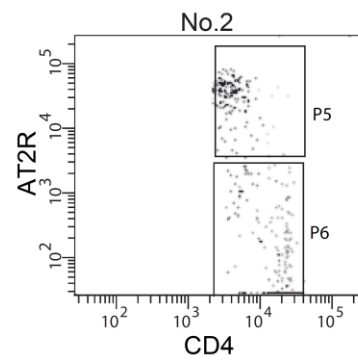
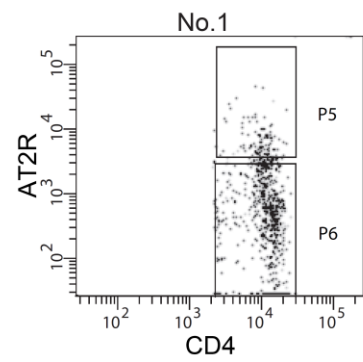
Appendix 2. FACS dot plots of patients with heart failure (n=9)







Appendix 1.



Appendix 1 and Appendix 2. FACS dot plots of healthy donors and patients with heart failure. Mononuclear cells (MNCs) were isolated from human peripheral blood using Ficoll centrifugation and stained with mouse anti-human CD4-PE and goat polyclonal anti-AT2R followed by indirect staining with secondary antibody anti-goat Alexa Fluor 488. Cells were analyzed and sorted using a BD FACS Aria II. Healthy donors, n=28; Heart failure n=9. Taken from Skorska A et al., *JCMM* (2015)